Investigation of antimicrobial strategies using various titanium dental implant surfaces to prevent peri-implantitis: *in vitro* models of *Streptococcus* spp.

PhD Thesis

Annamária Venkei MSc.

2022

Szeged

PhD Thesis

Investigation of antimicrobial strategies using various titanium dental implant surfaces to prevent peri-implantitis: *in vitro* models of *Streptococcus* spp.

Annamária Venkei MSc.

Department of Medical Microbiology, Albert Szent-Györgyi Health Center and
Albert Szent-Györgyi Medical School, University of Szeged

Graduate School of Clinical Science, Research in Dental Medicine

Supervisors:

Krisztina Ungvári DMD, PhD

Department of Prosthodontics, Faculty of Dentistry, University of Szeged

Anette Stájer DMD, PhD

Vice Dean, Head of the Dentistry Clinic, Acting Head of Department, Department of Prosthodontics, Faculty of Dentistry, University of Szeged

2022

Szeged

PUBLICATIONS RELATED TO AND INCLUDED IN THE THESIS

I. **Venkei A**, Ungvári K, Eördegh G, Janovák L, Urbán E, Turzó K: Photocatalytic enhancement of antibacterial effects of photoreactive nanohybrid films in an *in vitro Streptococcus mitis* model. *Archives of Oral Biology*. 2020; 117:104837. doi: org/10.1016/j.archoralbio.2020.104837. **IF: 2.635**

II. **Venkei A**, Eördegh G, Turzó K, Urbán E, Ungvári K: A simplified *in vitro* model for investigation of the antimicrobial efficacy of various antiseptic agents to prevent peri-implantitis. *Acta Microbiol Immunol Hung.* 2020; 67 (2):127-132. doi: 10.1556/030.2020.01080. PMID: 32160783. **IF: 2.048**

ΣIF:4.683

PUBLICATIONS RELATED TO, BUT NOT INCLUDED IN THE THESIS

I. Niller HH, Masa R, **Venkei A**, Mészáros S, Minárovits J: Pathogenic mechanisms of intracellular bacteria. *Current Opinion in Infectious Diseases*. 2017; 30:309-315 doi: 10.1097/QCO.0000000000000363. **IF: 3.782**

II. Barrak I, Baráth Z, Tián T, **Venkei A**, Gajdács M, Urbán E, Stájer A: Effects of different decontaminating solutions used for the treatment of peri-implantitis on the growth of *Porphyromonas gingivalis*-an *in vitro* study. *Acta Microbiol Immunol Hung*. 2020; doi: 10.1556/030.2020.01176. **IF: 2.048**

ΣIF: 5.83

TABLE OF CONTENTS

ABBREVIATIONS

Ag	silver
Ag-TiO_2	silver-titanium-dioxide
AgNPs	silver nanoparticles
AMR pathogen	antimicrobial resistant pathogen
Au	gold
BHI	brain–heart infusion
BSA	bovine serum albumin
C	carbon
CD	chlorine dioxide
CFU	colony forming unit
CHX	chlorhexidine-digluconate
CL	chemiluminescence
CO_2	carbon dioxide
CP_4	commercially pure, grade 4 titanium
ELISA	enzyme-linked immunosorbent assay
FITC	fluorescein isothiocyanate
H_2O	dihydrogen-monoxide (water)
H_2O_2	hydrogen peroxide
MALDI-TOF MS	matrix assisted laser desorption ionization-time of flight mass spectrometer
MTT	3-(4,5-dimethylthiazol-2-yl)-2,5-diphenyltetrazolium bromide
NPs	nanoparticles
O_2	oxygen
O^{2-}	oxide
O_2^-	superoxide anions
$^{\cdot}OH$	hydroxyl radicals
OD	optical density
PBS	phosphate buffered saline

p (EA-co-MMA)	poly (ethyl acrylate-co-methyl methacrylate)
PI	povidone-iodine
ROS	reactive oxygen species
RLU	relative light unit
SEM	scanning electron microscope
SEM-EDS	scanning electron microscopy-energy dispersive X-ray spectrometry
S. salivarius	*Streptococcus salivarius*
S. mitis	*Streptococcus mitis*
SPR	surface plasmon resonance
Ti	titanium
TiO_2	titanium-dioxide
UV	ultraviolet
Zn	zinc

1. INTRODUCTION

It is not the possession of truth, but
the success which attends the seeking
after it, that enriches the seeker
and brings happiness to him.
/Max Planck/

With an improvement in the quality of human life and the expansion of the average human lifespan, materials with specific biomedical applications have become more remarkable [1].

Dental implants have become today an important treatment option for oral rehabilitation in partially or totally edentulous patients, with reliable long term results [2]. The documented high survival rate of osseointegrated dental implants has led to their acceptance as a potential treatment alternative for missing teeth [3]. Despite the high success rate of dental implants, it is still difficult to prevent implant failures due to some risk factors, such as insufficient osseointegration, bacterial infection, unfavorable micro-movements, surgical trauma, premature overloading, improper surgical placement, metal fatigue, and inadequate quality and quantity of bone tissue surrounding the implant. Furthermore, smoking, hormones, poor dental hygiene, diabetes, or genetic history may have an impact on the success of implantation [4–6].

Among these factors, osseointegration between the bone and an implant and bacterial adhesion on the implant surface can have a significant influence on dental implant survival [7]. In the implantation procedure, microbial adhesion, proliferation, and biofilm formation on the implant surface can lead to severe inflammation [8]. Inflammatory processes, i.e., peri-implant mucositis and peri-implantitis occurring after the implantation procedure may lead to implant failure or implant loss. In the case of peri-implant mucositis, the inflammation is localized only to the soft tissues, and it is reversible with efficient conservative therapy. The more progressive form is peri-implantitis, a destructive inflammatory reaction, which affects the supporting soft and hard tissues that surround the implant. It has been shown that the inflammation is more pronounced and the inflammatory process goes deeper and faster around the dental implant, which can lead to the loss of the implant with a high chance (**Figure 1**) [8–10]. According to Derks et al. the mean prevalance of peri-implant mucositis and peri-implantitis is 43 % and 22 %, respectively [11].

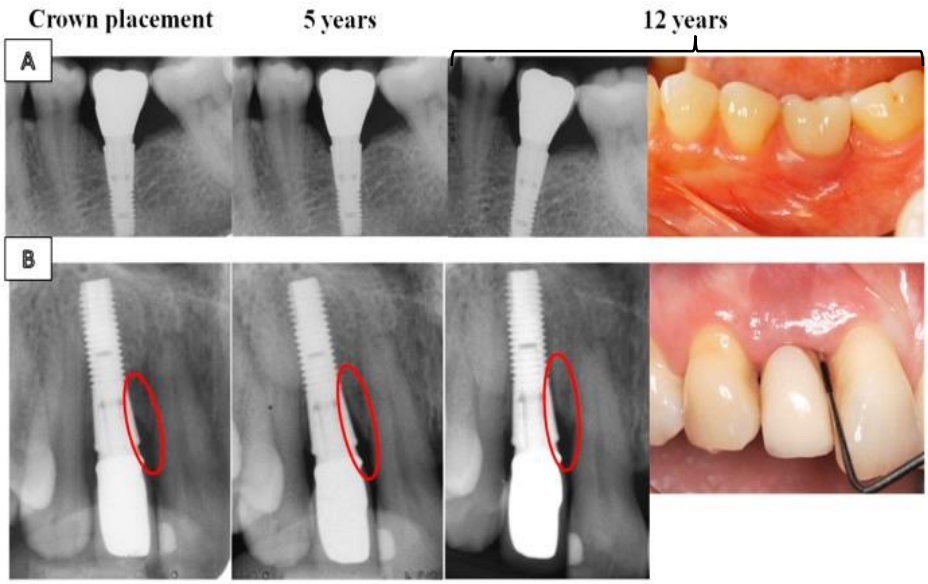

Figure 1. Clinical and radiographic illustrations of (A) a case with no bone loss. Baseline (crown placement), 5 and 12 years of follow-up. (B) a case with progressive bone loss. Baseline (crown placement), 5 and 12 years of follow-up. The figure and legend are reprinted from references [12]. Asensio et al. [12] adapted from Donati et al. [13] with the permission of John Wiley and Sons. The figure has been slightly modified.

Consequently, understanding the etiology, mechanism, and treatment protocol of inflammatory processes is necessary for clinicians involved in implant dentistry.

However, why is it a big challenge to improve implant success? The bacterial biofilm is a structurally and functionally well-organized, cooperating community of different microorganisms. Within the biofilm, the bacteria adapt to environmental stress, such as anoxia and nutrient limitation by presenting a modified metabolism, gene expression pattern, and protein production, which can lead to a lower metabolic activity and as a result reduced rate of cell division. In addition, due to these adaptations, the biofilm forming bacteria become more resistant to antimicrobial therapy by inactivating the antimicrobial agents or reducing the molecular pathways for the cellular function that the antimicrobials interfere with [14–15]. Therefore, the initial treatment of peri-implantitis is based on preventing bacterial adhesion and proliferation on implant surfaces, but it is hard to eliminate them in an effective way.

Titanium (Ti) and its alloys are widely used in manufacturing dental implants, maxillofacial, and orthopedic prostheses due to their favorable properties [16]. Modern Ti implants are constantly engineered, and the surface is usually modified to improve the ossseointegration process [12]. Now, a critical next step in the evolution of implant coatings is improving of osseointegration with antibacterial properties. Many modifications that led to an antimicrobial property of dental implants have been introduced in recent years, including

antibiotics, nanoparticles (NPs), such as gold (Au), zinc (Zn), or silver (Ag), or other compounds bound to the surface [17]. There is also a constantly growing need to develop biomaterials that can be implanted in jawbone tissues for the rehabilitation of the damaged chewing apparatus. Understanding the interaction between biomaterial and microorganism is very important for the development of antibacterial implants.

As the number of patients undergoing restorative therapy through dental implants increases, peri-implantitis is considered to be a remarkable and growing problem in dentistry [18]. In the treatment of peri-implantitis, decontamination of the implant surface should be performed to resolve inflammation and stop further bone loss [19]. Therefore, effective antimicrobial strategies are needed for the treatment of peri-implant inflammation in the routine clinical practice.

1.1 Members of the oral microbiome

The oral microbiota is a diverse community of microorganisms, consisting of over 700 different bacterial species, viruses, mycoplasmas, *Archaea*, protozoa, and fungal species. These microorganisms persist on all surfaces as multispecies biofilms and form the resident oral microbiome, which generally exists in balance with the host and provides important benefits that contribute to overall health and well-being [20].

The formation of a conditioning film on the clean dental surfaces mainly consisting of salivary glycoproteins, the so-called acquired pellicle connecting the oral hard tissue and environments, facilitate the initial adhesion of bacteria to the oral surfaces. The pioneer bacterial species adhere to the pellicle by a weak binding mechanism. The stronger bacterial adherence to the pellicle is developed via receptor-pairs between bacterial surface adhesins and glycoprotein receptors in the acquired pellicle [21]. The predominant pioneer colonizers are oral streptococci, such as *Streptococcus mitis* and *Streptococcus salivarius*, followed by Gram-positive rods, especially *Actinomyces* species. Then other Gram-positive and Gram-negative bacteria adhere to the early forming Gram-positive biofilm. Strict anaerobic bacteria, such as *Fusobacterium* and *Porphyromonas* species play an important role in the formation of the mature dental biofilm as these species co-aggregate with both the initial Gram-positive bacteria and the following colonizers [22,23].

Socransky and colleagues have assigned the organisms of the subgingival microbiota into groups or complexes based on their association with health and various diseases (**Figure 2**) [24,26]. These investigators have used different colors to denote the association of particular bacterial complexes with periodontal infections. The green, yellow, blue, and purple complexes indicate early colonizers of the subgingival flora. Orange and red complexes sign late colonizers associated with the mature subgingival biofilm. Each member of bacterial complexes is associated with health or disease. For example, the species in the red complex are more likely to be associated with periodontal diseases [24,26].

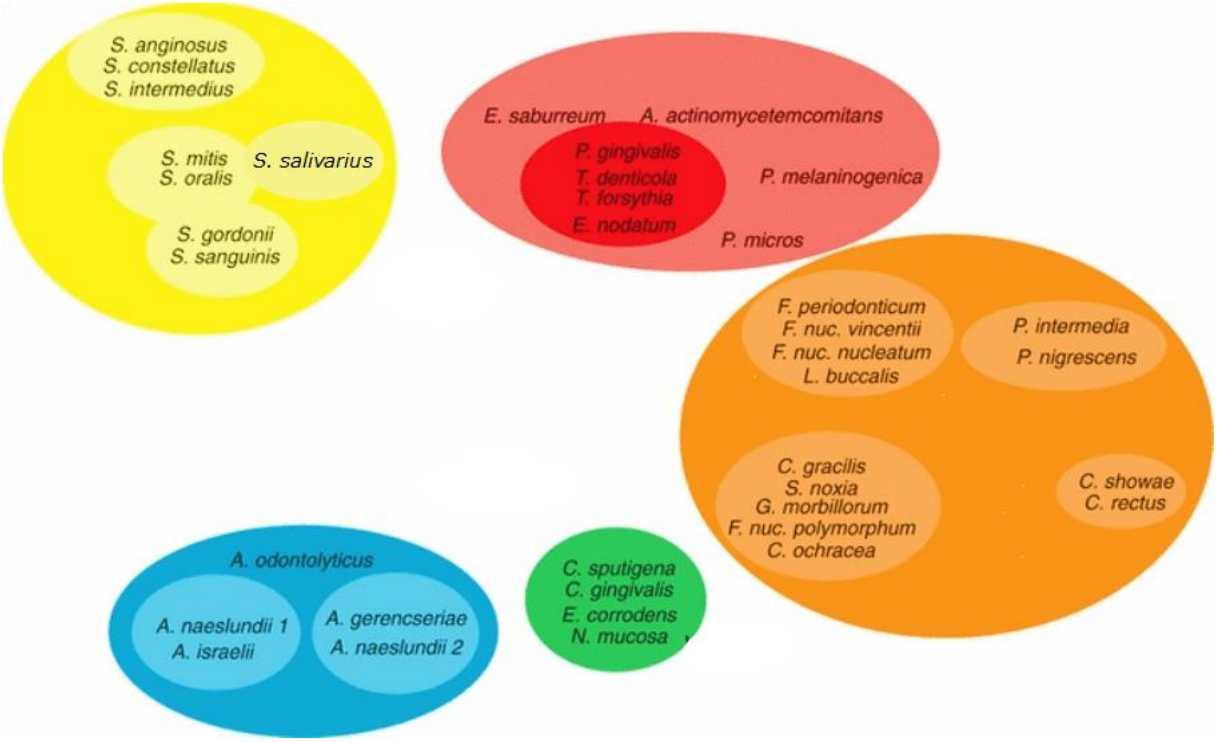

Figure 2. Microbial complexes in subgingival biofilm. Figure 2 is reprinted from reference [24]; however, *S. salivarius* was added to the figure based on the results of Grant et al. [25] who mention *S. salivarius* as a member of the yellow complex.

1.2 The oral microbiome as one of the most complex microbial communities in the human body

During the development of the biofilm, bacteria are in metabolically active state and they use nutrients from saliva. This results in the formation of an extracellular matrix that contributes to the co-adherence of the bacteria on the oral surfaces and ensures protection of the biofilm forming bacteria [27]. The processing of co-adhesion can promote microbial

interactions by co-locating organisms next to the physiologically relevant partner species, thereby providing nutritional co-operation and food chains, gene transfer (i.e., antibiotic resistance genes) and cell–cell signalling (**Figure 3**) [28]. A typical example of the physical and functional associations is observed among *Candida* species and pioneer colonizer bacteria. *Candida albicans* can co-aggregate with oral streptococci and can form synergistic partnerships in which the yeast promotes the biofilm formation of pioneer colonizer bacterium, while streptococci strengthen the invasive property of *Candida* [29].

In this structured community, there is a stable microbial homeostasis in the view of nutritional interdependencies between biofilm forming bacteria. The primary feeder bacteria metabolic products become the main nutrient source for the secondary feeder, resulting in complex synergistic metabolic interactions among them [30]. Laboratory studies have shown that bacterial cells are able to communicate with and respond to neighbouring cells in biofilms by a quorum sensing communication system, as a "universal language" for interspecies communication. Quorum signal molecules, such as autoinducer-1 and -2 play a significant role in the sensitization and adaptation of bacterial cells to environmental stress, and thereby regulate the virulence capacity of the biofilm [31].

In addition to synergistic connections, antagonistic interactions also contribute to the ecological stability of the oral microbiome [32]. The production of antagonistic compounds, such as bacteriocins, hidrogen peroxide (H_2O_2), organic acids, or various enzymes provide benefits for a microorganism in competition for microbial well fare. The most studied oral streptococci produce bacteriocins or bacteriocin-like substances, which may even have an antimicrobial effect, for example, mutacin produced by *S. mutans* or salivaricin by *S. salivarius* [33]. However, antagonism can also have a beneficial effect on communities living in the biofilm, protecting them from colonization by exogenous bacteria, which is the so-called colonization resistance mechanism [34].

Within the biofilm, there is a very close relationship between bacteria that provide optimal condition for horizontal gene transfer among species, which may ultimately also serve as a protection for the members of the biofilm [28].

Dental biofilms are part of the resident oral microflora, and in health, numerous interactions contribute to the stability and flexibility of the ecosystem against environmental disturbances. In the state of microbial homeostasis, the oral microbiome interacting with the

immune system ensures the required benefits for the host, while if it is stressed, the balance is broken and diseases may develop [35]. In dental diseases, similarly to the treatment protocol of other bacterial infections, the using of antibiotics is the first well-tried method. However, due to the existence of resistance genes and their inter-species transfer within oral biofilm, *β*-lactamase producing bacteria are frequently present in oral biofilms, and they could protect neighbouring bacterial species that should be susceptible to the effects of the antibiotics [36].

The oral biofilm was characterized as a structurally and functionally well organized community of microbes (**Figure 3** [28]). Furthermore, it was suggested that multispecies biofilms and other microbial consortia may transmit adaptive traits between ancestral and descendant microbiomes [37]. These features may cause difficulties in the effective prevention of diseases caused by bacteria and the development of adequate strategies to promote the fight against microorganisms.

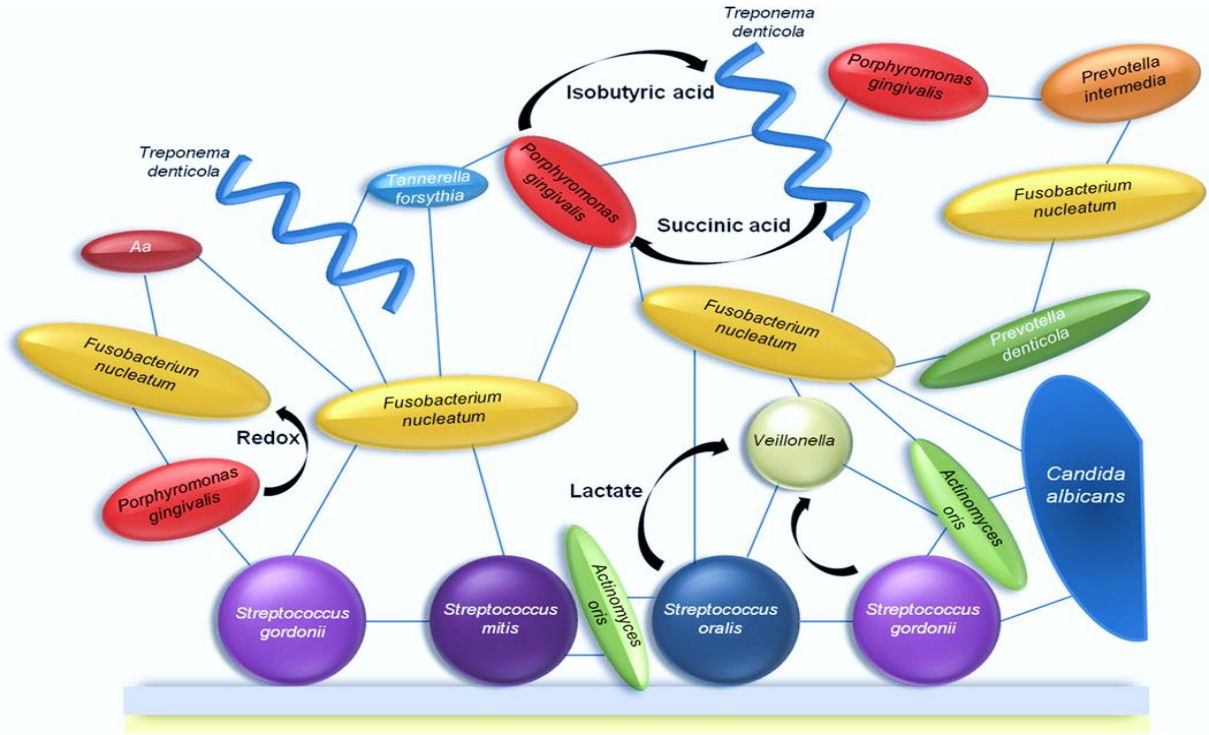

Figure 3. Bacterial cell-to-cell interactions in the dental plaque biofilm. One example of mutualism is displayed between *P. gingivalis* and *T. denticola*. Both release a metabolic factor that the other can utilize, thus enhancing the growth of both species. Lines linking the microorganisms represent adhesive interactions. Aa= *Aggregatibacter actinomycetemcomitans.* Figure and legend are reprinted from reference [28].

1.3 Bacterial adhesion and biofilm formation as one of the main barriers in successful implant intervention

The process of biofilm formation on implant surface (**Figure 4**) is similar to the biofilm formation on the natural teeth. Initial adhesion of bacteria from the oral cavity begins by hydrophobic, electrostatic, and van der Waals forces, which bring the cells closer to the implant surface. After this irreversible attachment, bacterial metabolic activity is upregulated, and migration spread from the colonized neck part of an implant along the implant body in the deeper hard tissue region, and peri-implantitis may occur as an inflammation reaction around implants due to the bacterial toxins [38].

Various types of bacteria can affect the peri-implant inflammation. Among them, the amounts of *Tanarella forsythia*, *Porphyromonas gingivalis*, *Treponema socranskii*, *Staphylococcus aureus*, *Staphylococcus anaerobius*, *Streptococcus intermedius*, and *S. mitis* are approximately four times as high as found on healthy implant sites [39]. These species constituted 30 % of peri-implant microflora at the infected sites [39], which indicates the importance of the study of these strains. Beside these results, we can conclude that a primary strategy to avoid implant-associated infections is to inhibit pioneer bacteria from adhering to implant in the first place, which emphasises the importance of investigating pioneer colonizing bacteria. Therefore, we selected *Streptococcus* species in our experiments, such as *S. mitis* and *S. salivarius*.

The extensive inflammation triggered by bacteria can cause the progressive loss of the supporting bone or even the implant [8]; therefore, an effective biomaterial surface modification with antibacterial function is required to prevent pioneer colonizer adhesion and biofilm formation on implant surfaces.

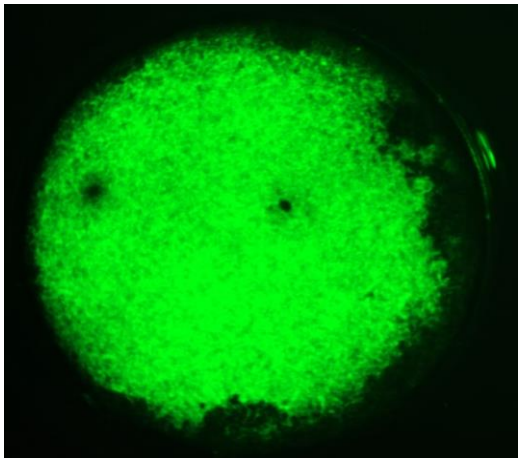

Figure 4. *S. mitis* biofilm formation on Ti implant surface, stained by acridin orange, FITC 1x. Source: own image.

1.4 Modification of Ti dental implant surface for the prevention of bacterial proliferation and biofilm formation

In 1947, J. Cotton introduced Ti and its alloys, like implant materials with medical applications, and since then, the expansive spread of Ti and its alloys has started in the industry or biomedical field [40]. Nowadays, Ti and its alloys are widely used in dentistry (e.g., dental implants and dentures) and orthopedics (e.g., artificial bone, plates, joints, and screws) [41]. Globally, more than 200 million people use orthopedic metal implants for different bone-related diseases, and the number is increasing. Replacement of a missing tooth and restoration of the oral function with surface-modified Ti implant is the main goal in oral implantology [42]. Titanium and its alloys are popular due to their favorable properties, such as excellent mechanical properties, outstanding bio-corrosion resistance, relatively low modulus of elasticity, and high biocompatibility [17]. When Ti is exposed to oxygen (O_2) containing milieu, it forms an oxide (O^{2-}) layer, which provides resistance to corrosion and protection of the underlying metal [43]. Brånemark has discovered that there is a direct interface between living bones and the implant surface, and he has defined this phenomenon as "osseointegration" [44]. The O^{2-} layer does not only boost good biocompatibility but also makes Ti biologically inert, and the treatment of implant surface is usually carried out for the modification of the O^{2-} layer [43].

The surface treatment of Ti implant can be classified into physical, chemical, and biochemical methods [45]. Surface conditions of Ti implants, such as surface roughness, surface charge, surface energy, and chemical composition have great significance in the osseointegration process. To improve the clinical outcomes of implants, surface modifications are being utilised, mainly for the improvement of implant wettability, cell-implant adhesion and attachement, cell proliferation and osseointegration, and also to provide shorter healing time from implant placement to restoration [45]. Goyal et al. [46] have observed that the increased roughness can simultaneously increase the surface area of the implant, consequently boost cell migration and attachment, and improve ossseointegration. Parsikia et al. [47] have found that the surface topography of Ti is optimal when the commercially pure (CP4) Ti surface is blasted followed by a two-step chemical treatment (acid-alkali). Based on their results, the rougher Ti surface promots shorter healing process than the smoother. In current implantology practice, the standard sand blasted, acid etched Ti surface is the most commonly used surface

modification of the root part of the implant, since it provides appropriate roughness for osteoblast cells, thereby granting the anchorage of the implant in the bone [48]. However, in contrast to osteoblast cells, epithelial and fibroblast cells have different needs; therefore, the neck part of the implant, where epithelial cells are attached, is usually polished for a smoother surface, while fibroblast cells need a machined surface [48]. The goal of surface modifications is to find an optimal surface (e.g., with a right roughness) for several functional parts of an implant (root and neck), which is in contact with various biological tissues (alveolar bone, and connective and epithelial tissue) (**Figure 5**).

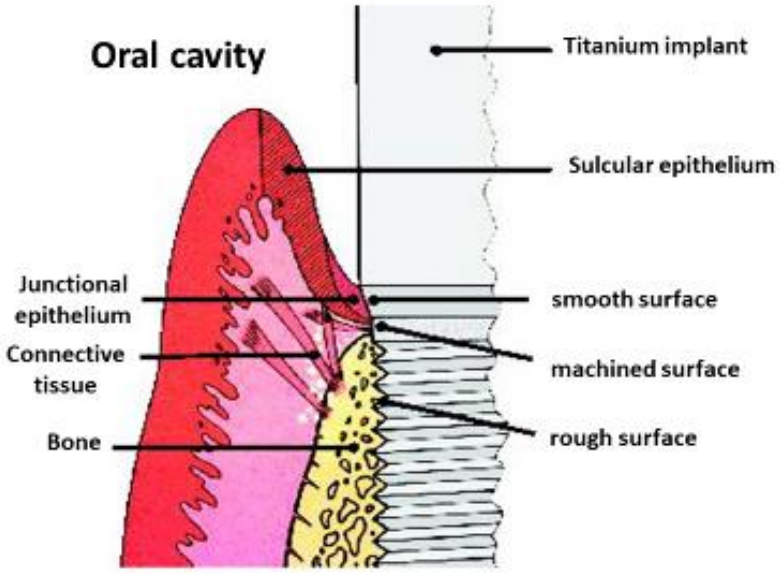

Figure 5. The various types of biological tissues (epithelial, connective tissue, and alveolar bone) in contact with the Ti implant will determine the ideal features of the surface of the implant at its given position. Figure and legend are reprinted from reference [48]. The figure has been slightly modified.

Besides this, it is important to arrest the bacterial adhesion due to the phenomena called the “race for the surface”. Tissue cell integration and bacterial adhesion compete for the real estate on the implant’s surface. If this race is won by tissue cells, the biomaterial surface is covered by a cellular layer. On the other hand, if the race is won by bacteria, the implant surface will become colonized by bacteria, and tissue cell functions are inhibited by bacterial virulence factors [49]. For the elimination of this phenomenon, new innovations have appeared in the field of implantology.

Apart from surface modifying techniques, by some additive technologies, depositions can be gained from the implant surface, which are known as coatings. Various combinations of

surface coatings have been utilised to improve biocompatibility and antibacterial potentials of the implants. Among the different alternatives, coating implants with antimicrobial peptides, growth factors, antibiotic components, nanomaterials, or polymers are the most used techniques [17]. However, due to the continuous development of biomaterials science and biotechnology, the photoactivable bioactive materials have been released and more frequently used. Photocatalytic surface coatings are considered to be one of the best solutions for disinfecting the affected surfaces [50].

1.4.1 Antibacterial photocatalytic coating

Titanium-dioxide (TiO_2) is a typical non-toxic photo-chemically active semiconductor with high photoactivity, which can be used to reduce the number of adhered microbes on Ti surfaces with self-sterilizing effects. Based on literature data, Ti has considerable antibacterial activity; however, the photocatalytic application makes it a more ideal biomaterial for the industry [51]. Titanium-dioxide surfaces undergo photo-activation, when they are irradiated with photon energies under aerobic conditions, causing the photoexcitation of electrons in its valence band to be promoted to its conduction band, creating an electron-hole pair. This electron-hole pair then reacts with dissolved O_2 and water (H_2O) to form reactive radical species (ROS). The generation of superoxide anions (O_2^-) and of hydroxyl radicals ($^{\cdot}OH$) can also lead to the production of further ROS such as H_2O_2. The interaction of ROS with microorganisms can induce bacterial cell damage or cell death, for example, through reaction with essential components of the microorganism or ROS can block biofilm formation by confusion of biofilm gene expression and transcription process (**Figure 6**) [52]. The mechanism of TiO_2 photo-catalysis was discovered by Fujishima and Honda in 1972, and since then, it has been used in many fields of industry and biomedicine [53].

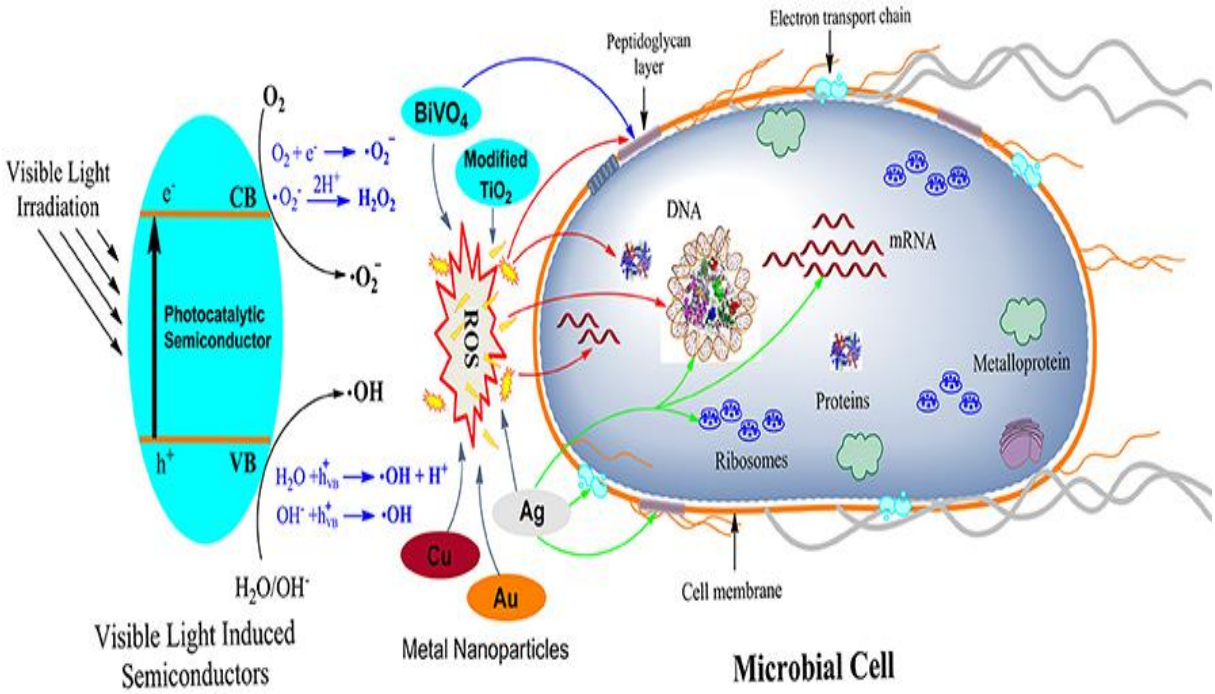

Figure 6. The possible mechanisms of antimicrobial activities exhibited by different photocatalytic semiconductors. In the left side of the figure, the activation of the photocatalytic semiconductor by visible light is shown. Red colored arrows point to the targets of ROS generated by various semiconductors. The blue color arrow represents the target of bismuth vanadate ($BiVO_4$). Ag, Cu, and Au metal NPs are also known to generate ROS and targets different parts in the cell. The green color arrow represents targets of AgNPs. Different targets in the microbial cells are labeled within the cell. Figure and legend are reprinted from reference [52].

1.4.2 Silver as photoactive nanoparticle

Nano-coatings, compared with conventional coatings, have excellent mechanical properties, such as lower porosity, higher hardness, oxidation, and corrosion resistance. In addition, the nanosurface coating with antibacterial properties will be an appropriate technique in solving the implant-related infections [54,55]. Nanomaterials can be used as antibacterial agents on the surface of Ti, and they have a potential to effectively increase the bactericidal properties [52]. Metallic antibacterial agents have remarkable research value because of their strong antibacterial activity, good biocompatibility, and excellent stability [56]. They can be fixed on the Ti surface by using a carrier or coated. Nanoparticles with a particle size in the range of 1–100 nm have specific properties, such as small size effect and large specific surface area [57]. Among NPs, Ag has many advantages, which makes it the most studied and widely used metal-based antibacterial agent.

Modification of TiO_2 by loaded Ag alters the structure and mode of photocatalytic action because Ag can act as an electron trap. The electrons can then be transferred to molecular O_2 to form ROS (**Figure 6**). AgNPs have the ability to boost the photoactive properties of TiO_2 due to surface plasmon resonance (SPR) mechanism. Surface plasmon resonance is a phenomenon that originates from the collective oscillation of conduction electrons of NPs upon interacting with electromagnetic radiation. As a result, the surface Ag component induces visible-light-driven photocatalysis and the semiconductor TiO_2 has photocatalytic activity, and its absorption spectrum extends in the visible light range [52, 58–60]. In this way, the harmful ultra violet (UV) irradiation necessary for the excitation of conventional TiO_2 could be triggered by visible light in the presence of Ag-TiO_2 photocatalyst [58–60].

However, Ag is a well-known antibacterial agent in the absence of light. The antibacterial activity of AgNP against bacteria is variable [61]. The NP can adhere to the cell membrane and penetrate the bacteria causing deactivation of cellular enzymes, disruption of membrane permeability, leading to cell lysis and death [62]. Another mode of action is the induction of morphological changes, such as cytoplasm constriction and detachment of the cell wall membrane and DNA condensation [63]. Moreover, the bacteria are generally unable to develop resistance against AgNP [64], and all these properties of AgNP well demonstrate that it has a huge potential to be used as an antimicrobial agent. Currently, the biggest challenge in the field of biomedical research with regard AgNP is to enable the stable release of Ag at a suitable concentration on the surface of the Ti implant.

1.5 Rescuing a failing implant - treatment possibilities of peri-implantitis

When peri-implant mucositis or peri-implantitis has been diagnosed by the clinician, many different factors and parameters have to be considered before a treatment plan is constructed and treatment may begin. One of the main goals of peri-implantitis treatment is the removal of the bacterial biofilm and the disinfection of the implant surface. Treatment protocols of peri-implantitis include two main approaches: surgical or non-surgical (conservative) therapy [65]. If the implant is in a condition to be retained, treatment should focus mostly on controlling the infection. Non-surgical therapy should always be the first step, as this provides the clinician time to evaluate the healing response of the tissues. During conservative therapy, clinicians remove local irritants from the implant surface with or without surface

decontamination and may apply some additional adjunctive therapies. The decontamination is usually being perfomed mechanically via the use of air abrasive devices or mechanical depurators or chemical agents [65].

The therapy of peri-implantitis in the surgical phase is a more complex process, it should be started with surgical debridement of the damaged peri-implant tissue and continue with decontamination of the affected implant surface. The implant surface can be cleaned by mechanical (air-powder abrasive) or chemical agents (chlorhexidine-digluconate (CHX), H_2O_2, or citric acid) or with laser irradiation. Topical and/or systemic antibiotics as adjunct to peri-implant surgery treatment are commonly used, for example, tetracycline, amoxicillin, augmentin, metronidazol, or penicillin. Surgical treatment protocol, if it is needed, promotes the regeneration of any bone defect by guided tissue regeneration with or without the use of bone grafts or barrier membranes [66–68].

For the chemical decontamination of implant surfaces, several agents have been suggested; however, there is a lack of consensus regarding the techniques/ antiseptic agents to be used for decontamination [69]. The most suitable chemical agent for disinfecting the peri-implant region has not yet been identified because of the lack of comprehensive *in vitro* and *in vivo* experiments [69]. Several disinfectants have been tested with varying success.

Chlorhexidine-digluconate is an effective bactericidal and broad-spectrum antimicrobial agent and currently is the "gold standard" antiseptic in oral hygiene [70]. Chlorhexidine-digluconate is useful in many clinical fields including periodontology, endodontology, oral surgery, and operative dentistry. This agent primarily attacks on the bacterial cell membrane causing leakage of cell components of Gram-positive and Gram-negative bacteria; nonetheless, fungicidal and virucidal effects are also known [71]. Chlorhexidine-digluconate can adhere to the bacteria, preventing their attachment to the dental surfaces. The adhesion of it to salivary proteins inhibits the formation of the biofilm [72]. *Porphyromonas gingivalis* is often difficult to eliminate since being embedded in the biofilm may make it resistant to higher concentration of antimicrobial agents. However, CHX can penetrate in to the plaque, and Noiri et al. [73] have reported that CHX eliminated *P. gingivalis* embedded in biofilm more effectively than compared to antimicrobial agents.

Chlorine dioxide (CD) is also effective in eliminating biofilms. It has excellent bactericidal, virucidal, sporocidal properties, and the main advantage of using CD is that it can

replace antibiotics, avoiding the selection of antibiotic resistant bacterial species [74]. CD interrupts various cellular processes in bacteria due to its direct interactions with amino acids and RNA molecules [75].

However, the use of CD as an antiseptic was hindered because CD solutions were not stable enough. In 2006, a new membrane separation process was invented by Noszticzius et al. [76], which can produce hyperpure, and therefore a significantly more stable CD solution [76]. This solution has been commercially available in Hungary since 2008 under the name of Solumium.

Povidone-iodine (PI) or betadine is a potent microbial agent; it has a wide spectrum of antibacterial and antiviral effects [77]. The information with regard to its effect on biofilms is limited [78]; however, it can destroy the bacterial cell membrane leading to cytosol leakage, and finally to cell death [77].

The above mentioned chemical agents are also commonly applied in dental practice, but well-designed *in vitro* and *in vivo* studies with adequate sample size are warranted in order to establish a protocol for decontamination of peri-implant site during the treatment.

2. AIMS OF THE THESIS

The Faculty of Dentistry of the University of Szeged has been conducting research on surface modifications of Ti implant and favorable osseointegration process for years. Turzó et al. have established the main directions of peri-implantitis research. Experts from other disciplines, such as Ungvári et al. Janovák et al. and many other researchers have joined this project, creating a multidisciplinary collaboration to find new, innovative surfaces for medical application.

Connecting to their results, the aim of my work was to investigate antimicrobial strategies by using various Ti implant surfaces that support the prevention of peri-implantitis. For that, I applied *in vitro* testing methods with relevant pioneer colonizer bacteria, such as *S. mitis* and *S. salivarius*. These methods are regularly used for testing the antimicrobial potential of Ti implant surface, before performing the more expensive and time consuming *in vivo* or clinical studies.

The treatment of peri-implantitis is a very complex and complicated process. For this reason, the present doctoral work focuses on two main strategies. I tested the antibacterial effect of newly developed photoreactive nanohybrid films containing TiO_2 and plasmonic Ag-TiO_2 on Ti based implant surface to find a new opportunity for the conservative treatment or even prevention of peri-implant infections. Furthermore, since in the treatment protocol of peri-implantitis disinfection of implant surfaces is also crucial, I compared the *in vitro* bacterial killing effect of three widely used disinfectant agents (CHX, PI, CD) on *S. mitis* and *S. salivarius* mono-species biofilm models on Ti discs surfaces.

The points to be examined for nanohybrid surfaces were the following:

- *Investigation of the newly developed photocatalyst containing polymer based hybrid layer.*
- *Determination of the anti-adhesive effect of nanohybrid films without visible light illumination by 3- (4,5-dimethylthiazol-2yl)-2,5-diphenyltetrazolium bromide (MTT) assay.*
- *Evaluation of the visible light induced photocatalysis on adhered bacterial cells on different surfaces compared with dark controls by MTT and protein assay.*

- *A further goal was to determinate the effective illumination time that can be short enough in peri-implant treatment process.*
- *To investigate whether the reduced Ag content of the nanohybrid film can be sufficiently effective in killing pioneer colonizer bacteria.*

The points to be examined for antiseptic agents were the following:

- *Comparison of the antibacterial effect of three different decontamination solutions using monobacterial streptococci models.*
- *Investigation of the response of pioneer colonizer streptococci to antiseptic treatment in distinct laboratory conditions.*

3. MATERIALS AND METHODS

3.1 Antibacterial property of nanocomposite polymers

3.1.1 Pretreatment of the Ti discs for the experiments

Titanium discs (1.5 mm thick and 9 mm in diameter) were cut from CP4 Ti rods (Denti System®, Szentes, Hungary). CP4 Ti is available in 4 grades depending on the carbon (C) and iron contents [79]. This type of Ti contains only very small amounts of other elements: the O_2 content is lower than 0.40 %, the nitrogen is not more than 0.05 %, and the C is less than 0.10 % [79]. When we investigated the antibacterial effect of photoreactive nanohybrid films, the surfaces were sandblasted and acid etched by the manufacturer for root part of an implant (**Figure 7A**). Before the experiments, sample discs were uniformly cleaned in acetone (puriss, Molar Chemicals, Hungary), and then with 70 % ethanol (puriss, Molar Chemicals, Hungary) for 15 min, in an ultrasonic bath and rinsed with ultrapure water (Milli-Q® system, Merck, USA) three times. Finally, all cleaned Ti discs were sterilized at 160 °C for 45 min [80].

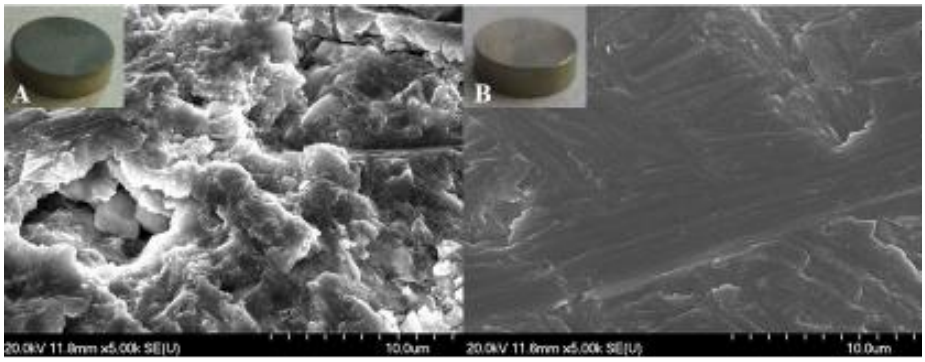

Figure 7. Surface characteristic of sand blasted, acid etched (A) and polished surface (B) by scanning electron microscope (x10), which are used in our experiments. Sand blasted and acid etched surfaces show a rough surface compared with the smoother polished surface. Source: own image.

3.1.2 Preparation of photoreactive nanohybrid films

The pure Ti discs were coated with polymer-based photocatalytic composite thin film with 60 wt% photocatalyst and 40 wt% polymer content. Two different photocatalysts were used for the experiment: the well-known UV- excitable P25 TiO_2 (99.9 %, Degussa- Evonik P25) and plasmonic Ag-TiO_2 photocatalyst with 0.001 wt% Ag content. Polyacrylate based binder material [poly (ethyl acrylate-co-methyl methacrylate; p (EA-co-MMA) (Eudragit NE

30 D, Evonik)] served as a mechanically stable polymer bed for the surface immobilized photocatalyst particles. The 10 wt% aqueous suspension consisting of photocatalyst particles (6 wt%) and polymer binder (4 wt%) was homogenized by sonicator (Elma Hans Schmidbauer GmbH&Co. KG, Stuttgart, Germany) for 30 min (**Figure 8A**). The spray-coated method was used (R180 type Airbrush spray gun, 3 bar operating pressure, 15 cm distance from the surface) to take the suspension up onto the surface of the discs, in a density of approximately 2 mg/disc, and then the film was dried (**Figure 8B**). After sterilization at 160 °C for 45 min, the samples were photo bleached by UV-C irradiation (Vilber Lourmat, Marne-la-Vallée, France) at 254 nm wavelength for 60 min before the experiments in order to partially photodegrade the polymer component of the nanohybrid film, so the surface ratio of uncoated photocatalyst NPs increased on the surface of the film. With this procedure, we provided the direct link between the bacteria and the NPs [59]. The process of the synthesis of polymer-based photocatalytic suspension was detailed elsewhere [59].

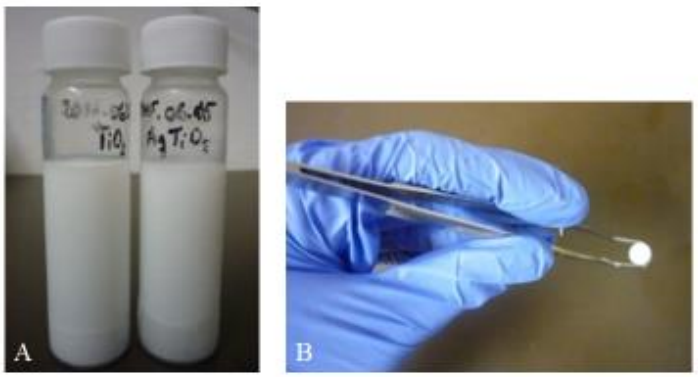

Figure 8. Aqueous suspension consisting of photocatalyst particles and polymer binder (A) and the photocatalytic film on Ti implant surface (B). Source: own image.

3.1.3 Investigation of the polymer based composite layers

The surface of the polymer based composite layer with photocatalyst loading was examined by scanning electron microscope (SEM) (SEM, Hitachi S-4700 microscope), applying a secondary electron detector and 5 kV acceleration voltage. Energy dispersive X-ray spectra were also measured by using the Röntec EDX detector at 20 keV.

The amount of ˙OH was measured from the reaction of luminol and H_2O_2 (50 % aqueous solution, Molar Chemicals, Hungary) using the chemiluminescence (CL) probe method, which has been developed by Hirakawa et al. [81].

The results were calculated from the CL data obtained with Sirius L Single Tube luminometer (Berthold Detection Systems, Budapest). Six milligrams of luminol (≥97.0 % (HPLC)), Sigma-Aldrich) was diluted in 1 mL of 0.1 M sodium hydroxide (puriss, Molar Chemicals, Hungary) solution and filled out to 20 mL with distilled water (Milli-Q® system, Merck, USA). The nanohybrid films were immersed in 40 mL of distilled water and illuminated and shaken continuously during the experiment with a magnetic stirrer. The distance of the light source from the nanohybrid films was 10 cm. The samples were taken after a given time interval (0–360 min) of illumination; 100 µL of the samples was added to 100 µL of luminol solution, and the intensity of the CL was measured immediately with the luminometer [81, 82]. Based on the calibration curve (0–5 mM), the concentration of ·OH radicals is directly proportionate to the measured relative light unit (RLU) values as follows: C_{H2O2} (mM) = measured RLU value/41866, R^2 = 0.9977. For quantitative characterization of the free radical concentration from the RLU data, the calculated equivalent concentration of H_2O_2 (mM) is displayed as a function of illumination time with the used light source.

The photocatalytic activity of the hybrid layers was also verified through bovine serum albumin (BSA) (BSA, ≥98.0 %, Merck, USA) photodegradation tests [83]. The photocatalytic activity, i.e., the decreasing concentration of the BSA (Merck, USA) solution was measured with a Horiba Jobin Yvon Fluoromax-4 spectrofluorometer, and the fluorescence spectra were taken after 0, 30, 60, 120, 180, and 240 min of UV light illumination. The concentration of the initial BSA (Merck, USA) solution was 114 ppm, while the extinction wavelength was λ_{ex}= 290 nm.

3.1.4 Illumination conditions

For photocatalytic illumination, a 15 W low-pressure mercury lamp was used with an UV-visible light source (Lighttech, Dunakeszi, Hungary). The spectrum of the UV lamp was determined by a grating spectrometer (Ocean Optics QE6500, Dunedin, Florida, USA). The 300 lines/mm grating and the 200 µm entrance slit of the spectrometer allowed 6 nm spectral resolution. The spectrum was recorded by directing the light of the lamp onto the entrance slit of the spectrometer across the glass plates, which were used in the experiments. The tissue culture plates were covered with glass plates in order to exclude the UV light during the

illumination periods. The illuminating light source intensity was 1.26 x 10^{-6} einstein/secundum (s), and the plates were positioned 10 cm from the light source.

The emission spectrum of the light source was intense only in the visible range, i.e., these photocatalytic tests were performed under visible light illumination, see in **Figure 9.** The measured spectral lines (368, 409, 439, 490, 548, 615, 633, and 712 nm) corresponded to the emission lines of mercury vapor, and the phosphorescent coating. Weak UV spectral lines of mercury vapor below 320 nm were completely eliminated by the use of glass plates. Therefore, in our experiments, the photocatalytic antibacterial effect was initiated by the above mentioned intense visible spectral lines ($\lambda > 400$ nm).

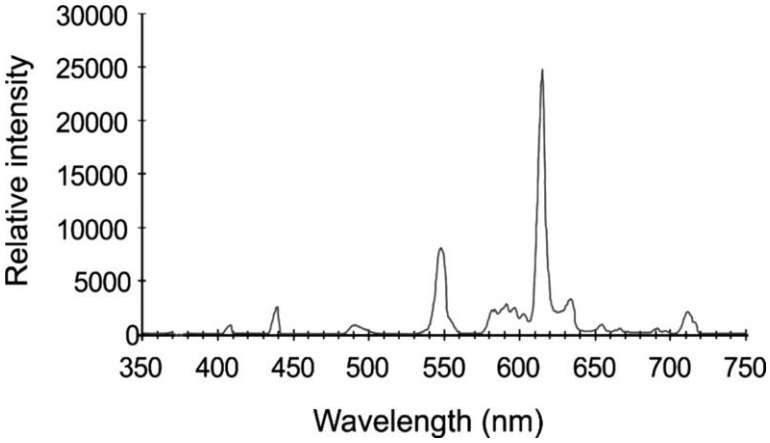

Figure 9. Emission spectrum of the light source used during the antimicrobial experiments.

3.1.5 Culture conditions of *S. mitis*

A clinical isolate of *S. mitis* from a patient who had clinical symptoms of peri-implantitis was used in our experiments. The isolate was recommended by courtesy of the Albert Szent-Györgyi Health Center and the Department of Medical Microbiology, Albert Szent-Györgyi Medical School, University of Szeged. The isolates were previously identified by matrix assisted laser desorption ionization-time of flight mass spectrometer (MALDI-TOF MS) (Bruker Daltonics, Bremen, Germany).

After the isolation and identification, the bacteria were stored at –80 °C in Brain Heart Infusion (BHI) broth (Oxoid, UK) supplemented with 12 % (v/v) glycerol. The strains were streaked and incubated at 37 °C for 24 hours (h) in 5 % CO_2 aerobic atmosphere on blood agar plate containing 5 % cattle blood (BioMérieux, S. A. Marcyl'Etoile, France) for experiments. Isolated colonies of bacteria after overnight incubation on blood agar were inoculated into 50 mL 1 % glucose bouillon broth (Merck, USA). After incubation at 37 °C for 3 h under aerobic

atmosphere, enriched with 5 % carbon-dioxide, the optical density (OD) of the mono-bacterial culture corresponded to 0.5 McFarland density (OD_{620nm}=0.089), which means approximately 10^8 colony forming unit (CFU)/mL.

3.1.6 Investigation of the photocatalytic-induced antibacterial activity of nanohybrid coatings by MTT assay

Two mL of the exponentially growing *S. mitis* culture was pipetted onto the surface of the control and surface modified Ti discs, placed into 24-well hydrophilic surface plate (Sarstedt, Nümbrecht, Germany) and incubated with the mono- bacterial culture for 4.5 h under aerobic conditions. In order to investigate the visible light-induced antibacterial activity of nanohybrid films, illuminated and dark sample groups were prepared. In the "illuminated" group, the discs with adhered *S. mitis* bacteria were illuminated for 5, 10, or 15 min at 37 °C under standardized conditions, while in the "dark" group, the discs were kept in the dark at 37 °C. Non-coated, sandblasted, and acid etched Ti discs, which generally applied in dental practice, were used as controls of nanohybrid surface modifications.

The plate wells were covered with glass plates to prevent the antibacterial effect of the lamp by its UV range (**see Figure 9**). In this way, we provided the enforcement of the photocatalytic antibacterial effect by visible spectral lines.

In order to follow the growth of *S. mitis* on the various surfaces under dark and illuminated conditions MTT (Sigma-Aldrich, Darmstadt, Germany) measurements were used [84]. After the illumination, the samples were washed with phosphate buffered saline (PBS) (Thermo Scientific, Waltham, Massachusetts, USA), then 50 µL MTT solution (1 mg/ml final concentration; MTT powder dissolved in ultrapure water) was added to 0.5 mL PBS on the samples and incubated at 37 °C for 4 h. After this incubation period the solution was removed from each well. Then the formazan crystals, which are the crystallized form of the dye and generated by active bacterial cells, were solubilized with 200 µL of 0.04 mM HCl (Scharlab, Barcelona, Spain) in absolute isopropanol (Molar Chemicals, Halásztelek, Hungary) and with 40 µL of 10 % sodium dodecyl sulfate (Sigma-Aldrich GmbH, Darmstadt, Germany). The OD of solubilized formazan crystals, which indicates the level of cell metabolic activity was

measured at 550 nm with an ELISA (Enzyme-Linked Immunosorbent Assay) reader (Anthos Labtech Elisa Reader, Vienna, Austria) (**Figure 10**).

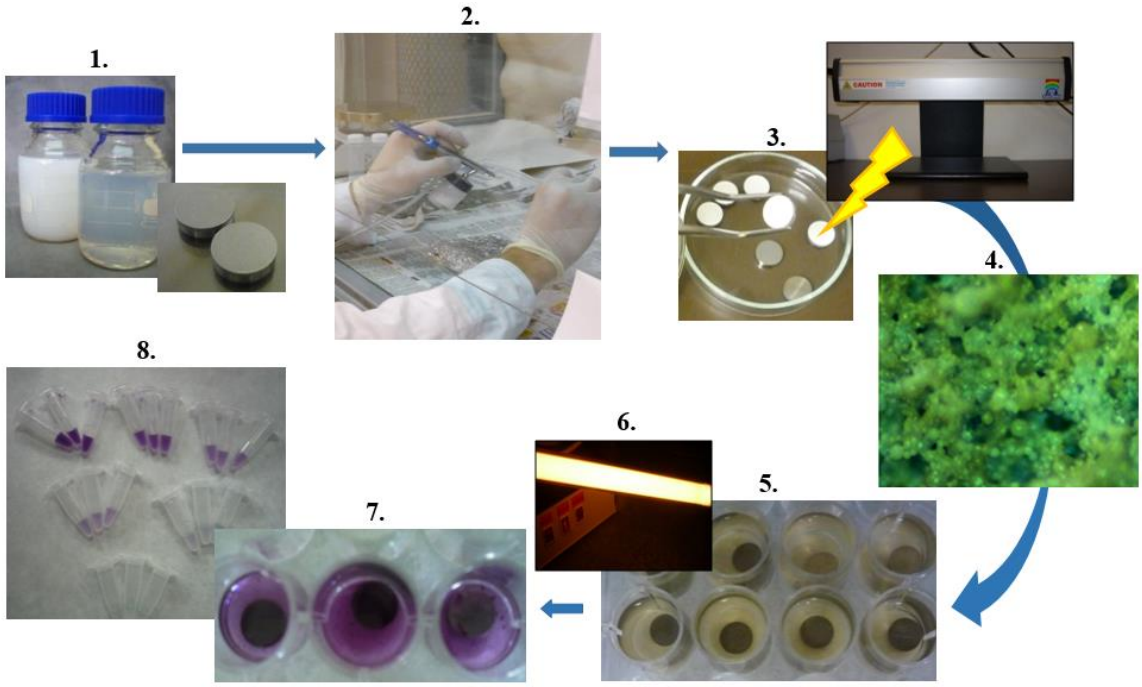

Figure 10. Progress diagram of the investigation of nanohybrid coating antibacterial effect. Polymer-based photocatalytic suspension (1) is taken up on the surface of sand blasted, acid etched Ti by spray-coating method (2). The prepared samples were photo bleached by UV-C irradiation (3) to partially photodegrade the polymer component of the nanohybrid film, so the surface ratio of uncoated photocatalyst NPs increased on the surface of the film (4: representative optical microscopic image of 60 w% Ag-TiO_2: 40 w% copolymer surface, 10x; 200x200µm). The mono-bacterial culture of *S. mitis* was incubated with the control and modified Ti discs (5). The photocatalytic-induced antibacterial activity of polymer based surfaces was triggered by visible light (6). Finally, the antibacterial effect of polymer based surfaces was determined with MTT (7) and protein assay (8). The progress diagram was created based on our own pictures.

3.1.7 Investigation of the photocatalytic-induced antibacterial activity of nanohybrid coatings by protein assay

The Micro BCA™ Protein assay kit (Thermo Scientific, Waltham, Massachusetts, USA) determines the protein content of the samples, which is proportionate to the overall bacterial biomass [85]. For parallel set of the samples, this assay kit was used. A calibration curve was created by using BSA as a control. After the illumination and the washing step with 0.5 mL PBS, (Thermo Scientific, Waltham, Massachusetts, USA) the remaining bacterial cells were disrupted in 0.5 mL lysis buffer (Thermo Scientific, Waltham, Massachusetts, USA). The lysate was centrifuged at 13.000 rpm for 10 min and the supernatants were removed. 150 µL

Micro BCA Working reagent (Thermo Scientific, Waltham, Massachusetts, USA) was added to each supernatant and the solutions were incubated at 37 °C for 2 h. The OD was determined at 550 nm with an ELISA reader. The protein concentration data were calculated based on the measured OD values according to the standard curve (**Figure 10**) [85].

3.1.8 Statistical analysis

The statistical analysis was performed in Statistica 13.4.0.14 (TIBCO Software Inc. USA) and CogStat 1.7.0. (Attila Krajcsi 2012-2018). In my nanohybrid films related study, after checking the normality and homogenity criterion, we compared the data with the help of the appropriate tests (Mann-Whitney U test, Kruskal-Wallis test, independent samples t-test, Welch probe, and one-way ANOVA). Statistical significance was set at $p<0.05$. The means ± SEM (standard error of the mean) were calculated for $OD_{550\,nm}$ values measured by plate reader based on four parallel experiments (four measures in each) carried out at different time points.

3.2 Antibacterial property of various antiseptic agents

3.2.1 Preparation of disc surfaces for the experiment

In our experiments, we used two different surface modified Ti discs. The discs (1.5 mm thick and 9 mm diameter) were cut from commercially pure (CP4) Ti rods (Denti System®, Hungary). Besides the sandblasted and acid etched surfaces, in our next research, we used polished surfaces, similarly to the transgingival part of a dental implant (**Figure 7B**). Before the experiments, the samples were cleaned with the same method as detailed in Section 3.1.1.

3.2.2 Culture condition of *Streptococcus* spp.

Clinical isolates of *S. mitis* and *S. salivarius* were used in our experiment. Similarly to *S. mitis* isolate, *S. salivarius* was also offered by respect of the Albert Szent-Györgyi Health Center and the Department of Medical Microbiology, Albert Szent-Györgyi Medical School, University of Szeged. Before the experiments, the isolates were identified by MALDI-TOF MS (Bruker Daltonics, Bremen, Germany). The storage and the preparation of the mono-bacterial culture of the strains were the same as detailed in Chapter 3.1.5.

3.2.3 Investigation of the antibacterial activity of the three different antiseptic agents on mono-species biofilms

Two mL mono-bacterial suspension was pipetted on the surfaces of discs in 24-well hydrophilic surface plate (Tissue Culture 24 well plate, Nümbrecht, Germany).

However, in this research, we used different incubation times for the two test bacteria, since our goal was to investigate the response of pioneer colonizer streptococci to antiseptic treatment in distinct laboratory conditions. Therefore, we incubated the *S. mitis* for 4.5 h on the surfaces of discs, like in our nanohybrid film experiments, while we extended the incubation time to 48 h in case of *S. salivarius*, where after 24 h, we changed the culture medium for fresh 1 % glucose bouillon.

After incubation at 37 °C in 5 % CO_2 the developed biofilms were washed with PBS to remove the non-adherent cells. Then, the attached bacterial cells were treated with 2 mL of three different oral antiseptics: CHX (Curasept ADS 220, 0.2 %, Switzerland), PI (Betadine, 10 %, Switzerland) and CD (Solumium dental, 0.12 %, Hungary) for 5 min, since it can be optimal in dental practice. The antiseptics were washed out from the implant surfaces by rinsing them with 1 mL PBS.

In order to follow the metabolic activity of the bacterial biofilm, MTT (Sigma-Aldrich, Darmstadt, Germany) assay was used. The steps of the assay were the same as used previously, see Chapter 3.1.6. The antibacterial effect of the antiseptics was compared with untreated control Ti discs with the developed biofilm, which were only rinsed with sterile PBS.

3.2.4 Statistical analysis

Statistical analysis was carried out by using Statistica 13 (Dell Inc. USA). After test of normality (Shapiro–Wilk test), the comparisons within group were evaluated by using one-way analysis of variance (ANOVA) followed by Tukey's post hoc test, and T-test was used for the comparison of independent samples. The means ± SEM (standard error of the mean) were calculated for $OD_{550\ nm}$ values measured by plate reader based on five parallel experiments (three measures in each group) carried out at different time points. Statistical significance was set at $p<0.05$.

4. RESULTS

4.1 Structural and photocatalytic characterization of the hybrid layers

Figure 11 presents the structure of the photocatalyst containing polymer based hybrid layer with different magnifications. Quasi-spherical microscale-aggregates of the primer photocatalyst particles can be observed on the composite surface with diameters ranging from 5 to 40 μm. Moreover, according to the scanning electron microscopy-energy dispersive X-ray spectrometry (SEM-EDS) pictures, at increased magnifications, nanostructures could be identified superposed on the microscale structure. This is due to the NPs aggregation during the composite film forming process; the initial Ag-TiO_2 photocatalytic particles with ~50 nm primary (nominal) particle size were aggregated into 5–40 μm microparticles. This structure ensures high porosity and accessibility, which is advantageous for the photocatalytic process.

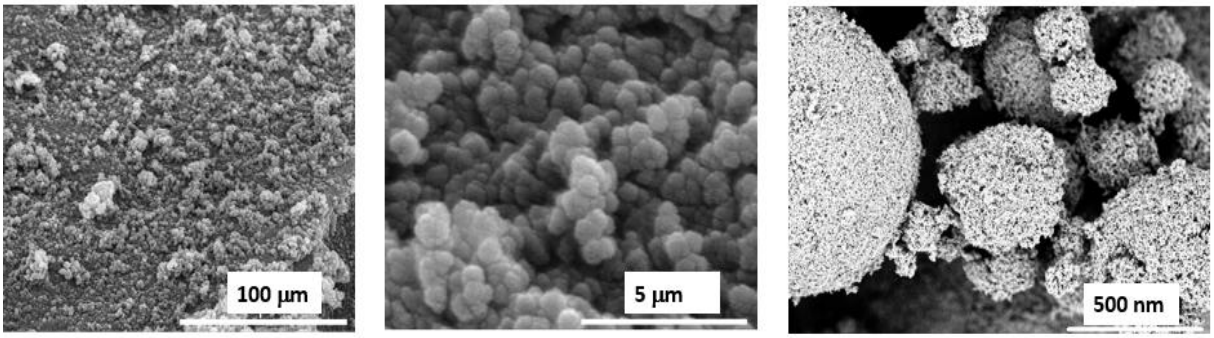

Figure 11. SEM-EDS images of the polyacrylate based composite thin films containing Ag-TiO_2 photocatalyst filler material with various magnifications.

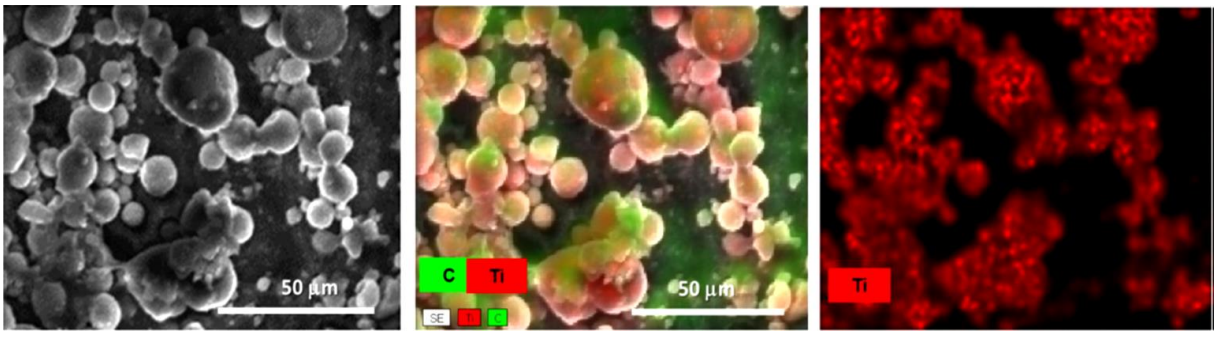

Figure 12. SEM-EDS images of polymer based photoreactive hybrid layer with the corresponding element distribution of carbon (C) and Ti.

Figure 12 shows the SEM-EDS image, and elemental mapping for C, Ti, and C/Ti content of the polymer based sample with 60 wt.% Ag-TiO_2 content. At this photocatalyst

content, both the C of the polymer (green colour) and the Ti content of the photocatalyst (red colour) are expressed on the surface. This dual presence of the components at optimal composition resulted surfaces with simultaneous photocatalytic and good mechanical properties.

To explore the Ag-TiO_2 photocatalytic reactions, the concentration of ROS produced during irradiation has been investigated with the CL method. The calculated equivalent concentration values of ROS such as H_2O_2 (mM) as a function of illumination time are presented in **Figure 13**. The amount of ˙OH that are produced by the photocatalysts was measured from the CL of luminol. The results showed that hybrid layer with 60 wt% photocatalyst content shows saturation curve during the studied time interval (0–360 min). This tendency is due to the previously reported partial polymer photodegradation; the illumination changes in the ratio of catalyst/polymer composition as the photocatalyst particles became uncoated [60]. This resulted in higher catalyst availability on the surface region. Due to this photocatalyst surface enrichment, the formation of free radical concentration displays saturation curves. It can be also seen that both the photocatalyst free polymer sample and the control sample show negligible photocatalytic effect.

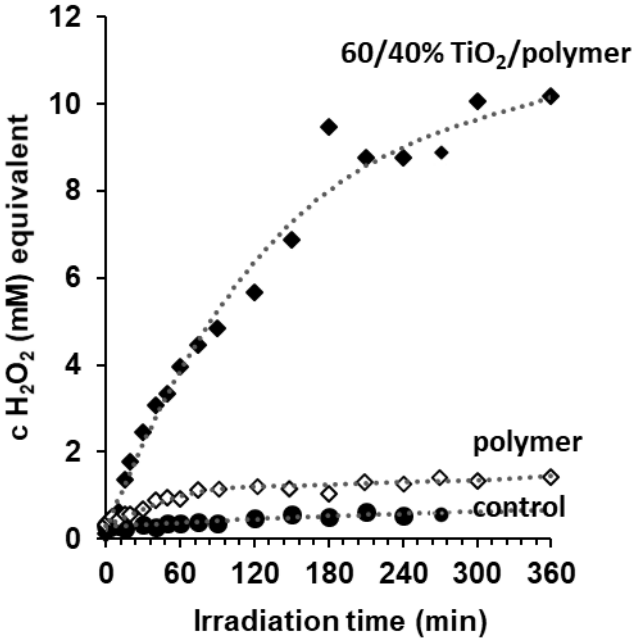

Figure 13. Characterization of the formation of free radicals on photoreactive hybrid thin films via RLU CL intensity measurements. Representation of the equivalent H_2O_2 concentration as a function of illumination time.

Next, the photocatalytic behavior of the Ag-TiO_2 containing hybrid layer was also demonstrated and studied in the case of BSA solution under UV- light irradiation (**Figures 14A**

and 14B). The results reveal that the surface adsorption of the BSA macromolecules was relatively high after 15 min contact time and after that the photooxidation of protein solution (c_0 = 114 ppm) almost reached the 100 % under the 4-hour UV irradiation time. Thus, the polymer based hybrid layers show obvious photocatalytic activity.

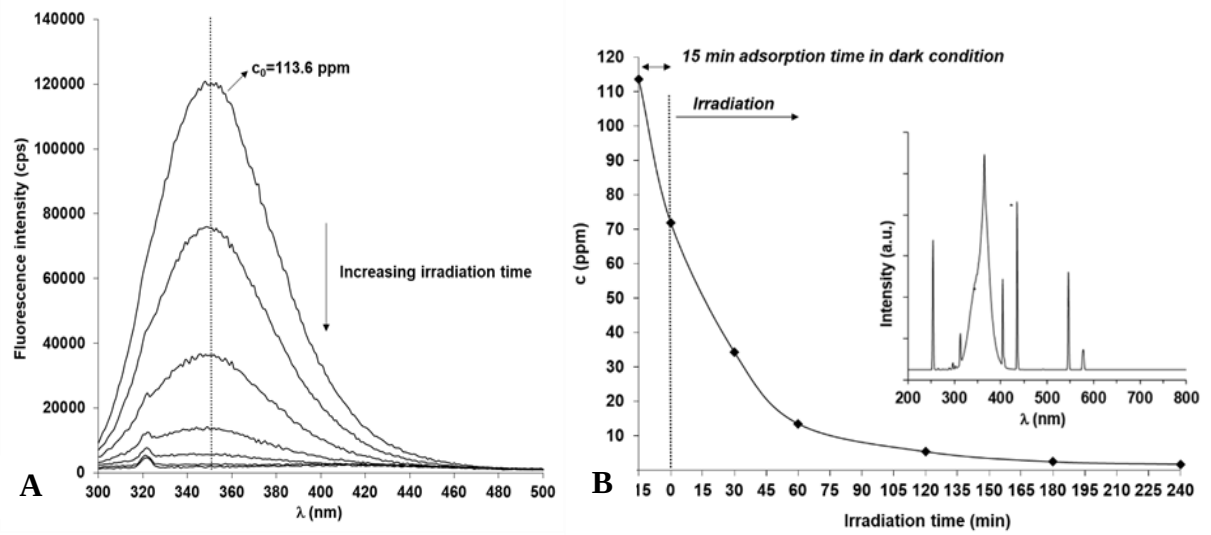

Figure 14. The effect of UV light irradiation on the fluorescence spectra of the aqueous BSA solutions (A) and the corresponding normalized concentration changes (B) of the protein solution. The inserted image shows the emission spectra of the used UV light source.

4.2 Assessment of the antibacterial activity of the modified surfaces using the MTT method

The relative adherence of *S. mitis* to the different dark control disc surfaces is illustrated in **Figure 15**. The MTT results confirmed that the relative adherence of *S. mitis* was different depending on the surface type even without illumination. The anti-adhesive effect of the 0.001 wt% Ag-TiO_2 nanohybrid was the most remarkable, however not significant (**Figure 15**).

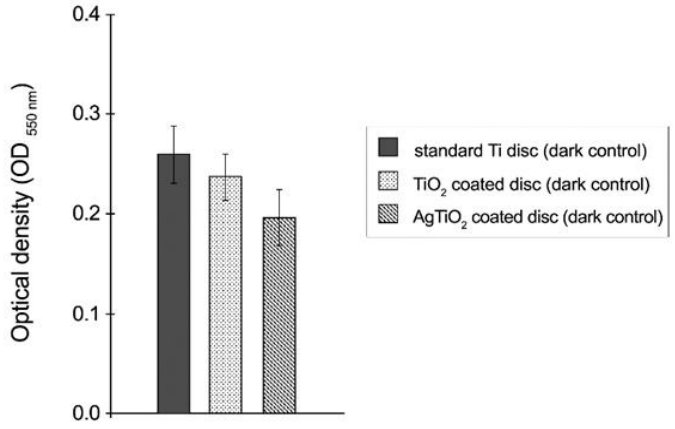

Figure 15. Relative adherence of *S. mitis* to the standard Ti and modified disc surfaces measured with MTT colorimetric assay without visible light illumination. The values were calculated from four independent experiments and are shown as mean ± SEM (standard error of mean).

In **Figure 16A**, the antibacterial effect of surface modifications and visible light illumination compared to their dark controls are plotted as the effect of illumination time. The number of metabolically active bacteria decreased on all Ti based surfaces during illumination for different time. Significant differences ($p<0.05$) were observed at 15 min illumination compared with dark controls in case of all surfaces. In cases of TiO_2 nanohybrid surfaces and standard Ti disc, we measured significant differences ($p<0.05$) between the 5 min and 15 min illuminated samples by the MTT method (**Figure 16B**). The metabolic activity of *S. mitis* on the Ag-TiO_2 nanohybrid film covered sample (OD_{550nm}=0.118±0.014) illuminated for 15 min was 40 % lower than its dark control (OD_{550nm}=0.196±0.028) (**Figure 16A**). 15 min of illumination with visible light enhanced the antibacterial effect of the Ag-TiO_2 coated surface. We observed the fluctuation of OD value in the test results of the standard Ti disc. The OD value rises after being illuminated for 10 min compared with 5 min illumination. The reason for this discrepancy may be a complex process.

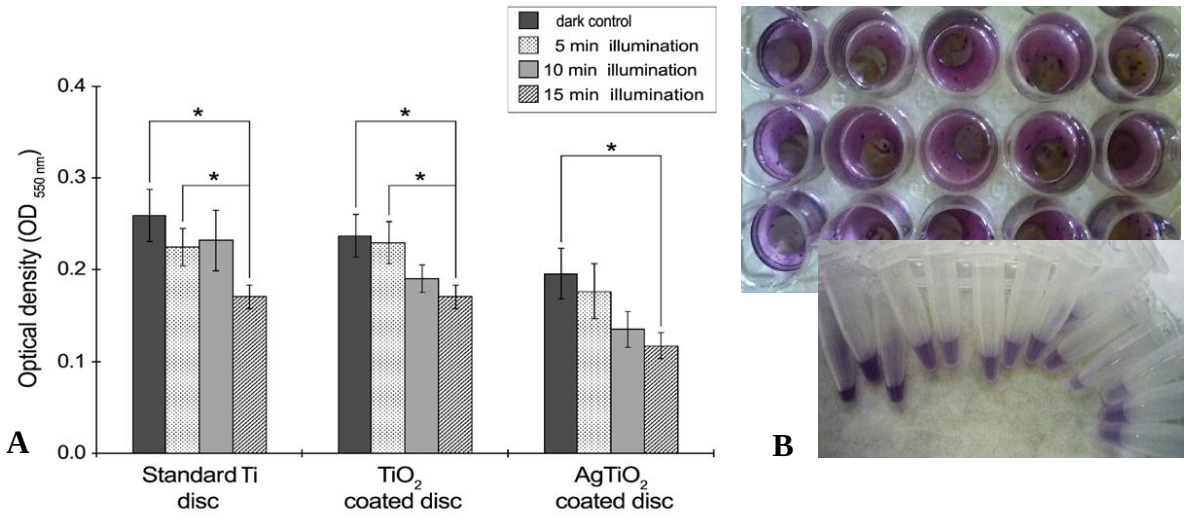

Figure 16. The antibacterial effect of visible light induced photocatalysis on the metabolically active bacterial cells adhered to the different surfaces compared with dark controls (A) using MTT colorimetric assay (B). The values were calculated from four independent experiments and are shown as mean ± SEM. Asterisks denote significant differences (* $p< 0.05$). Figure 16B: our own images.

4.3 Investigation of the various nanohybrid coatings photocatalytic activity

The antibacterial effect of photocatalytically activated nanohybrid surfaces after illumination for different times compared with the standard Ti discs (without illumination) is shown in **Figure 17**. We observed significant differences between the control Ti discs and both types of nanohybrid coatings in cases at 10 and 15 min illumination. The TiO_2 nanohybrid coatings eliminated significantly more metabolically active bacterial cells after 10 min (OD_{550nm}=0.191±0.015) and 15 min (OD_{550nm}=0.171±0.013) illumination compared with the control Ti discs (OD_{550nm}=0.260±0.028). We also found a significant difference between the 10 min illuminated Ag-TiO_2 nanohybrid film (OD_{550nm}=0.136±0.020) and the control Ti discs (OD_{550nm}=0.260±0.028). Furthermore, in our comparisons, the 15 min illuminated Ag-TiO_2 nanohybrid film (OD_{550nm}=0.118±0.014) had the most remarkable antibacterial effect, since it proved to be significantly better compared with the control Ti discs (OD_{550nm}=0.260±0.028). These findings demonstrated that the Ag-TiO_2 coated surface had remarkable antibacterial effect, which is obviously due to the Ag enhanced photocatalytical activity.

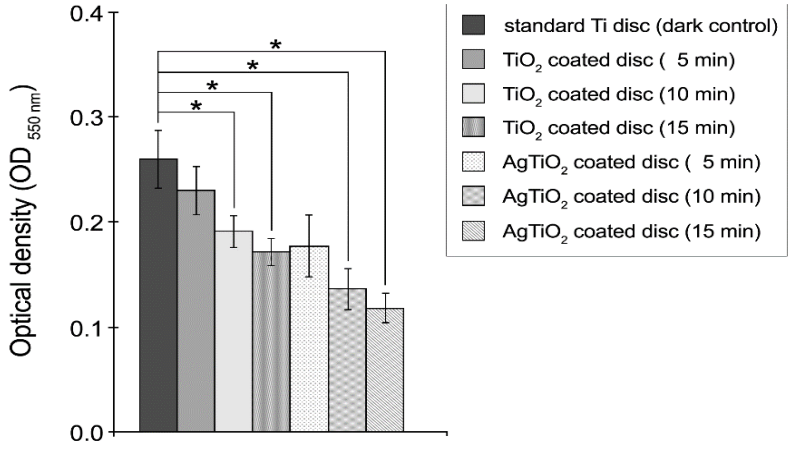

Figure 17. Comparison of the antibacterial effect of visible light illuminated TiO_2 and Ag-TiO_2 nanohybrid coatings with dark control Ti disc by MTT colorimetric assay. The values were calculated from four independent experiments and are shown as mean ± SEM. Asterisks denote significant differences (* $p < 0.05$).

4.4 The effect of the various surfaces on the total bacterial protein content

The remaining amounts of bacterial protein on the tested surfaces as a result of the illumination time are shown in **Figure 18**.

According to protein assay, the amounts of proteins on both nanohybrid surfaces were lower than on the control Ti after 15 min illumination, however not significantly. It can also be stated that no significant changes were observed in protein content reduction on Ag-TiO_2 surface, but this coating inhibited bacterial attachment and showed bactericid effect most of all.

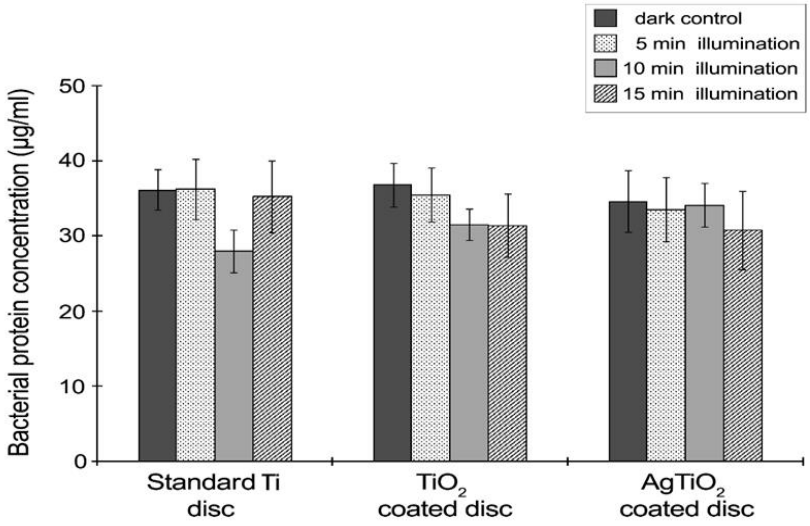

Figure 18. The antibacterial effects of various illumination times measured by the amount of the total bacterial protein on the nanohybrid surfaces and standard Ti discs. The protein concentration data were calculated based on the calibration curve of BSA. The values were calculated from four independent experiments and are shown as mean ± SEM.

4.5 Disinfectant efficacy of oral antiseptics on *S. mitis* biofilm determined by MTT colorimetric assay

The results of antimicrobial activity of antiseptics against *S. mitis* are shown in **Figure 19**. Evaluation of the three disinfectants antibacterial activity against the pioneer colonizer indicated that among antiseptics, the PI and CD showed significant differences both on the polished ($p=0.0005$) and the sand blasted, acid etched ($p=0.0004$) Ti surfaces compared with the untreated control Ti discs after the 5 min treatment time. We presented the measured OD values in **Figure 19**; however, we converted these data to percent values and mentioned them in this way in the text (data are not shown here). The attachment to the control Ti surface was considered 100 % (highest OD value), and the number of metabolically active cells on the surfaces was expressed in relative percentages in the results section. Based on our MTT results, all antiseptic decreased the cell metabolic activity in biofilm on sand blasted, acid etched, and polished surfaces. However, the PI and CD showed significant cell reduction on both surfaces

($p<0.05$). The PI was the most effective antiseptic against the *S. mitis* cells incubated for 4.5 h, since it decreased the number of active cells with 37 % ($OD_{550nm} = 0.043 \pm 0.001$) on polished surface compared with the control disc ($OD_{550nm} = 0.068 \pm 0.008$) after 5 min treatment time ($p=0.0012$). We observed completely similar tendency with regard to the sand blasted, acid etched surfaces. The decrease of the metabolically active cells was 33 % ($OD_{550nm} = 0.044 \pm 0.001$) after rinsing with PI compared with the untreated control Ti discs ($OD_{550nm} = 0.065 \pm 0.007$) ($p=0.0007$).

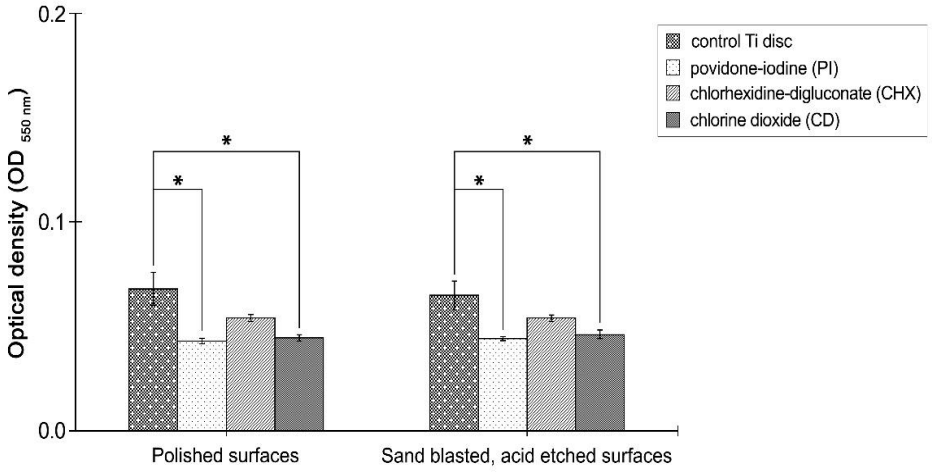

Figure 19. Determination of the antibacterial efficiency of different antiseptic agents by MTT colorimetric assay for *S. mitis*. The values were calculated from five independent experiments and are shown as mean ± SEM. Asterisks denote significant differences (*$p<0.05$).

4.6 Disinfectant efficacy of oral antiseptics on *S. salivarius* biofilm determined by colorimetric MTT assay

The disinfectants dissolving effects on *S. salivarius* biofilm developed for a prolonged incubation time (48 h) are detailed in **Figure 20**. According to our results, all tested agents significantly decreased the amount of metabolically active cells in *S. salivarius* biofilm on polished surfaces compared with the untreated Ti surfaces *in vitro* ($p<0.0001$). The most pronounced antibacterial activity was attributed to PI, which eliminated 65 % ($OD=0.048 \pm 0.003$) of biofilm forming cells on polished surface after 5 min treatment time ($p=0.0002$). However, the CD also eliminated a remarkable percent of the biofilm (60 %) ($OD=0.056 \pm 0.001$) compared with the control polished discs ($OD=0.139 \pm 0.01$, $p=0.0002$). Considering the three agents, significant differences could be observed between the PI and CHX ($p=0.0002$), and in this respect, between the CD and CHX ($p=0.0006$) as well.

Compared with the control discs, each of the three antiseptics studied decreased the metabolic activity of *S. salivarius* biofilms on polished surfaces as well as on sand blasted, acid etched surfaces ($p<0.0001$) (**Figure 20**).

Furthermore, the PI and CD showed significantly higher antibacterial activity against *S. salivarius* compared with the CHX treatment (PI vs. CHX $p=0.0007$, CD vs. CHX $p=0.0212$). We also observed that the metabolic activity of control *S. salivarius* cells was lower on the sand blasted, acid etched Ti surface than on the polished surface ($p=0.0063$) (**Figure 20**). We did not notice such a difference in case of control *S. mitis* biofilms (see **Figure 19**).

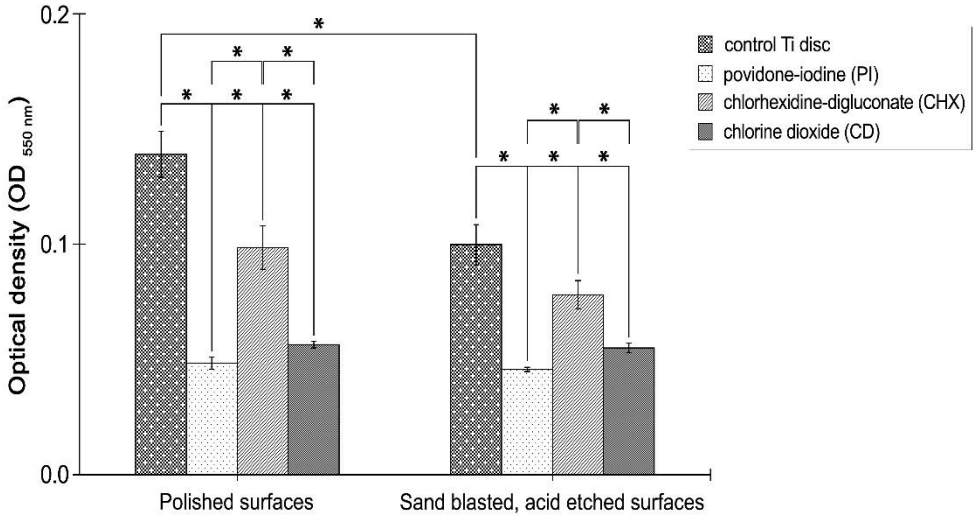

Figure 20. Effect of antiseptics on the *S. salivarius* cells using MTT colorimetric assay. The values were calculated from five independent experiments and are shown as mean ± SEM. Asterisks denote significant differences (*$p<0.05$).

5. DISCUSSION

The use of Ti dental implants is becoming a widely accepted method among dentists for replacing missing teeth [86]. However, dental implants are constantly exposed to oral bacteria by partial contact with the jawbone and gums [87]. Bacterial infection on and around the implant (peri-implantitis) is one of the most common causes of implant failures [8]. Therefore, there is a growing need to develop surfaces to control the spread of implant related infections and find alternative agents, which may kill a broader spectrum of microbial species without any harmful effect on the surrounding human cells. Nonetheless, coating manufacturers are facing a major challenge these days in the form of superbugs, multidrug resistant microbes, and viruses [88]. The antimicrobial resistant (AMR) pathogens cause high impact in the international health epidemic. Globally, it was noticed that 700,000 deaths could be attributed to AMR per year, and the numbers are expected to rise dramatically unless action is taken [89]. The development of antimicrobial resistance will enhance peri-implant disease in the coming years [90]. Therefore, the need for effective antimicrobial agents and compounds is mandatory in order to prevent the risk of superinfection. The presence of antimicrobial agents that do not alter colonization resistance will lead to a decrease in the risk of development and spread of resistant strains among patients [90]. Furthermore, actually there is no gold standard in the treatment of peri-implantitis.

The methods of my doctoral work are simplified *in vitro* basic models using *Streptococcus* spp. These models serve, however, as a basis for the investigation of more complex biofilm forming communities.

5.1 Evaluation of the antibacterial effect of nanocomposite surfaces in the light of my results

Photocatalytic surface coatings are one of the promising remedies to eliminate pathogens from surfaces exposed to them from the most commonly touched surfaces used in the everyday life, such as mobile phones or from medical devices [88, 91]. TiO_2 is a widely used photocatalyst for antimicrobial coatings due to it is broad-spectrum bactericide property with self-sterilizing effect, and it could reduce the number of adhered microbes [52, 53]. TiO_2 has been doped with metals/non-metals or other chemical modifiers to extend the photocatalytic

activity of the semiconductor in the visible region and boost the photocatalytic process [52, 58–60].

Our interest led us to investigate the antibacterial potential of two photocatalytic nanocomposite films: TiO_2 and Ag-TiO_2 (with 0.001 wt% plasmonic Ag content) as new coatings on Ti implant surfaces. Basically, first, we studied the structural and photocatalytic properties of composite layers with various methods. Similarly to Mérai et al. we detected both the C and Ti component of the nanofilms on the surface of the composite layers using high-resolution elemental mapping (see **Figures 11 and 12**) [92]. The C component represented the polyacrylate binder providing mechanical stability for the composite films, whereas the Ti component contributed to the photocatalytic activity of the nanohybrid films.

The presence of visible light induced ROS was also verified and quantified by CL probe method developed by Hirakawa et al. [81]. During this method, a luminometric assay is applied to determine the concentration of ROS responsible for microbial inactivation. In this way, the active O_2 species measured could be expressed as the equivalent H_2O_2 concentration. In general, it is known that the TiO_2 photocatalytic reactions proceed mainly by the contributions of active O_2 species, such as $^{\cdot}OH$, O_2^- and H_2O_2 [93]. In the photocatalytic reactions, H_2O_2 would be formed in both processes of reduction and oxidation, that is, dimerization of $^{\cdot}OH$, disproportionation of O_2^- and reduction of O_2^-. Then, H_2O_2 might be taken into account to understand the details in TiO_2 photocatalysis. The lifetime of the free radicals can be measured in femto- or picoseconds [94]. However, the degradation of the formed H_2O_2 (which is produced from $^{\cdot}OH$) is slow at room temperature; it can be measured with a luminometer [95]. According to this phenomenon, the measured H_2O_2 concentration is proportionate to the various free radicals produced under illumination of the photocatalysts. The amount of $^{\cdot}OH$ that are produced by the photocatalysts was measured from the CL of luminol. As our results demonstrated in **Figure 13** at relatively low light intensities, a sufficient amount of ROS is formed on the irradiated photocatalyst surface.

The photocatalytic efficacy of the Ag-TiO_2 coating was also tested with a model-biomacromolecule (BSA). We experienced the effective photooxidation of the studied BSA protein, which phenomenon was attributed not only to the photoreactivity of Ag-TiO_2, but also increased surface adsorption of polymer chains on the NPs surface. Mariam et al. have published in their research about the interaction between NPs and biomacromolecules [96] and

mentioned that the AgNPs have a strong ability to quench the intrinsic fluorescence of BSA via the formation of a complex between BSA and AgNPs. Thus, AgNPs have a multifunctional role, they increase both the photocatalytic efficiency and the interaction between the macromolecules and NPs [96]. Thus, our physicochemical findings (**Figures 11**, **12**, and **13**) suggest that the new polymer based surfaces are suitable for photocatalytic application.

The antibacterial effect of nanohybrid coatings to eliminate clinically relevant pathogenic strains (methicillin resistant *Staphylococcus aureus* (MRSA), *Escherichia coli* or *Pseudomonas aeruginosa*) and oral *S. salivarius* has been previously observed [97, 82, 83]. Based on these results, we wished to study the antibacterial effect of nanohybrid coatings on biofilms formed by pioneer colonizing oral streptococci *in vitro*.

Although AgNPs are capable to destroy pathogenic bacteria, they may also affect the viability of human cells in a dose dependent manner [86, 98, 99]. For this reason, it is important to control the concentration of NPs to kill bacteria on the implant surfaces with minimal or no harmful effects to the living human tissue. Currently, the precise concentration of AgNPs that are antibacterial and biocompatible with osteoblast cell are poorly understood [86]. Therefore, we reduced the Ag content of the coatings to 0.001 wt%, which was a significant reduction compared the amount of 0.5 wt% used by Györgyey [97] and Tallósy et al. [82, 83]. In parallel with our experiments, other members of our research team, Masa et al. [100] have investigated the biocompatibility of Ag-TiO_2 coated surfaces with human epithelial cells and MG-63 osteosarcoma cells and observed that such coatings were well tolerated by human cells *in vitro*.

Furthermore, we applied short illumination time in the photocatalytic process, such as 5, 10, 15 min, which can be short enough to be applicable in dental practice. *S mitis*, a significant oral microbiome member was chosen for our investigations, since it has remarkable role in oral biofilm formation, providing the basis for the subsequent colonization of facultative and obligate anaerobic bacteria [22, 23].

In contrast with most of the studies in our field, we did not use the classic CFU counting method, instead, we used the MTT colorimetric assay and protein content assay and determined their sensitivity to detect the antibacterial effect. The quantification of CFU per mL or g of sample is the gold standard method for the enumeration of bacteria or fungi in microbiology. However, in our research, we could not use it because of the following reasons: for CFU counting, we must prepare serial dilutions of the sample, plate the diluted suspensions and count

the number of CFUs. Before all these steps, we have to harvest the adhered bacteria from the surfaces of treated discs using a rough mechanical force such as sonication, [101] which can also result in the removal of NPs that are included in the dilutions and can lead to false results. Therefore, the CFU method is a completely different method from the MTT assay. For this reason, MTT data cannot be converted to CFU data.

The MTT tetrazolium assay has been widely used as a high throughput screening method for the determination of mitochondrial enzymatic activity in cells, which does not only show the number of viable cells (used as proliferation assay), but it also indicates the degree of mitochondrial activity that reflects cellular stress or dying cells (used as cytotoxicity test). Viable cells with active metabolism convert MTT into a purple colored formazan product. Died cells lose the ability to convert MTT into formazan; thus, color formation serves as an exact and convenient marker only for the viable cells [84]. The MTT method was previously tested efficiently on epithelial cell culture and on *S. salivarius* by our research group [102, 97].

Haase et al. [103] have recalculated their MTT data to viability percentage with the use of a suitable control in their work [103]. However, we could not use this or similar experimental settings in our research, since the Ti implant itself has some antibacterial activity as well, consequently we could not attribute 100 % viability for it [104]. Moreover, the 24-well plastic plate surface is totally different from the Ti dental implant surface, so we also could not use it as a standard control for 100 % viability. For these reasons, similarly to Zhou et al. [105], we applied the MTT assay and plotted our MTT graphs based on the measured OD values in our first study.

According to our MTT results, the AgNP-coated Ti surface showed effective anti-adhesive potency against the pioneer colonizer *S. mitis* under dark conditions, and this property may even make it suitable for the prevention of peri-implantitis. These findigs have been confirmed by several researchers. For example, Zhao et al. [106] have reported in their article that the deposition of AgNPs on TiO_2 nanotube surfaces enhanced the anti-adhesive properties of the biomaterial, and besides this, they have provided satisfactory osteoconductivity [106]. In this context, it is worth highlighting the results of Masa et al. [100]. They have found that the attachment of epithelial cells on the NP-modified surfaces relatively high, but the proliferation is poor. In case of MG-63 cells, it seemed to be still sensitive to AgNPs, in spite of the reduced, 0.001 wt% AgNPs concentration, which could be explained by the presence of the NPs.

However, based on their results, it can be emphasized that the tested coatings are biocompatible and besides their antibacterial potential, they are also well tolerated by epithelial cells of human origin [100].

Based on our results, the number of metabolically active bacteria decreased on all Ti based surfaces under illumination for a different time, compared with their dark control, indicating the visible light-driven ROS generation. The standard sandblasted, acid etched Ti disc surfaces showed visible light induced antibacterial property, too; 15 min of illumination with visible light resulted in the most remarkable killing compared to Ti discs kept in the dark. In addition, we found that the metabolic activity of *S. mitis* on the Ag-TiO_2 nanohybrid film covered sample illuminated for 15 min was 40 % lower than its dark control. This time span of illumination is tolerable in the dental practice. In this context, it is worth mentioning that a previous study has reported considerable photodegradation of the cell wall components of *E. coli* and MRSA using Ag-TiO_2 photocatalyst particles [83]. According to these results, after 120 min irradiation, the bacterial cell wall was totally degraded, i.e., the formation of peptidoglycan cross links is totally prevented due to the presence of ROS, which are produced during the process of the visible light induced photocatalysis [83]. The observed fluctuation of OD values in **Figure 16** may be attributable the growth dynamics of mono-bacterial culture. Shany-Kdoshmin et al. have mentioned in their work that periodonto-pathogenic bacteria could show different light tolerance during exposure to blue light, which can support our observations [107].

Next, we compared the antibacterial effect of photocatalytically activated nanohybrid surfaces after illumination for various times with the standard Ti disc (without illumination). Both types of nanohybrid coatings showed significant antibacterial effect in cases of 10 and 15 min illuminations compared with the Ti disc. Furthermore, in our comparisons, the 15 min illuminated Ag-TiO_2 nanohybrid film had the most remarkable antibacterial effect, since it proved to be significantly better compared with the control Ti discs as well as surpassed the TiO_2 nanohybrid coating in its photocatalytic cell damaging antibacterial activity. These findings demonstrated that the addition of plasmonic properties of noble metal NPs (e.g., AgNPs) enhances the photocatalytic activity of TiO_2 under visible light. Therefore, we established that plasmonic photocatalysis may play a key role in eliminating the development of the bacterial biofilm.

We also investigated the effects of photocatalytic damage on the total bacterial cell protein content, measured by Micro BCA™ Protein assay kit. Besides the MTT method, protein measurement is also a previously used method by our research team [85]. We were interested in the investigation of how the protein assay measurements support our OD values measured with MTT assay, since the literature data about the comparison of these two methods are absent.

Therefore, we used a simplified, time-saving assay, which does not have any influence on cell viability and applicable in antibacterial studies [108, 109].

Our measured protein concentrations suggested that the illuminated Ag-TiO_2 nanohybrid surface had efficient bactericidal effect and inhibited bacterial attachment. The observed tendency of decreasing protein concentration in the case of photoreactive coatings is presumably attributed to the photooxidation of the organic macromolecules in spite of the short irradiation time (5–15 min), although our protein assay data could not support the statistically significant differences between the various surfaces demonstrated with the MTT assay. It was primarily due to the different sensitivities between these methods. The MTT assay measures only the metabolically active cells [84], while the protein-based assay represents all the proteins in the viable and non-viable cells [85, 110]. The MTT assay appeared to be more sensitive in detecting the antibacterial effect. Our data support the observation of Fotakis et al. that is, in case of bacterial biofilm studies the MTT assay is a more sensitive method compared with protein assay [111].

5.2 Antibacterial efficacy of oral antiseptics on *Streptococcus* spp.

We created an *in vitro* model to evaluate the antibacterial effect of three widely used antiseptics in dental practice. The peri-implant inflammation caused by pathogens can spread apically from the colonized neck part of the Ti implant towards the deeper bone tissue region. For this reason, we used two different surface roughnesses of dental implant (polished and sand blasted, acid etched) to model this complex process on the two test bacteria (*S. mitis* and *S. salivarius*) [112].

According to McDonnell et al. [113], CHX is one of the most well-known and widely used antiseptic agent in dentistry, but based on our results, it showed significant cell reduction only in case of *S. salivarius* after 5 min exposure time. CHX reduced 29 % of metabolically active cells, while the other two agents destroyed double amounts of proliferating *S. salivarius*.

Based on MTT data, PI and CD were the two most effective antiseptic agents against *S. mitis* and *S. salivarius.* Moreover, both agents were proved to be significantly better compared with CHX in the elimination of the *S. salivarius* biofilm developed for 48 h. Our results are in concordance with Herczegh et al. [114], who have established in their work that CD was more effective compared with CHX after 5 min treatment time.

Our model demonstrated that the PI was the most effective in the *in vitro* elimination of both bacterial biofilms. However, in case of *S. mitis*, we could not observe significant difference between PI and CD. In this context, it is worth mentioning our other *in vitro* studies, where we compared the antibacterial effect of PI, CHX, and citric acid against *P. gingivalis* [115]. Our results suggested that PI seemed to be superior in this comparison against anaerobic periodonthopatogenic bacteria [116], but not significantly [115]. Hosaka et al. [117] have reported that even 0.5 min application of PI was effective in the *in vitro* killing both of *P. gingivalis* and *Fusobacterium nucleatum*, and according to a clinical study, CD has also been effective in reducing plaque accumulation and the counts of *F. nucleatum* in the saliva [118].

However, choosing an ideal antiseptic for the therapy of peri-implantitis is influenced not only by the effectiveness, but also by the lack of side effects of the agent. CHX is the most widely used gold standard antiseptic for plaque control [70], but CHX has some adverse properties. It stains the teeth or it can cause oral mucosa desquamation as well as a burning sensation on the oral mucosa [119, 120]. However, the anti-discoloration system (ADS) presented in Curasept used in our experiment can reduce the risk of discoloration and eliminates the unpleasant taste-disturbance [121]. PI has also adverse effects including allergy or hypersensitivity to the solution, and it can cause a reversible yellowish discoloration as well, although the short durations of using PI in low concentration could decrease these effects [122, 123]. In our experiment, we used a short, 5 min exposure time; furthermore, Kanagalingam et al. have reported in their review that there have been no clinical reports on the development of microbial resistance after PI treatment, while in contrast, bacterial resistance to CHX has been observed [124]. Based on our MTT assay data, we determined that PI could be a promising oral antiseptic in the prevention of peri-implantitis.

According to other researchers [125], CD can react with four amino acids (cysteine, methionine, tyrosine, and tryptophan), which have a vital role in the living organisms, and microbes can not develop resistance against CD. Furthermore, it can cause no real harm to

humans as it is not able to penetrate the deep tissues [125]. CD is effective in relatively low concentrations, and the new membrane technology developed by Noszticziusz et al. [125] allows the production of high purity CD solution without any by-products. These properties could make it an ideal antiseptic besides PI in dental practice to treat inflammation caused by microoganisms.

5.3 Future possibilities of antibacterial strategies in infection control

The visible light induced antibacterial property of Ag-TiO_2 may open a new potential for the treatment of peri-implant infections, which is more efficient than the currently used medical alternatives. For instance, if primary peri-implantitis develops, the complete elimination of bacteria from the implant surface might be achieved by the visible light illumination of the Ag-TiO_2 surface with a dental curing lamp. The photocatalytically-induced release of ROS from the implant surface may be more effective in bacterial killing than surgical decontamination because it does not damage the surface. The main therapeutic goal in the treatment of implant related infections is the complete removal of bacteria from the surgical site, including the implant surface and the surrounding tissues. The surrounding tissues can be decontaminated by surgical debridement, but actually, it is a challenge to free the implant surface from bacterial attachment. The currently applied surgical decontamination of the implant surfaces does not guarantee the complete elimination of bacteria, and it can also have a negative impact on the osseointegration process. The tested Ag-TiO_2 surface may offer an alternative solution for this problem. Moreover, the visible light induced antibacterial property of the Ag-TiO_2 supplemented with PI or CD rinsing could control the infection at the surgical site and can open a totally new direction in dental practice. However, this assumption is currently theoretical, but it is worth investigating this assumption in the future.

Nevertheless, in consideration of the pandemic in 2020 caused by severe acute respiratory syndrome coronavirus 2 (SARS-CoV-2), humanity has received a warning sign that more attention needs to be paid to control the new emerging infectious diseases. Due to the current SARS-CoV-2 crisis, the development of antimicrobial coatings and the application of antimicrobial disinfectant agents have quickly become hot topics [88].

Other researchers have investigated these photoreactive composite films with regard to their virucidal effect using pseudorabies virus as a model virus. Their results demonstrated that illuminated photoreactive nanocomposite surfaces showed a significant antiviral effect [126].

Recent studies have also investigated all of the three decontamination agents tested by our group, highlighting their significant efficacy in killing the new type of coronavirus [127–130]. Based on the observations until now, the antibacterial strategies outlined in the present thesis are promising, and they may be applicable in other areas as well, including other microbial species (viruses or fungal spp.) or more complex microbial communities to control existing or emerging infections in the future.

6. SUMMARY AND CONCLUSIONS

Due to the cooperation of industry with medicine, Ti and its alloys are widely used for oral implantation, and the demand for implant therapy is constantly expanding with the increasing of human life expectancy. Nonetheless, once exposed to the external environment, Ti implants are also set out to microbial adhesion and biofilm formation, which finally can trigger local inflammation in the surrounding tissues. Since dental implant placement is becoming more and more popular for people who are in need of tooth replacement or restoration, the incidence of inflammation is also frequent. Furthermore, antibiotics are often used in the treatment of peri-implantitis, which further aggravates the situation with the emergence of new resistant strains.

Therefore, novel surface modifications such as using antimicrobial coatings on Ti implant and effective disinfection strategies are necessary for the prevention and treatment of inflammation caused by microorganisms around implantable medical devices.

The aim of the present doctoral work was to develop antimicrobial strategies using Ti dental implants for the effective prevention of peri-implantitis using *Streptococcus* species *in vitro* models.

We investigated the direct interaction between the photoreactive composite coating material and the abundant pioneer colonizer in the oral cavity, *S. mitis*, and we also determined the effective illumination time that was short enough to be used in everyday dental practice. Furthermore, we monitored the antibacterial activity of nanohybrid coatings at the physiologically acceptable 0.001 wt% Ag content level for the human patients by two different methods.

The main conclusions of this study are:

- The new polymer based surfaces showed favorable surface properties and good *in vitro* photocatalytic activity due to their physicochemical properties; thus, the nanocomposite materials proved their suitability for the photocatalysis induced bacterial elimination.

- The results of our *in vitro* experiments suggested that the Ag-TiO_2 (with reduced Ag content) containing surface had a remarkable anti-adhesive potential under dark conditions.
- Ag-TiO_2 showed antibacterial property against *S. mitis* cells after 15 min of visible light illumination, due to the photocatalytic mechanism.

Furthermore, we compared the antimicrobial effects of three antiseptics (CHX, PI, and CD) on *S. mitis* and *S. salivarius* in mono-species biofilm models adhering to Ti surfaces using MTT colorimetric assay.

The following conclusions can be drawn from this experiment:

- Our data indicated that PI and CD had remarkable eliminating property against both streptococci in the biofilm after 5 min of treatment time on the Ti surfaces. Compared to CHX, PI and CD proved to be more effective against the biofilms of pioneer colonizers.

7. ACKNOWLEDGEMENTS

I would like to express my deep sense of gratitude to my supervisors, **Dr. Anette Stájer** and **Dr. Krisztina Ungvári**, who supported and encouraged me during my scientific years. I am thankful for their scientific guidance, motivation, advice, and patience.

Besides my supervisors, I also want to express my warm gratitude to **Prof. Emer. Dr. Elisabeth Nagy** for the help, advice, and her constructive comments and encouragement, which contributed significantly to the present form of PhD thesis.

I am grateful to our head of department, **Prof. Dr. Katalin Burián** for her continuous support and trust during my scientific work.

I would like to thank **Prof. Dr. Edit Urbán** and **Dr. Kinga Turzó** who established our scientific work, by introducing me into the beauties of studying the relationship between biomaterials and living organisms.

I would like to thank **Prof. Dr. János Minárovits** for his professional help in proofreading my thesis.

I would like to thank our collaborating partners **Prof. Emer. Dr. Imre Dékány**, **Dr. László Janovák** and **Dr. Ágota Imre-Deák,** who provided us the polymer suspensions.

I am also grateful to my earlier colleagues, **Prof. Emer. Dr. Kornél L. Kovács**, **Dr. Zsolt Tóth**, **Dr. Anett Nagy-Demcsák**, **Dr. Roland Masa**, **Dr. Henrietta Guti Pelsőczi-Kovácsné**, **Zsófia Papp,** and **Mária Horváth** for their help and encouragement during my PhD years.

I also would like to thank to **Zsuzsanna Kiss-Dózsai** for her technical support in the preparation of the illustrations in my work.

I am grateful to tha **Denti System®** (Hungary) for supplying thee titanium discs for the experiments.

I am also grateful to my **current colleagues** at Department of Medical Microbiology, Albert Szent-Györgyi Medical School for their patience while I was writing my PhD thesis.

Finally, I would like to express my warmest gratitude to my **husband** and my **family** for their support, encouragement, and patience, which got me through the most difficult periods of my scientific years and helped me to reach my goals.

8. FINANCIAL SUPPORT

The present work was supported by the following grants:

- GINOP-2.3.2-15-2016-00011- Molecular research of oral diseases, Hungary.
- UNKP-20-5 New National Excellence Program of the Ministry for Innovation of Technology.
- János Bolyai Research Scholarship of the Hungarian Academy of Sciences.
- GINOP-2.3.2-15-2016-00013 by the Hungarian Government and the European Union.
- 20391-3/2018/FEKUSTRAT grant of the Hungarian Ministry of Human Capacities.

9. REFERENCES

1. Chen FM, Liu X: Advancing biomaterials of human origin for tissue engineering. *Prog. Polym. Sci.* **2016**; 53:86-168.
2. Dong H, Zhou N, Liu H, Huang H, Yang G, Chen L, Ding M, Mou Y: Satisfaction analysis of patients with single implant treatments based on a questionnaire survey. *Patient Prefer. Adherence.* **2019**; 13:695–704.
3. Del Fabbro M, Testori T, Kekovic V, Goker F, Tumedei M, Wang HL: A systematic review of survival rates of osseointegrated implants in fully and partially edentulous patients following immediate loading. *J. Clin. Med*. **2019**; 8:2142.
4. An Do T, Son Le H, Shen YW, Huang HL, Fuh LJ: Risk factors related to late failure of dental implant—A systematic review of recent studies. *Int. J. Environ. Res. Public Health*. **2020**; 17:3931.
5. Rosenberg ES, Torosian JP, Slots J: Microbial differences in 2 clinically distinct types of failures of osseointegrated implants. *Clin. Oral Implants Res*. **1991**; 2:135.
6. Schou S, Holmstrup P, Hjorting-Hansen E, Lang NP: Plaque-induced marginal tissue reactions of osseointegrated oral implants: a review of the literature. *Clin. Oral Implants Res*. **1992**; 3:149.
7. Nguyen-Hieu T, Borghetti A, Aboudharam G: Peri-implantitis: From diagnosis to therapeutics. *J. Investig. Clin. Dent*. **2012**; 3:79–94.
8. Renvert S, Roos-Jansaker AM, Claffey N: Non-surgical treatment of peri-implant mucositis and peri-implantitis: a literature review. *J. Clin. Periodontol*. **2008**; *35*:305-315.
9. Norowski PA Jr, Bumgardner JD: Review. Biomaterial and antibiotic strategies for peri-implantitis. *J. Biomed. Mater. Res. Part B: Appl. Biomater.* **2009**; 88:530–543.
10. Zitzmann NU, Berglundh T: Definition and prevalence of periimplant diseases. *J. Clin Periodontol.* **2008**; 35:286–291.
11. Derks J, Tomasi C: Peri-implant health and disease. A systematic review of current epidemiology. *J. Clin. Periodontol.* **2015**; 42:158.
12. Asensio G, Vazquez-Lasa B, Rojo L: Achievements in the topographic design of commercial titanium dental implants: towards anti-peri-implantitis surfaces. *J. Clin. Med*. **2019**; 8:1982.

13. Donati M, Ekestubbe A, Lindhe J, Wennstrom JL: Implant-supported single-tooth restorations. A 12-year prospective study. *Clin. Oral Implants Res.* **2016**; 27:1207–1211.
14. Stoodley P, Hall-Stoodley L: Evolving concepts in biofilm infections. *Cell. Microbiol*. **2009**; 11:1034–1043.
15. Donlan RM, Costerton JW: Biofilms: survival mechanisms of clinically relevant microorganisms. *Clin. Microbiol. Rev*. **2002**; 15:167–193.
16. Long M, Rack HJ: Titanium alloys in total joint replacement- a materials science perspective. *Biomat*. **1998**; 19:1621-1639.
17. Dong H, Liu H, Zhou N, Li Q, Yang G, Chen L, Mou Y: Surface modified techniques and emerging functional coating of dental implants. *Coatings*. **2020**; 10:1012.
18. Derks J, Schaller D, Håkansson J, Wennström JL, Tomasi C, Berglundh T: Effectiveness of implant therapy analyzed in a swedish population: prevalence of peri-implantitis. *J. Dent. Res*. **2016**; 95:43-49.
19. Prathapachandran J, Suresh N: Management of peri-implantitis. *Dent. Res. J*. **2012**; 9:516-521.
20. Wade WG: The oral microbiome in health and disease. *Pharmacol. Res.* **2013**; 69:37-143.
21. Marsh PD, Do T, Beighton D, Devine DA: Influence of saliva on the oral microbiota. *Periodontol. 2000.* **2016**; 70: 80– 92.
22. Segata N, Haake SK, Mannon P, Lemon KP, Waldron L, Gevers D et al.: Composition of the adult digestive tract bacterial microbiome based on seven mouth surfaces, tonsils, throat and stool samples. *Genome Biol*. **2012**; 13:42.
23. Benitez-Páez A, Belda-Ferre P, Simón-Soro A, Mira A: Microbiota diversity and gene expression dynamics in human oral biofilms. *BMC Genom*. **2014**; 15:311-323.
24. Haffajee AD, Socransky SS, Patel MR, Song X: Microbial complexes in supragingival plaque. *Oral Microbiol. Immun.* **2008**; 23:196-205.
25. Grant M, Kilsgård O, Åkerman S, Klinge B, Demmer RT, Malmström J, Jönsson D: The human salivary antimicrobial peptride profile according to the oral microbiota in health, periodontitis and smoking. *J. Innate. Immun.* **2019**; 11:432-443.
26. Socransky SS, Haffajee AD, Cugini MA, Smith C, Kent RL Jr: Microbial complexes in subgingival plaque. *J. Clin. Periodontol.* **1998**; 25:134-144.

27. Do T, Devine DA, Marsh PD: Oral biofilms: molecular analysis, challenges, and future prospects in dental diagnostics. *Clin. Cosmet. Investig. Dent.* **2013**; 5:11-9.
28. Wright CJ, Burns LH, Jack AA, Back CR, Dutton LC, Nobbs AH et al.: Microbial interactions in building of communities. *Mol. Oral Microbiol*. **2013**; 28:83-101.
29. Xu H, Jenkinson HF, Dongari Bagtzoglou A: Innocent until proven guilty: mechanisms and roles of *Streptococcus- Candida* interactions in oral health and disease. *Mol. Oral Microbiol*. **2014**; 29: 99-116.
30. Hojo K, Nagaoka S, Ohshima T, Maeda N: Bacterial interactions in dental biofilm development. *J. Dent. Res*. **2009**; 88:982-990.
31. Rickard AH, Palmer RJ Jr, Blehert DS, Campagna SR, Semmelhack MF, Egland PG et al.: Autoinducer 2: a concentration-dependent signal for mutualistic bacterial biofilm growth. *Mol. Microbiol.* **2006**; 60:1446-1456.
32. Stacy A, Everett J, Jorth P, Trivedi U, Rumbaugh KP, Whiteley M: Bacterial fight-and-flight responses enhance virulence in a polymicrobial infection. *Proc. Natl. Acad. Sci. USA.* **2014**; 111:7819-24.
33. Merritt J, Qi F: The mutacins of *Streptococcus mutans*: regulation and ecology. *Mol. Oral Microbiol*. **2012**; 27:57-69.
34. Jakubovics NS, Yassin SA, Rickard AH: Community interactions of oral streptococci. *Adv. Appl. Microbiol*. **2014**; 87:43-110.
35. Marsh PD, Head DA, Devine DA: Ecological approaches to oral biofilms: control without killing. *Caries Res*. **2015**; 49:46-54.
36. Rams TE, Degener JE, van Winkelhoff AJ: Prevalence of β-lactamase-producing bacteria in human periodontitis. *J. Periodontal Res*. **2013**; 48:493-9.
37. Ereshefsky M, Pedroso M: Rethinking evolutionary individuality. *Proc. Natl. Acad. Sci. USA.* **2015**; 112:10126-32.
38. Kreve S, Dos Reis AC: Bacterial adhesion to biomaterials: What regulates this attachment? A review. *Jpn. Dent. Sci. Rev*. **2021**; 57: 85-96.
39. Persson GR, Renvert S: Cluster of bacteria associated with peri-implantitis. *Clin. Implant Dent. Relat. Res*. **2014**; 16:783-93.
40. Meffert RM, Langer B, Fritz ME: Dental implants: a review. *J. Periodontol.* **1992**; 63:859-870.

41. Kaur M, Singh K: Review on titanium and titanium based alloys as biomaterials for orthopaedic applications. *Mater. Sci. Eng. C.* **2019**; 102:844-862.
42. Lei ZM, Zhang HZ, Zhang EL, You JH, Ma XX, Bai XZ: Antibacterial activities and biocompatibilities of Ti-Ag alloys prepared by spark plasma sintering and acid etching. *Mater. Sci. Eng. C.* **2018**; 92:121-131.
43. Liu X, Chu PK, Ding C: Surface modification of titanium and titanium alloys, and related materials for biomedical applications. *Mater. Sci. Eng. R. Rep.* **2004**; 47:49-121.
44. Brånemark PI: Osseointegration and its experimental background. *J. Prosthet. Dent.* **1983**; 50:399-410.
45. Jemat A, Ghazali MJ, Razali M, Otsuka Y: Surface modifications and their effects on titanium dental implants. *Biomed. Res. Int.* **2015**; Article ID:791725.
46. Goyal N, Priyanka R: Effect of various implant surface treatments on osseointegration—a literature review. *Indian J. Dent. Sci.* **2012**; 4:154–157.
47. Parsikia F, Amini P, Asgari S: Influence of mechanical and chemical surface treatments on the formation of bone-like structure in CPTi for endosseous dental implants. *Appl. Surf. Sci.* **2012**; 259:283–287.
48. Turzo K: Surface aspects of titanium dental implants, biotechnology - molecular studies and novel applications for improved quality of human life. Reda Helmy Sammour, IntechOpen. **2012**.
49. Gristina AG: Biomaterial- centered infection: microbial adhesion versus tissue integration. *Science*. **1987**; 237: 1588-95.
50. Chouirfa H, Bouloussa H, Migonney V, Falentin-Daudré C: Review of titanium surface modification techniques and coatings for antibacterial applications. *Acta Biomater.* **2019**; 83: 37-54.
51. Visai L, De Nardo L, Punta C, Melone L, Cigada A, Imbriani M, Arciola CR: Titanium oxide antibacterial surfaces in biomedical devices. *Int. J. Artif. Organs.* **2011**; 34:929–946.
52. Regmi C, Joshi B, Ray SK, Gyawali G and Pandey RP: Understanding mechanism of photocatalytic microbial decontamination of environmental wastewater. *Front. Chem*. **2018**; 6:33.
53. Fujishima A, Honda K: Electrochemical photolysis of water at a semiconductor electrode. *Nature*. **1972**; 238:37–38.

54. Lin J, Chen H, Fei T, Zhang J: Highly transparent superhydrophobic organic-inorganic nanocoating from the aggregation of silica nanoparticles. *Colloids Surf. A Physicochem. Eng. Asp.* **2013***;* 421:51–62.
55. Ranjbar Z, Rastegar S: Nano mechanical properties of an automotive clear-coats containing nano silica particles with different surface chemistries. *Prog. Org. Coatings.* **2011***;* 72:40–43.
56. Ahmed KBA, Raman T, Veerappan A: Future prospects of antibacterial metal nanoparticles as enzyme inhibitor. *Mater. Sci. Eng. C Mater. Biol. Appl.* **2016**; 68:939-947.
57. Guo Z, Chen Y, Wang Y, Jiang H, Wang X: Advances and challenges in metallic nanomaterial synthesis and antibacterial applications. *J. Mater. Chem. B.* **2020**; 8:4764-4777.
58. Veres Á, Rica T, Janovák L, Dömök M, Buzás N, Zöllmer V et al.: Silver and gold modified plasmonic TiO_2 hybrid films for photocatalytic decomposition of ethanol under visible light. *Catal. Today*. **2012**; 181:156-162.
59. Veres Á, Janovák L, Bujdosó T, Rica T, Fodor E, Tallósy SP et al.: Silver and phosphate functionalized reactive TiO_2/polymer composite films for destructions of resistent bacteria using visible light. *J. Adv. Oxid. Technol*. **2012**; 15:205.
60. Veres Á, Ménesi J, Juhász Á, Berkesi O, Ábrahám N, Bohus G et al.: Photocatalytic performance of silver-modified TiO_2 embedded in poly (ethyl-acrylate-co-methyl metacrylate) matrix. *Colloid Polym. Sci*. **2014**; 292:207-217.
61. Yang Z, Gu H, Sha G, Lu W, Yu W, Zhang W et al.: TC4/Ag metal matrix nanocomposites modified by friction stir processing: surface characterization, antibacterial property, and cytotoxicity *in vitro*. *ACS Appl. Mater. Interfaces.* **2018***;* 10: 41155–41166.
62. Sanjivkumar M, Vaishnavi R, Neelakannan M, Kannan D, Silambarasan T, Immanuel G: Investigation on characterization and biomedical properties of silver nanoparticles synthesized by an actinobacterium Streptomyces olivaceus. *Biocatal. Agric. Biotechnol*. **2019**; 17:151-159.
63. Campoccia A, Montanaro L, Arciola CR: A review of the biomaterials technologies for infection resistant surfaces. *Biomaterials.* **2013**; 34: 8533-8554.

64. MubarakAli D, Thajuddin N, Jeganathan K, Gunasekaran M: Plant extract mediated synthesis of silver and gold nanoparticles and its antibacterial activity against clinically isolated pathogens. *Colloids Surf. B: Biointerfaces.* **2011**; 85:360-365.
65. Caccianiga G, Rey G, Caccianiga P, Leonida A, Baldoni M, Baldoni A et al.: Peri-implantitis management: surgical versus non-surgical approach using photodynamic therapy combined with hydrogen peroxide (OHLLT—Oxygen High Level Laser Therapy): A retrospective controlled study. *Appl. Sci.* **2021**; 11:5073.
66. Roos-Jansaker AM, Renvert S, Egelberg J: Treatment of periimplant infections: A literature review. *J. Clin. Periodontol*. **2003**; 30:467–485.
67. Schwarz F, Bieling K, Bonsmann M: Nonsurgical treatment of moderate and advanced periimplantitis lesions: A controlled clinical study. *Clin. Oral. Invest*. **2006**; 10:279–288.
68. Khoury F, Buchmann R: Surgical therapy of peri-implant disease: A 3-year follow-up study of cases treated with 3 different techniques of bone regeneration. *J. Periodontol*. **2001**; 72:1498–1508.
69. Machtei EE: Treatment alternatives to negotiate peri-implantitis. *Advances Med.* **2014**; 2014:13.
70. Kolliyavar B, Shettar L, Thakur S: Chlorhexidine: the gold standard mouth wash. *J. Pharm. Biomed. Sci*. **2016**; 6:106–109.
71. Southard SR, Drisko CL, Killoy WJ, Cobb CM, Tira DE: The effect of 2% chlorhexidine digluconate irrigation on clinical parameters and the level of *Bacteroides gingivalis* in periodontal pockets. *J. Periodontol.* **1989**; 60:302-309.
72. Löe H, Schiott CR: The effect of mouthrinses and topical application of chlorhexidine on the development of dental plaque and gingivitis in man. *J. Periodontal Res.* **1970**; 5:79-83.
73. Noiri Y, Okami Y, Narimatsu M, Takahashi Y, Kawahara T, Ebisu S: Effects of chlorhexidine, minocycline, and metronidazole on *Porphyromonas gingivalis* strain 381 in biofilms. *J. Periodontol.* **2003**; 74:1647-1651.
74. Meneghin SP, Reis FC, de Almeida PG, Ceccato-Antonini SR: Chlorine dioxide against bacteria and yeasts from the alcoholic fermentation. *Braz. J. Microbiol*. **2008**; 39:337-43.
75. Young RO: Chlorine dioxide (CLO_2) as a non-toxic antimicrobial agent for virus, bacteria and yeast (*Candida albicans*). *Int. J. Vaccines Vaccin*. **2016**; 2(6):00052.

76. Noszticzius Z, Wittmann M, Kály-Kullai K, Beregvári Z, Kiss I, Rosivall L et al.: Chlorine dioxide is a size-selective antimicrobial agent. *PLoS One.* **2013**; 8 (11): e79157.
77. Eggers M: Infectious disease management and control with povidone iodine. *Infect. Dis. Ther*. **2019**; 8:581–593.
78. Durani P, Leaper D: Povidone-iodine: use in hand disinfection, skin preparation and antiseptic irrigation. *Int. Wound J*. **2008**; 5:376–387.
79. Park JB, Kim YK: Metallic biomaterials, 2nd ed. In: Bronzino JD, editor. The Biomedical Engineering Handbook. Boca Raton: CRC Press and IEEE Press, Second Edition; Vol. 1, **2000**; p. 37-5–37-11.
80. Sikirić MD, Gergely C, Elkaim R, Wachtel E, Cuisinier FJ, Füredi-Milhofer H: Biomimetic organic-inorganic nanocomposite coatings for titanium implants. *J. Biomed. Mater. Res. A.* **2009**; 89:759-771.
81. Hirakawa, T, Nosaka, Y: Properties of $O_2^{\bullet-}$ and $OH^{\bullet}$ formed in TiO_2 aqueous suspensions by photocatalytic reaction and the influence of H_2O_2 and some ions. *Langmuir*. **2002**; 18:3247–3254.
82. Tallósy SP, Janovák L, Ménesi J, Nagy E, Juhász Á, Balázs L et al.: Investigation of the antibacterial effects of silver modified TiO_2 and ZnO plasmonic photocatalysts embedded in polymer thin films. *Environ. Sci. Pollut. R.* **2014**; 19:11155–11167.
83. Tallósy SP, Janovák L, Nagy E, Deák Á, Juhász Á, Csapó E et al.: Adhesion and inactivation of Gram-negative and Gram-positive bacteria on photoreactive TiO_2/polymer and Ag–TiO_2/polymer nanohybrid films. *Appl. Surf. Sci*. **2016**; 371:139-150.
84. Mosmann, T: Rapid colorimetric assay for cellular growth and survival: Application to proliferation and cytotoxicity assays. *J. Immunol. Methods*. **1983**; 65:55–63.
85. Stájer A, Urbán E, Pelsőczi-Kovács I, Mihalik E, Rakonczay Z, Nagy K et al.: Effect of caries preventive products on the growth of bacterial biofilm on titanium surface. *Acta Microbiol. Immunol. Hung*. **2012**; 59:51–61.
86. Salaie RN, Besinis A, Le H, Tredwin C, Handy RD: The biocompatibility of silver and nanohydroxyapatite coatings on titanium dental implants with human primary osteoblast cells. *Mater. Sci. Eng. C Mater. Biol. Appl*. **2020**; 107:110210.

87. Choi SH, Jang YS, Jang JH, Bae TS, Lee SJ, Lee MH: Enhanced antibacterial activity of titanium by surface modification with polydopamine and silver for dental implant application. *J. Appl. Biomater. Funct. Mater*. **2019**; 17:2280800019847067.
88. Kumaravel V, Nair KM, Mathew S, Bartlett J, Kennedy JE, Manning HG et al.: Antimicrobial TiO_2 nanocomposite coatings for surfaces, dental and orthopaedic implants. *Chem. Eng. J*. **2021**; 416:129071.
89. Humphreys G, Fleck F: United Nations meeting on antimicrobial resistance, World Health Organization. Bulletin of the World Health Organization 94 **2016**; 638.
90. Khalil D, Hultin M: Peri-implantitis microbiota, an update of dental implantology and biomaterial. Mazen Ahmad Almasri, IntechOpen. **2018**.
91. Qadir M, Lin J, Biesiekierski A, Li Y, Wen C: Effect of anodized TiO_2–Nb_2O_5–ZrO_2 nanotubes with different nanoscale dimensions on the biocompatibility of a $Ti_{35}Zr_{28}Nb$ Alloy, *ACS Appl. Mater*. *Interfaces.* **2020**; 12:6776-6787.
92. Mérai L, Varga N, Deák Á, Sebők D, Szenti I, Kukovecz Á et al.: Preparation of photocatalytic thin films with composition dependent wetting properties and self-healing ability. *Catal. Today*. **2019**; 328:85–90.
93. Xu YX, Riedl H, Holec D, Chen L, Du Y, Mayrhofer PH: Thermal stability and oxidation resistance of sputtered Ti\\Al\\Cr\\N hard coatings. *Surf. Coat Technol*. **2017**; 324:48–56.
94. Sawada T, Yoshino F, Kimoto K, Takahashi Y, Shibata T, Hamada N et al.: ESR detection of ROS generated by TiO_2 coated with fluoridated apatite. *J. Dent. Res*. **2010**; 8:848–853.
95. Perez-Benito JF: Iron (III)-hydrogen peroxide reaction: Kinetic evidence of a hydroxyl-mediated chain mechanism. *J. Phys. Chem. A*. **2004**; 108:4853–4858.
96. Mariam J, Dongre PM, Kothari DC: Study of interaction of silver nanoparticles with bovine serum albumin using fluorescence spectroscopy. *J. Fluoresc*. **2011**; 21:2193-2199.
97. Györgyey Á, Janovák L, Ádám A, Kopniczky J, Tóth LK, Deák Á et al.: Investigation of the *in vitro* photocatalytic antibacterial activity of nanocrystalline TiO_2 and coupled TiO_2/Ag containing copolymer on the surface of medical grade titanium. *J. Biomater. Appl.* **2016**; 31:55–67.
98. Ewald A, Glückermann SK, Thull R, Gbureck U: Antimicrobial titanium/silver PVD coating on titanium. *Biomed. Eng. Online.* **2006**; 5:22.

99. Gunputh UF, Le H, Lawton K, Besinis A, Tredwin C, Handy RD: Antibacterial properties of silver nanoparticles grown *in situ* and anchored to titanium dioxide nanotubes on titanium implant against *Staphylococcus aureus*. *Nanotoxicology*. **2020**; 14:97-100.
100. Masa R, Deák Á, Braunitzer G, Tóth Z, Kopniczky J, Pelsőczi IK et al.: TiO_2/Ag-TiO_2 nanohybrid films are cytocompatible with primary epithelial cells of human origin: an *in vitro* study. *J. Nanosci. Nanotechnol.* **2018**; 18:3916-3924.
101. Schmidlin PR, Müller P, Attin T, Wieland M, Hofer D, Guggenheim B: Polyspecies biofilm formation on implant surfaces with different surface characteristics. *J. Appl. Oral Sci.* **2013**; 21:48–55.
102. Ungvári K, Pelsőczi- Kovács I, Kormos B, Oszkó A, Rakonczay Z, Kemény L et al.: Effects on titanium implant surfaces of chemical agents used for the treatment of peri-implantitis. *J. Biomed. Mater. Res. B Appl. Biomater.* **2010**; 94:222–229.
103. Haase H, Jordan L, Keitel L, Keil C, Mahltig B: Comparison of methods for determining the effectiveness of antibacterial functionalized textiles. *Mater. Sci. Eng. C.* **2017**; 61:965–978.
104. Ferraris S, Spriano S: Antibacterial titanium surfaces for medical implants. *Mater. Sci. Eng. C.* **2016**; 61:965–978.
105. Zhou Y, Wang S, Zhou X, Zou Y, Li M, Peng X et al.: Short-time antibacterial effects of dimethylaminododecyl methacrylate on oral multispecies biofilm *in vitro*. *BioMed Res. Int.* **2019**; 1-10.
106. Zhao L, Chu PK, Zhang Y, Wu Z: Antibacterial coatings on titanium implants. *J. Biomed. Mater. Res. B: Appl. Biomater.* **2009**; 91:470-480.
107. Shany-Kdoshim S, Polak D, Houri-Haddad Y, Feuerstein O: Killing mechanism of bacteria within multi-species biofilm by blue light. *J. Oral Microbiol.* **2019**; 11:1628577.
108. Yuan Z, Ouyang P, Gu K, Rehman T, Zhang T, Yin Z et al.: The antibacterial mechanism of oridonin against methicillin-resistant *Staphylococcus aureus* (MRSA). *Pharm. Biol.* **2019**; 57:710–716.
109. Itohiya H, Matsushima Y, Shirakawa S, Kajiyama S, Yashima A, Nagano T et al.: Organic resolution function and effects of platinum nanoparticles on bacteria and organic matter. *PLoS One*. **2019**; 14(9).

110. Eiampongpaiboon T, Chung WO, Bryers JD, Chung KH, Chan, DCN: Antibacterial activity of gold-titanates on Gram-positive cariogenic bacteria. *Acta Biomater. Odontol. Scand*. **2015**; 1:51–58.
111. Fotakis G, Timbrell JA: *In vitro* cytotoxicity assays: Comparison of LDH, neutral red, MTT and protein assay in hepatoma cell lines following exposure to cadmium chloride. *Toxicol. Lett.* **2006**; 160:171–177.
112. Dhir S: Biofilm and dental implant: the microbial link. *J. Indian Soc. Periodontol.* **2013**; 17:5–11.
113. McDonnell G, Russell AD: Antiseptics and disinfectants: activity, action, and resistance. *Clin. Microbiol. Rev.* **1999**; 12:147–79.
114. Herczegh A, Gyurkovics M, Agababyan H, Ghidán Á, Lohinai Z: Comparing the efficacy of hyper-pure chlorine-dioxide with other oral antiseptics on oral pathogen microorganisms and biofilm *in vitro*. *Acta Microbiol. Immunol. Hung.* **2013**; 60:359–373.
115. Barrak I, Baráth Z, Tián T, Venkei A, Gajdács M, Urbán E et al.: Effects of different decontaminating solutions used for the treatment of peri-implantitis on the growth of *Porphyromonas gingivalis*-an *in vitro* study. *Acta Microbiol. Immunol. Hung*. **2020**.
116. Rafiei M, Kiani F, Sayehmiri K, Sayehmiri F, Tavirani M, Dousti M et al.: Prevalence of anaerobic bacteria (*P. gingivalis*) as major microbial agent in the incidence periodontal diseases by meta-analysis. *J. Dent (Shiraz)*. **2018**; 19:232-242.
117. Hosaka Y, Saito A, Maeda R, Fukaya C, Morikawa S, Makino A et al.: Antibacterial activity of povidone-iodine against an artificial biofilm of *Porphyromonas gingivalis* and *Fusobacterium nucleatum*. *Arch. Oral Biol.* **2012**; 57:364–368.
118. Shinada K, Ueno M, Konishi C, Takehara S, Yokoyama S, Zaitsu T et al.: Effects of a mouthwash with chlorine dioxide on oral malodor and salivary bacteria: a randomized placebo-controlled 7-day trial. *Trials.* **2010**; 11:14.
119. Addy M, Moran J, Griffiths AA, Wills-Wood NJ: Extrinsic tooth discoloration by metals and chlorhexidine. I. Surface protein denaturation or dietary precipitation? *Br. Dent. J.* **1985**; 159:281–285.
120. Kenrad B: Toxin effects from chlorhexidine gluconate: case report. *Tandlaegebladet*. **1990**; 94:489–491.

121. Marrelli M, Amantea M, Tatullo M: A comparative, randomized, controlled study on clinical efficacy and dental staining reduction of a mouthwash containing chlorhexidine 0.20% and Anti Discoloration System (ADS). *Ann. Stomatol. (Roma).* **2015**; 6:35–42.
122. Rath T, Meissl G: Induction of hyperthyroidism in burn patients treated topically with povidone-iodine. *Burns Incl. Therm. Inj*.**1988**; 14:320–322.
123. Chua J, Dominguez E, Mae C, Sison CMC, Berba R: The efficacy of povidone-iodine oral rinse in preventing ventilator- associated pneumonia: a randomized, double blind, placebo controlled (VAPOR) trial: preliminary report. *Phil. J. Microbiol. Infect. Dis.* **2004**; 33:153–161.
124. Kanagalingam J, Feliciano R, Hah JH, Labib H, Le TA, Lin JC: Practical use of povidone-iodine antiseptic in the maintenance of oral health and in the prevention and treatment of common oropharyngeal infections. *Int. J. Clin. Pract.* **2015**; 69:1247–56.
125. Noszticzius Z, Wittmann M, Kaly-Kullai K, Beregvari Z, Kiss I, Rosivall L et al.: Chlorine dioxide is a size-selective antimicrobial agent. *PLoS One.* **2013**; 8: e79157.
126. Boldogkői Z, Csabai Z, Tombácz D, Janovák L, Balassa L, Deák Á et al.: Visible light-generated antiviral effect on plasmonic Ag-TiO_2-based reactive nanocomposite thin film. *Front. Bioeng. Biotechnol*. **2021**; 9:709462.
127. Frank S, Capriotti J, Brown SM, Tessema B: Povidone-iodine use in sinonasal and oral cavities: a review of safety in the COVID-19 era. *Ear, Nose, Throat J.* **2020**; 99:586-593.
128. Ogata N, Miura T: Inhibition of the binding of spike protein of SARS-CoV-2 coronavirus to human angiotensin-converting enzyme 2 by chlorine dioxide. *Ann. Pharmacol. Pharm.* **2020**; 5:1195.
129. Huang YH, Huang JT: Use of chlorhexidine to eradicate oropharyngeal SARS-CoV-2 in COVID-19 patients. *J. Med. Virol.* **2021**; 93:4370- 4373.
130. Hatanaka N, Xu B, Yasugi M, Morino H, Tagishi H, Miura T et al.: Chlorine dioxide is a more potent antiviral agent against SARS-CoV-2 than sodium hypochlorite. *J. Hosp. Infect.* **2021**; 118:20-26.

PUBLICATIONS RELATED TO AND INCLUDED IN THE THESIS

I.

Archives of Oral Biology 117 (2020) 104837

Contents lists available at ScienceDirect

Archives of Oral Biology

journal homepage: www.elsevier.com/locate/archoralbio

Photocatalytic enhancement of antibacterial effects of photoreactive nanohybrid films in an *in vitro Streptococcus mitis* model

Annamária Venkei[a], Krisztina Ungvári[b], Gabriella Eördegh[b], László Janovák[c,*], Edit Urbán[a], Kinga Turzó[d]

[a] Institute of Clinical Microbiology, Faculty of Medicine, University of Szeged, 6725 Szeged, Semmelweis u. 6., Hungary
[b] Department of Oral Biology and Experimental Dental Research, Faculty of Dentistry, University of Szeged, 6720 Szeged, Tisza Lajos krt. 64., Hungary
[c] Interdisciplinary Excellence Centre, Department of Physical Chemistry and Materials Science, Faculty of Science and Informatics, University of Szeged, 6720 Szeged, Rerrich Béla tér 1., Hungary
[d] Dental School, Medical Faculty, University of Pécs, 7621 Pécs, Dischka Gy. u. 5., Hungary

ARTICLE INFO

Keywords:
Peri-implantitis
Nanoparticles
Photocatalysis
Pioneer colonizer
Antimicrobial activity

ABSTRACT

Objective: Bacterial adhesion and colonization on implanted devices are major etiological factors of peri-implantitis in dentistry. Enhancing the antibacterial properties of implant surfaces is a promising way to reduce the occurrence of inflammations. In this *in vitro* study, the antibacterial potential of two nanocomposite surfaces were investigated, as possible new materials for implantology.

Material and methods: The structural and photocatalytic properties of the TiO_2 and Ag-TiO_2 (with 0.001 wt% plasmonic Ag content) photocatalyst containing polymer based composite layers were also studied and compared to the unmodified standard sandblasted and acid etched Ti discs (control). The presence of visible light induced reactive oxygen species was also verified and quantified by luminol based chemiluminescence (CL) probe method. The discs with adhered *Streptococcus mitis* were illuminated for 5, 10 and 15 min. The antibacterial effect was determined by the metabolic activities of the adhered and proliferated bacterial cells and protein assay at each time point.

Results: The Ag-TiO_2 containing surfaces with obvious photocatalytic activity eliminated the highest amount of the metabolically active bacteria, compared to the control discs in the dark, after 15 min illumination.

Conclusions: The plasmonic Ag-enhanced and illuminated surface exhibits significantly better antibacterial activity under harmless visible light irradiation, than the control Ti or TiO_2 containing copolymer. The studied surface modifications could be promising for further, more complex investigations associated with dental research on infection prevention in connection with oral implantation.

1. Introduction

With the expansion of the average human lifespan, the need for tooth replacement has increased to which modern implantology is an adequate response (Hultin, Gustafsson, & Klinge, 2000; Jungner, Lundqvist, & Lundgren, 2005). In the field of implantology titanium (Ti) implants offers a predictable, long-term implant lifetime, both for general medical and dental applications (Albrektsson, Branemark, Hansson, & Lindström, 1981; Meffert, Langer, & Fritz, 1992).

Inflammatory processes, *i.e.* peri-implant mucositis and peri-implantitis, occurring after the implant placement intervention, may lead to implant failure. Peri-implant mucositis is a reversible implant-related inflammation, localized to the soft tissues, however it can develop into serious peri-implantitis. Peri-implantitis is a destructive inflammatory reaction with the loss of the supporting bone around a dental implant, which can ultimately lead to the loss of the implant (Caton et al., 2018). Among complications microbial colonization and biofilm formation are major etiological factors of peri-implantitis (Renvert, Roos-Jansaker, & Claffey, 2008).

In order to prevent bacterial attachment and biofilm formation on implant surfaces, research has focused on the development of new antibacterial surfaces by the application of surface coatings or modification of the surface architecture (Bazaka, Jacob, Crawford, & Ivanova, 2012; Li et al., 2019; Yuan, Ouyang, Luo et al., 2019). Recent evolution in the field of nanotechnology led to the construction of silver (Ag)-based bactericidal surfaces, which are very promising in combating

* Corresponding author.
E-mail address: janovakl@chem.u-szeged.hu (L. Janovák).

https://doi.org/10.1016/j.archoralbio.2020.104837
Received 28 February 2020; Received in revised form 19 May 2020; Accepted 30 June 2020

against even antibiotic resistant bacteria (Rai, Deshmukh, Ingle, & Gade, 2012).

In spite of the widespread use of silver nanoparticles (AgNPs), little is known about their biological effects *e.g.* on the host tissues and a great number of unidentified signal pathways are associated with AgNPs (Ge et al., 2014; Masa, Deák, Braunitzer, Tóth, & Kopniczky, 2018; McShan, Ray, & Yu, 2014). However, in the case of plasmonic photocatalysts, AgNPs can also be used in combination with titanium-dioxide (TiO_2) (Khan, Qazi, Hashmi, Awan, & Zaidi, 2013). In this plasmonic photocatalyst, visible light is harvested due to the surface plasmon resonance, attributed to the AgNPs, while the metal-semiconductor interface takes part in the separation of the generated holes and electrons (Mérai et al., 2019). The surface Ag component acts as a charge separator resulting visible-light-driven photocatalysis (Awazu et al., 2008; Ma, Dai, Yu, & Huang, 2016; Tanaka, Teramura, Hosokawa, Kominami, & Tanaka., 2017). As a result, the semiconductor TiO_2 has photocatalytic activity and its absorption spectrum extends in the visible light range (red shift) (Veres, Rica et al., 2012). In this way the harmful ultra violet (UV) irradiation necessary for the excitation of conventional TiO_2 could be triggered by visible light exposure in the presence of Ag-TiO_2 photocatalyst. Moreover, it is also worth to note, that besides this noble metals doped semiconductor photocatalysts, upconversion fluorescence could also applied for convert visible light or near-infrared light to UV for TiO_2 activation. (Qi et al., 2019) These multi-strategies for TiO_2 activation is promising for its application in clinical antibacterial materials and surfaces.

Earlier study reported that photoreactive nanohybrid films containing TiO_2 and plasmonic Ag-TiO_2 NPs in polymer matrix were successfully used for sterilizing surfaces and proposed as a prevention strategy against clinically relevant pathogenic bacterial strains (Tallósy et al., 2016). Moreover, our research group observed these coatings cytocompatible properties with epithelial cells (Masa et al., 2018). Based on these results our working hypothesis was that a nanohybrid film with visible light-induced photocatalytic activity could be effective in controlling the bacterial proliferation on Ti used in implantology because in dentistry, blue light is widely used for tooth bleaching and restoration procedures involving composite resin. In addition, many dentists use magnification loupes to enable them to provide more accurate dental treatment. Therefore, the use of light is indispensable in dental treatment (Yoshino & Yoshida, 2018). In this context, the main purpose of our work was to test a novel nanohybrid film loaded with either TiO_2 or with Ag-TiO_2 NPs. Since the recent data in the literature have demonstrated the potential toxicological side effects of AgNP in animal experiment (Wen et al., 2017), therefore we reduced the concentration of AgNPs from 0.5 wt% to 0.001 wt% compared to the amounts applied earlier (Tallósy et al., 2016). Our further goal was to evaluate the antibacterial activity of nanohybrid films containing photosensitizer additives in an *in vitro* experimental setting under dark and illuminated conditions against one of the abundant pioneer colonizer oral bacterium, *Streptococus mitis*, which has a great importance in biofilm formation in oral cavity (Li et al., 2004). Furthermore, we investigated the polymer based composite layers and we compared two different methods (determined the metabolic activities of bacterial cells and protein assay) and determined their sensitivity to detect the antibacterial effect.

2. Materials and methods

2.1. Preparation of antibacterial surfaces

Titanium discs (1.5 mm thick and 9 mm in diameter) were cut from commercially pure (CP4) Ti rods (Denti System, Szentes, Hungary). The surfaces of discs were sandblasted and acid etched. The samples were cleaned with acetone (puriss, Molar Chemicals, Hungary), then with 70 % ethanol (puriss, Molar Chemicals, Hungary) for 15 min (min), and finally rinsed with ultrapure water (Milli-Q® system, Merck, USA) three times. The discs were coated with polymer-based photocatalytic composite thin film with 60 wt% photocatalyst and 40 wt% polymer content. Two different photocatalysts were used for the test: the well-known UV - excitable P25 TiO_2 (99.9 %, Degussa- Evonik P25) and plasmonic Ag-TiO_2 photocatalyst with 0.001 wt% Ag content. Polyacrylate based binder material [poly (ethyl acrylate-co-methyl methacrylate; p (EA-co-MMA) (Eudragit NE 30 D, Evonik)] served as a mechanically stable polymer bed for the surface immobilized photocatalyst particles. The 10 wt% aqueous suspension consisting of photocatalyst particles (6 wt%) and polymer binder (4 wt%) was homogenized by sonication (Elma Hans Schmidbauer GmbH&Co. KG, Stuttgart, Germany) for 30 min then spray-coated (R180 type Airbrush spray gun, 3 bar operating pressure, 15 cm distance from the surface) onto the surface of the discs, in a density of approximately 2 mg/discs and the film was dried. After sterilization at 160 °C for 45 min, the samples were photo bleached by UV-C irradiation (Vilber Lourmat, Marne-la-Vallée, France) at 254 nm wavelength for 60 min before the experiments in order to partially photodegrade the polymer component of the nanohybrid film, so the surface ratio of uncoated photocatalyst nanoparticles increased on the surface of the film. With this procedure we granted the direct link between the bacteria and the nanoparticles. The detailed process of the synthesis of polymer-based photocatalytic suspension has been published elsewhere (Veres, Janovák et al., 2012).

2.2. Investigation of the polymer based composite layers

The surface of the polymer based composite layer with photocatalyst loading were examined by scanning electron microscope (SEM, Hitachi S-4700 microscope), applying a secondary electron detector and 5 kV acceleration voltage. Energy dispersive X-ray spectra were also measured using the Röntec EDX detector at 20 keV.

The amount of hydroxyl radicals (˙OH) was measured from the reaction of luminol and hydrogen peroxide (H_2O_2) (50 % aqueous solution, Molar Chemicals, Hungary). The results were calculated from the chemiluminescence (CL) data with Sirius L Single Tube luminometer (Berthold Detection Systems, Budapest). Six milligrams of luminol (≥ 97.0 % (HPLC), Sigma-Aldrich) was diluted in 1 mL of 0.1 M sodium hydroxide (puriss, Molar Chemicals, Hungary) solution and filled out to 20 mL with distilled water (Milli-Q® system, Merck, USA). The nanohybrid films were immersed in 40 mL of distilled water (Milli-Q® system, Merck, USA) and illuminated and shaken continuously during the experiment with a magnetic stirrer. The distance of the light source from the nanohybrid films was 10 cm. The samples were taken after a given time interval (0–360 min) of illumination, 100 µL of the samples was added to 100 µL of luminol solution, and the intensity of the chemiluminescence was measured immediately with the luminometer (Hirakawa & Nosaka, 2002; Tallósy et al., 2014). Based on the calibration curve (0–5 mM), the concentration of ˙OH radicals is directly proportional to the measured relative light unit (RLU) values as follows: C_{H2O2} (mM) = measured RLU value/41866, $R^2 = 0.9977$. For quantitative characterization of the free radical concentration from the RLU data, the calculated equivalent concentration of H_2O_2 (mM) is displayed as a function of illumination time with the used light source.

The photocatalytic activity of the hybrid layers was also verified through bovine serum albumin (BSA, ≥ 98.0 %, Merck, USA) photodegradation tests (Tallósy et al., 2016). The photocatalytic activity, *i.e.* the decreasing concentration of the BSA solution (BSA, ≥ 98.0 %, Merck, USA) were measured with a Horiba Jobin Yvon Fluoromax-4 spectrofluorometer and the fluorescence spectra were taken after 0, 30, 60, 120, 180 and 240 min of UV light illumination. The concentration of the initial BSA solution (BSA, ≥ 98.0 %, Merck, USA) was 114 ppm, while the extinction wavelength was $\lambda_{ex} = 290$ nm (slit: 5).

2.3. Conditions of bacterial cultivations

A clinical isolate of *S. mitis*, from a patient who had clinical

symptoms of peri-implantitis, was used in our experiments. The isolate was previously identified by matrix assisted laser desorption ionization-time of flight (MALDI-TOF) mass spectrometer (Bruker Daltonics, Bremen, Germany). Before the experiments the strain was stored at –80 °C in Brain Heart Infusion (BHI) broth (Oxoid, Basingstoke, UK), supplemented with 12 % (v/v) of glycerol. The strain was streaked and incubated at 37 °C for 24 h (h) in aerobic environment enriched with 5 % carbon-dioxide on blood agar plates containing 5% cattle blood (BioMérieux, S. A. Marcyl'Etoile, France) for subsequent use. Isolated colonies of *S. mitis* after overnight incubation on blood agar were inoculated into 50 mL 1% glucose bouillon broth (Merck, USA) After incubation at 37 °C for 3 h under aerobic atmosphere, enriched with 5 % carbon-dioxide, the optical density of the culture corresponded to 0.5 McFarland density, (OD_{620nm} = 0.089) which means approximately 10^8 colony forming units (CFU)/mL. Two ml of this exponentially growing culture was pipetted onto the surface of the control and surface modified Ti discs, placed into 24-well hydrophilic surface plate (Sarstedt, Nümbrecht, Germany) and incubated with the bacterial culture for 4.5 h under aerobic conditions. After that the discs with adhered bacteria were illuminated for different time under standardized conditions. The plate wells were covered with glass plates to prevent the antibacterial effect of the lamp by its UV range (see Section 2.4.). In this way we provided the enforcement of the photocatalytic antibacterial effect by visible spectral lines.

2.4. Illumination conditions

For illumination, a 15 W low-pressure mercury lamp was used with an UV–vis light source (Lighttech, Dunakeszi, Hungary). The spectrum of the UV lamp was determined by a grating spectrometer (Ocean Optics QE6500, Dunedin, Florida, USA). The 300 lines/mm grating and the 200 µm entrance slit of the spectrometer allowed 6 nm spectral resolution. The spectrum was recorded by directing the light of the lamp onto the entrance slit of the spectrometer across the glass plates, which were used in the experiments. The tissue culture plates were covered with glass plates in order to exclude the UV light during the illumination periods. The illuminating light source intensity was 1.26×10^{-6} einstein/secundum (s) and the plates were positioned 10 cm from the light source.

As shown on Fig. 1, the emission spectrum of the light source was intense only in the visible range, *i.e.* this photocatalytic tests were performed under visible light illumination. The measured spectral lines (368, 409, 439, 490, 548, 615, 633 and 712 nm) corresponded to the emission lines of mercury vapor, and the phosphorescent coating. Weak UV spectral lines of mercury vapor below 320 nm were completely eliminated by the application of the glass plates. Therefore, in our experiments the photocatalytic antibacterial effect was initiated by the above mentioned intense visible spectral lines ($\lambda > 400$ nm).

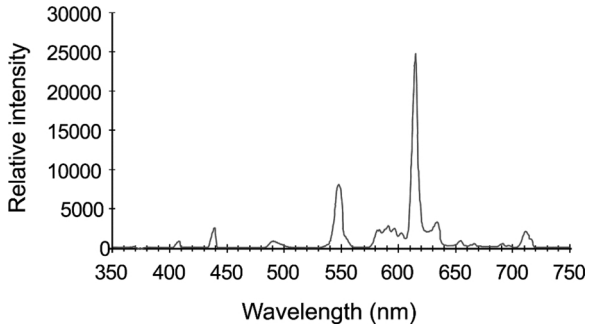

Fig. 1. Emission spectrum of the light source used during the antimicrobial experiments.

2.5. Investigation of the photocatalytic-induced antibacterial activity of nanohybrid coatings by MTT assay

In order to investigate the visible light-induced antibacterial activity of nanohybrid films, illuminated and dark sample groups were prepared. In the "illuminated" group the discs with bacteria were illuminated for 5, 10, or 15 min at 37 °C under standardized conditions, while in the "dark" group the discs were kept in the dark at 37 °C. The standard, sandblasted and acid etched Ti discs, which generally applied in dental practice, were used as controls of nanohybrid surface modifications.

In order to follow the growth of *S. mitis* on the various surfaces under dark and illuminated conditions 3-(4,5-dimethylthiazol-2-yl)-2,5-diphenyltetrazolium bromide (MTT) (Sigma-Aldrich, Darmstadt, Germany) measurements were used (Mosmann, 1983). After the illumination, the samples were washed with phosphate buffered saline (PBS) (Thermo Scientific, Waltham, Massachusetts, USA), then 50 µL MTT solution (1 mg/mL final concentration; MTT powder dissolved in ultrapure water (Milli-Q® system, Merck, USA)) was added to 0.5 mL PBS (Thermo Scientific, Waltham, Massachusetts, USA) on the samples and incubated at 37 °C for 4 h. After this incubation period the solution was removed from each well. Than the formazan crystals, which are the crystallized form of the dye and generated by active bacterial cells, were solubilized with 200 µL of 0.04 mM HCl (Scharlab, Barcelona, Spain) in absolute isopropanol (Molar Chemicals, Halásztelek, Hungary) and with 40 µL of 10 % sodium dodecyl sulfate (Sigma-Aldrich GmbH, Darmstadt, Germany). The optical density (OD) of solubilized formazan crystals, which indicates the level of cell metabolic activity was measured at 550 nm with an ELISA reader (Anthos Labtech Elisa Reader, Vienna, Austria).

2.6. Investigation of the photocatalytic-induced antibacterial activity of nanohybrid coatings by protein assay

The Micro BCA™ Protein assay kit (Thermo Scientific, Waltham, Massachusetts, USA) determines the protein content of the samples, which is proportional to the overall bacterial biomass (Stájer et al., 2012). For parallel set of the samples, this assay kit was used. A calibration curve was created using bovine serum albumin (BSA) (Thermo Scientific, Waltham, Massachusetts, USA) as a control. After the illumination and the washing step with 0.5 mL PBS, (Thermo Scientific, Waltham, Massachusetts, USA) the remaining bacterial cells were disrupted in 0.5 mL lysis buffer (Thermo Scientific, Waltham, Massachusetts, USA). The lysate was centrifuged at 13.000 rpm for 10 min and the supernatants were removed. 150 µL Micro BCA Working reagent (Thermo Scientific, Waltham, Massachusetts, USA) was added to each supernatant and the solutions were incubated at 37 °C for 2 h. The OD was determined at 550 nm with an ELISA reader (Anthos Labtech Elisa Reader, Vienna, Austria). The protein concentration data were calculated based on the measured OD values according to the standard curve (Stájer et al., 2012).

2.7. Statistical analysis

The statistical analysis was performed in Statistica 13.4.0.14 (TIBCO Software Inc. USA) and CogStat 1.7.0. (Attila Krajcsi 2012–2018). After checking the normality and homogenity criterion we compared the data with the appropriate tests (Mann-Whitney U test, Kruskal-Wallis test, independent samples t-test, Welch probe, one-way ANOVA). Statistical significance was set at $p < 0.05$. The means ± SEM (standard error of the mean) were calculated for OD_{550nm} values measured by plate reader based on four parallel experiments (four measures in each) carried out in different time points.

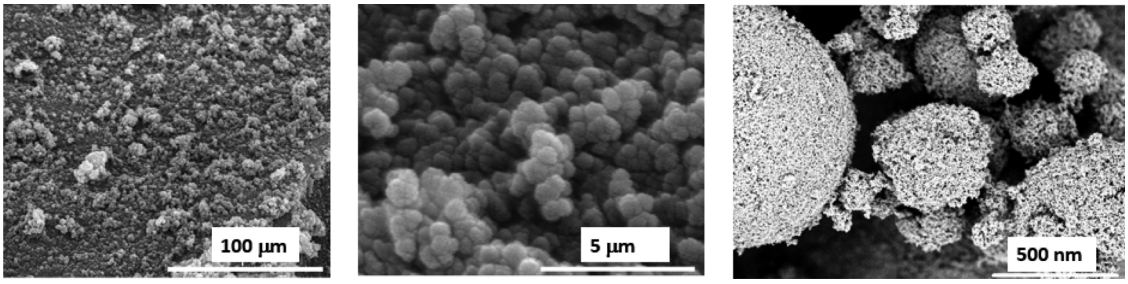

Fig. 2. SEM-EDS images of the polyacrylate based composite thin films containing Ag-TiO_2 photocatalyst filler material with different magnifications.

3. Results and discussion

3.1. Structural and photocatalytic characterization of the hybrid layers

Fig. 2 shows the structure of the photocatalyst containing polymer based hybrid layers with different magnifications. Quasi-spherical microscale-aggregates of the primer photocatalyst particles can be observed on the composite surface with diameters ranging from 5 to 40 µm. Moreover, according to the scanning electron microscopy-energy dispersive X-ray spectrometry (SEM-EDS) pictures, at increased magnifications, nanostructures could be identified superposed on the microscale structure. This is due to the nanoparticles aggregation during the composite film forming process: the initial Ag - TiO_2 photocatalyst particles with ~ 50 nm primary (nominal) particle size were aggregated into 5–40 µm microparticles. This structure ensures high porosity and accessibility which is advantageous for photocatalytic process.

Fig. 3 shows the SEM-EDS base image, and elemental mapping for carbon (C), Ti and C/Ti content of the polymer based sample with 60 wt % Ag-TiO_2 content. At this photocatalyst content both the C of the polymer (green colour) and the Ti content of the photocatalyst (red colour) expressed on the surface. This dual presence of the components at optimal composition resulted surfaces with simultaneous photocatalytic and good mechanical properties as will be seen in the next chapters.

To explore the Ag-TiO_2 photocatalytic reactions, the concentration of reactive radicals produced during irradiation have been investigated with several methods (Dai, Wang, & Yuan, 1998; Sun & Bolton, 1996). For example, Hirakawa et al. were developed a luminol based chemiluminescence (CL) probe method (Hirakawa & Nosaka, 2002). During this method the determination of the high oxidation potential free radicals responsible for the microbial inactivation the concentration of these species was measured by luminometric measurements. In this way, directly the active oxygen species was measured but it can be expressed as H_2O_2 equivalent concentration. In general, it is known that the TiO_2 photocatalytic reactions proceed mainly by the contributions of active oxygen species, such as $^{\cdot}OH$, $O_2^{-\cdot}$ and H_2O_2 (Xu et al., 2017). In the photocatalytic reactions, H_2O_2 would be formed in both processes of reduction and oxidation, that is, dimerization of ·OH, disproportionation of $O_2^{-\cdot}$ and reduction of O_2^{-}. Then, H_2O_2 might be taken into account to understand the details in TiO_2 photocatalysis. The lifetime of the free radicals can be measured in femto- or picoseconds (Sawada et al., 2010). However, the degradation of the formed H_2O_2 (which is produced from $^{\cdot}OH$) is slow at room temperature, it can be measured with a luminometer (Perez-Benito, 2004). According to this phenomenon, the measured H_2O_2 concentration is proportional to the different free radicals produced under illumination of the photocatalysts. The amount of $^{\cdot}OH$ that are produced by the photocatalysts was measured from the CL of luminol. The calculated equivalent concentration values of H_2O_2 (mM) as a function of illumination time are presented in Fig. 4. The results showed that hybrid layer with 60 wt% photocatalyst content shows saturation curve during the studied time interval (0–360 min). This tendency is due to the previously reported UV- induced partial polymer photodegradation: the illumination changes in the ratio of catalyst/polymer composition as the photocatalyst particles became uncoated (Veres et al., 2014). This resulted in higher catalyst availability on the surface region. Due to this photocatalyst surface enrichment the formation of free radical concentration displays saturation curves. It can be also seen that both the photocatalyst free polymer sample and the control sample show negligible photocatalytic effect.

Next, the photocatalytic behavior of the Ag-TiO_2 containing hybrid layer was also demonstrated and studied in the case of BSA solution under UV- light irradiation (Fig. 5). The results reveal that the surface adsorption of the BSA macromolecules was relatively high after 15 min contact time and after that the photooxidation of protein solution (c_0 = 114 ppm) almost reached the 100 % under 4 h UV irradiation time. Thus, the polymer based hybrid layers show obvious photocatalytic activity.

3.2. Assessment of the antibacterial activity of the modified surfaces using the MTT method

The biocompatible property and antibacterial effect of nanohybrid coatings to eliminate clinically relevant pathogenic strains (methicillin resistant *Staphylococcus aureus* (MRSA), *Escherichia coli* or Pseudomonas aeruginosa) within short time (60–120 min) was previously observed (Masa et al., 2018; Tallósy et al., 2016). Connecting to these research in our work we tested the coatings on dental materials, and compared the nanohybrid coatings with untreated standard Ti discs and determined

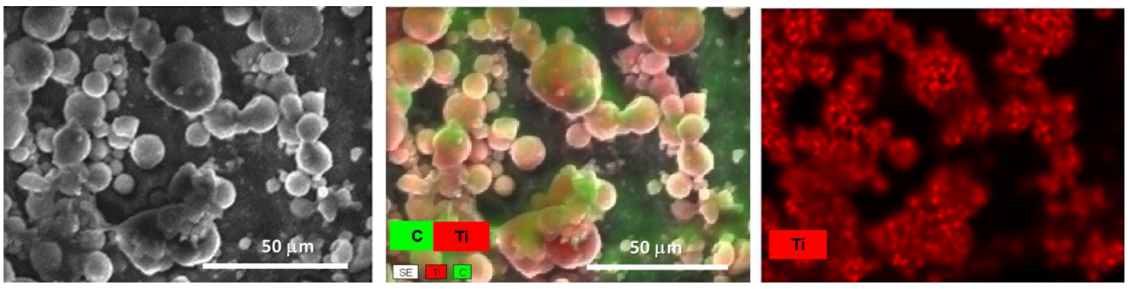

Fig. 3. SEM-EDS images of polymer based photoreactive hybrid layer with the corresponding element distribution of C and Ti.

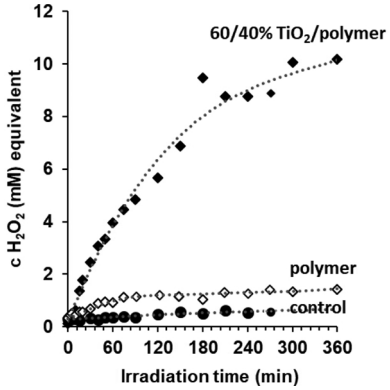

Fig. 4. Characterization of the formation of free radicals on photoreactive hybrid thin films *via* RLU chemiluminescense intensity measurements. Representation of the equivalent H_2O_2 concentration as a function of illumination time.

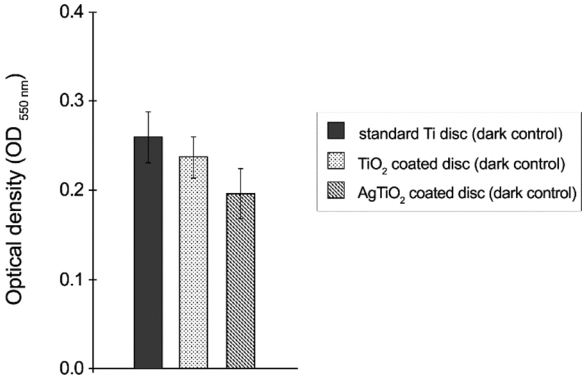

Fig. 6. Relative adherence of *S. mitis* to the standard Ti and modified discs surfaces measured the optical density values with MTT assay without visible light illumination.

the effective illumination time for helpful photocatalysis that is short enough to be applicable in dental practice. In our experiments *S. mitis* was used as one of the pioneer colonizer bacteria found in parodontopathogenic biofilms (Bernardi, Bianchi, Tomei, Continenza, & Macchiarelli, 2019). It has a key role in biofilm formation, providing the basis for the subsequent colonization of facultative and obligate anaerobes. (Li et al., 2004). Based on the literature it may be associated with inflammatory processes around the dental implant. According to Pokrowiecki et al. the amounts of this *streptococci* at infected peri-implant sites approximately four times higher than that found on healthy implants. (Pokrowiecki, Mielczarek, Zareba, & Tyski, 2017). These properties make it a significant oral microbiome member that makes it worth to investigating.

The antibacterial effects of the modified surfaces on the metabolically active *S. mitis* cells were measured by MTT colorimetric assay (Mosmann, 1983). The MTT tetrazolium assay has been widely used as a high throughput screening method for determination of mitochondrial enzymatic activity in cells, which not only indicates the number of viable cells (used as proliferation assay), but also presents the degree of mitochondrial activity that reflects cellular stress or dying cells (used as cytotoxicity test) (Monsees, 2016).Viable cells with active metabolism convert MTT into a purple colored formazan product. Died cells lose the ability to convert MTT into formazan, thus color formation serves as an exact and convenient marker only for the viable cells (Meerlo, Kaspers, & Cloos, 2011).

The Colonies Forming Units (CFU) determination is counting of viable cells, it is a widely used gold standard method in microbiology (Hazan, Que, Maura, & Rahme, 2012). However, it needs dilution series, followed by plating on agar media from each dilution therefore, it is a completely different method from MTT assay as a result our MTT data cannot be converted to CFU data.

Haase et al. recalculated their MTT data to viability percentage with the use of a suitable control in their work (Haase, Jordan, Keitel1, Keil1, & Mahltig, 2017). However, we could not use this or similar experimental setting in our research, since the Ti implant itself has some antibacterial activity as well, consequently we could not attribute 100 % viability for it (Ferraris & Spriano, 2016). Moreover, the 24-well plastic plate surface is totally different from the Ti dental implant surface, so we also could not use it as a standard control for 100 % viability. For these reasons, similarly to Zhou et al. work, we applied the MTT assay and plotted our MTT graphs based on the measured OD values (Zhou et al., 2019).

The relative adherence of *S. mitis* to the different dark control disc surfaces is illustrated on Fig. 6 based on OD measurements with MTT assay. The MTT results confirmed that the relative adherence of *S. mitis* was different depending on the surface type even without illumination. The antibacterial effect of the 0.001 wt% Ag-TiO_2 nanohybrid was the most remarkable (Fig. 6). The 0.001 wt% of Ag concentration is much smaller than those applied by earlier studies (Shi et al., 2015; Tallósy et al., 2016), but according to our findings proved to be effective.

In Fig. 7 the antibacterial effect of surface modifications and visible light illumination compared to their dark controls are plotted as the effect of illumination time. The number of metabolically active bacteria decreased on all Ti based surfaces during illumination for different

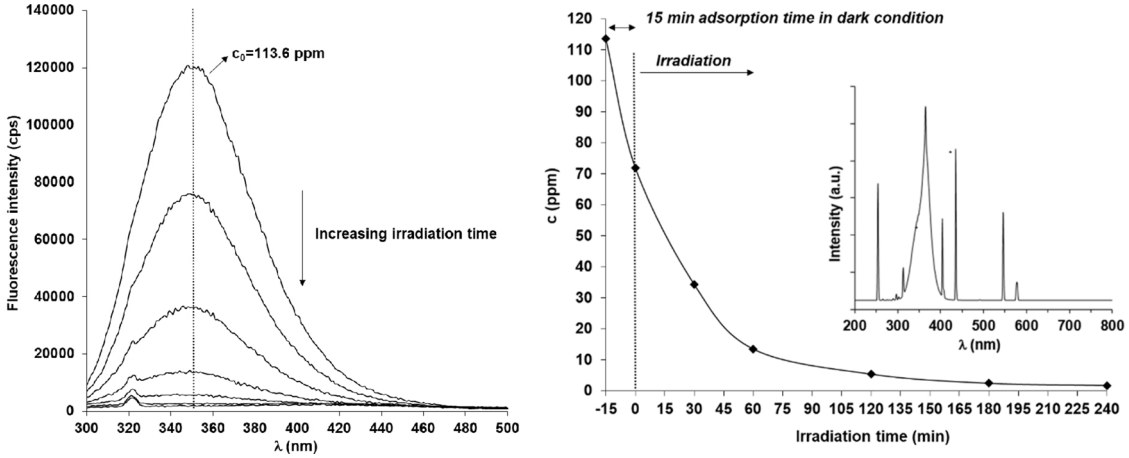

Fig. 5. The effect of UV light irradiation on the fluorescence spectra of the aqueous BSA solutions (a) and the corresponding normalized concentration changes (b) of the protein solution. The inserted image shows the emission spectra of the used UV light source.

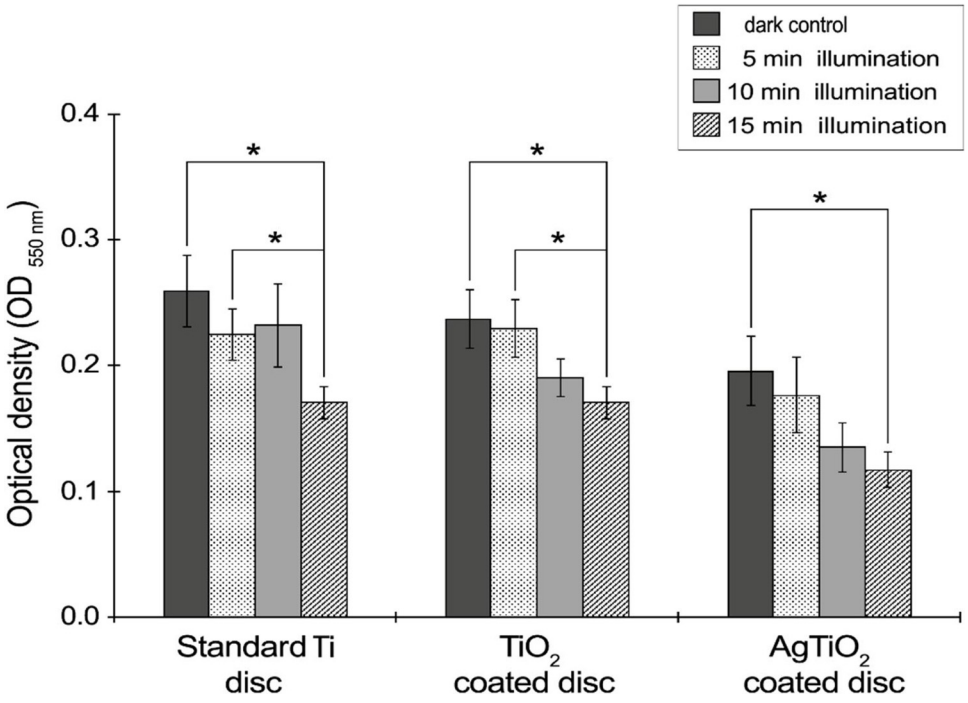

Fig. 7. The antibacterial effect of visible light induced photocatalysis on the metabolically active bacterial cells adhered to the different surfaces compared with dark controls using MTT colorimetric assay. The values were calculated from four independent experiments and are shown as mean ± SEM. Asterisks denote significant differences (* $p < 0.05$).

time. Significant differences ($p < 0.05$) were observed at 15 min illumination compared with dark controls in case of all surfaces. In cases of TiO_2 nanohybrid surfaces and standard Ti disc we measured significant differences ($p < 0.05$) between the 5 min and 15 min illuminated samples by the MTT method. The metabolic activity of *S. mitis* on the Ag-TiO_2 nanohybrid film covered sample (OD_{550nm} = 0.118 ± 0.014) illuminated for 15 min was lower than its dark control (OD_{550nm} = 0.196 ± 0.028) (Fig. 7). 15 min of illumination with visible light enhanced the antibacterial effect of the Ag-TiO_2 coated surface. This time span of illumination is acceptable in the dental practice. In this context it is worth to mention that previous study reported considerable photodegradation of the cell wall components of *E. coli* and MRSA using Ag-TiO_2 photocatalyst particles (Tallósy et al., 2016). According to these results, after 120 min irradiation the bacterial cell wall was totally degraded, *i.e.* the formation of peptidoglycan cross links are totally prevented due to the presence of free radicals, which were produced during the process of the visible light induced photocatalysis (Tallósy et al., 2016). The fluctuation of OD value in the test results of standard Ti disc was observed. The OD value rises after being illuminated for 10 min compared with 5 min illumination. Shany-Kdoshmin et al. mentioned in their work that periodonto-patogenic bacteria could show different light tolerance during exposure to blue light (Shany-Kdoshim, Polak, Houri-Haddad, & Feuerstein, 2019). According to our assumption this discrepancy may be due to the growth dynamics of bacterial cell mass under illumination.

The antibacterial effect of photocatalytically activated nanohybrid surfaces after illumination for different time compared with the standard Ti discs (without illumination), generally used in dental practice is shown in Fig. 8. We observed significant differences between the control Ti discs and both types of nanohybrid coatings in cases at 10 and 15 min illumination. The TiO_2 nanohybrid coatings eliminated significantly more metabolically active bacterial cells after 10 min (OD_{550nm} = 0.191 ± 0.015) and 15 min (OD_{550nm} = 0.171 ± 0.013) illumination compared with control Ti discs (OD_{550nm} = 0.260 ± 0.028). We also found significant difference between the 10 min illuminated Ag-TiO_2 nanohybrid film (OD_{550nm} = 0.136 ± 0.020) and the control Ti discs (OD_{550nm} = 0.260 ± 0.028). Furthermore, in our comparisons the 15 min illuminated Ag-TiO_2 nanohybrid film (OD_{550nm} = 0.118 ± 0.014) had the most remarkable antibacterial effect since it proved to be significantly better compared with the control Ti discs (OD_{550nm} = 0.260 ± 0.028). It has also been shown that the Ag-TiO_2 coated nanohybrid film surpassed the TiO_2 nanohybrid coating in its photocatalytic cell damaging antibacterial activity.

These findings demonstrated that the Ag-TiO_2 coated surface had remarkable antibacterial effect. It has been shown that the addition of plasmonic properties of noble metal nanoparticles (*e.g.* AgNPs) enhances the photocatalytic activity of TiO_2 under visible light (An et al., 2016), nevertheless the carrier polymer has negligible bactericidal effect compared with the nanoparticles containing films (Veres, Janovák et al., 2012). Therefore, we established, that plasmonic photocatalysis may play key role in eliminating the developing bacterial biofilm.

3.3. The effect of the different surfaces on the total bacterial protein content

The effects of photocatalytic damage on the total bacterial cell protein content are also reported here, measured by Micro BCA™ Protein assay kit - instead of using the regular microbiological procedure to count the rate of the CFU. In our research we could not use the CFU method because of the following reasons: for CFU units counting, we must prepare serial dilutions of the sample, plate the diluted suspensions and count the number of CFU. For the application of CFU method required the harvesting of adherent cells from implant surfaces with mechanical effect (*e.g.* sonication) (Schmidlin et al., 2013). This process can result the detachment of NPs from the surfaces which, in the dilution line, may cause incorrect results. Preparing of dilution line is a relatively time-consuming method, needs parallel inoculation, whereby it is labour intensive method and with a high sample size, these factors also can lead to incorrect results. Furthermore, we were interested in the investigation of how the protein assay measurements support our OD values measured with MTT assay, since the literature data about the comparison of these two methods are absent.

Therefore, we chose a simplified, time-saving assay, which do not have any influence on cell viability and applicable in antibacterial studies (Yuan, Ouyang, Gu et al., 2019; Itohiya et al., 2019).

The remaining amounts of bacterial protein on the tested surfaces as a result of the illumination time are shown in Fig. 9. The protein concentrations suggested that the illuminated Ag-TiO_2 nanohybrid surface

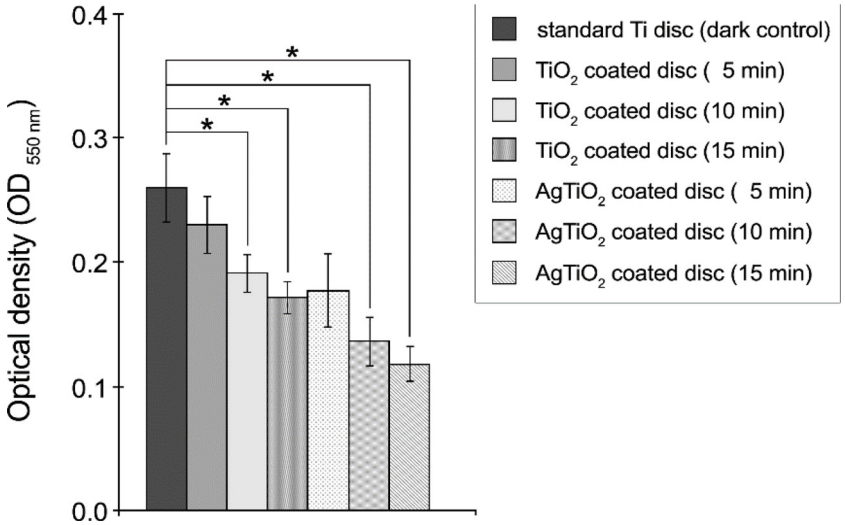

Fig. 8. Comparison of the antibacterial effect of visible light illuminated TiO2 and Ag-TiO2 nanohybrid coatings with dark control Ti disc by MTT colorimetric assay. The values were calculated from four independent experiments and are shown as mean ± SEM. Asterisks denote significant differences (* $p < 0.05$).

had efficient bactericidal effect and inhibited bacterial attachment. our results, the amounts of proteins on both nanohybrid surfaces were lower than on the dark control Ti after 15 min illumination. The observable tendency of decreasing protein concentration in the case of photoreactive coatings compared with dark control Ti is presumably attributed to the photooxidation of the organic macromolecules in spite of the short irradiation time (5 − 15 min), although our protein assay data could not support the statistically significant differences between the various surfaces demonstrated with the MTT assay. This was primarily due to the different sensitivities between these methods. The MTT assay measures only the metabolically active cells (Mosmann, 1983), while the protein-based assay represents all the proteins in the viable and non-viable cells (Eiampongpaiboon, Chung, Bryers, Chung, & Chan, 2015; Stájer et al., 2012). The MTT assay appeared to be more sensitive in detecting the antibacterial effect of nanohybrid coatings compared to the protein assay. Our data support the observation of Fotakis et al. that in case of bacterial biofilm studies the MTT assay is more sensitive method compared with protein assay (Fotakis & Timbrell, 2006).

4. Conclusions

In this study we investigated the direct interaction between the photoreactive composite coating material and the abundant pioneer colonizer in the oral cavity, *S. mitis* and determined the effective illumination time that is short enough to be applicable in everyday dental use. Furthermore, we monitored the antibacterial activity of nanohybrid coatings at the physiologically acceptable 0.001 wt% Ag content level for the human patients by two different methods. The results of our *in vitro* experiments suggested, that the Ag-TiO_2 containing photoreactive surface with visible light activity had remarkable antibacterial property against *S. mitis* cells after 15 min of illumination, because of the photocatalytic mechanism. This means an advantageous system for further *in vivo* experiments associated with peri-implantitis.

Further optimization of this experimental model system is needed to include saliva and extending the microbial spectrum to more complex pathogenic bacterial and fungal species usually involved in peri-implantitis. Research in these directions are in progress and will be reported in the near future.

Declaration of Competing Interest

The authors declare that there are no conflicts of interest.

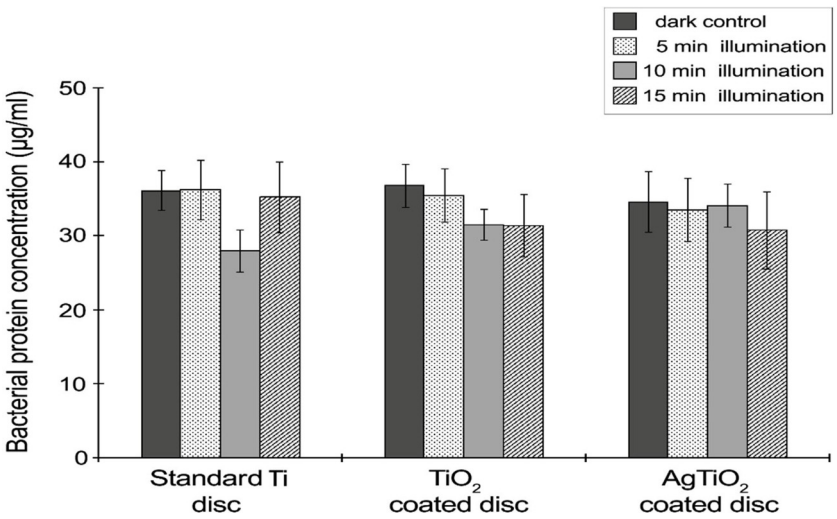

Fig. 9. The antibacterial effects of different illumination times measured by the amount of the total bacterial protein on the nanohybrid surfaces and standard Ti discs. The protein concentration data were calculated based on the calibration curve of BSA. The values were calculated from four independent experiments and are shown as mean ± SEM. Asterisks denote significant differences (* $p < 0.05$).

Acknowledgements

The present study was supported by the following grants: GINOP-2.3.2-15-2016-00011- Molecular research of oral diseases of the New National Excellence Program of the Ministry of Human Capacities, Hungary, UNKP-20-5New National Excellence Program of the Ministry For Innovation of Technology, János Bolyai Research Scholarship of the Hungarian Academy of Sciences, project GINOP-2.3.2-15-2016-00013 and the 20391-3/2018/FEKUSTRAT grant of the Hungarian Ministry of Human Capacities. The authors are grateful to Professor Kornél L. Kovács for his constructive suggestions. Special thanks to Denti System Ltd for supplying commercially pure titanium discs for the experiments.

References

Albrektsson, T., Branemark, P. I., Hansson, H. A., & Lindström, J. (1981). Osseointegrated titanium implants. Requirements for ensuring a long-lasting, direct bone-to-implant anchorage in man. *Acta Orthopaedica Scandinavica, 52*, 155–170. https://doi.org/10.3109/17453678108991776.

An, C., Wang, S., Sun, Y., Zhang, Q., Zhang, J., Wang, C., et al. (2016). Plasmonic silver incorporated silver halides for efficient photocatalysis. *Journal of Materials Chemistry A, 4*, 4336–4352. https://doi.org/10.1039/C5TA07719B.

Awazu, K., Fujimaki, M., Rockstuhl, C., Tominaga, J., Murakami, H., Ohki, Y., et al. (2008). A plasmonic photocatalyst consisting of silver nanoparticles embedded in titanium dioxide. *Journal of the American Chemical Society, 130*, 1676–1680. https://doi.org/10.1021/ja076503n.

Bazaka, K., Jacob, M. V., Crawford, R. J., & Ivanova, E. P. (2012). Efficient surface modification of biomaterial to prevent biofilm formation and the attachment of microorganisms. *Applied Microbiology and Biotechnology, 95*, 299–311. https://doi.org/10.1007/s00253-012-4144-7.

Bernardi, S., Bianchi, S., Tomei, A. R., Continenza, M. A., & Macchiarelli, G. (2019). Microbiological and SEM-EDS evaluation of titanium surfaces exposed to periodontal gel: *In vitro* study. *Materials, 12*, 1448. https://doi.org/10.3390/ma12091448.

Caton, J., Armitage, G., Berglundh, T., Chapple, I. L. C., Jepsen, S., Kornman, K. S., et al. (2018). A new classification scheme for periodontal and peri-implant diseases and conditions – Introduction and key changes from the 1999 classification. *Journal of Clinical Periodontology, 45*, S1–S8. https://doi.org/10.1111/jcpe.12935.

Dai, Q., Wang, D., & Yuan, C. (1998). A novel method for detecting •OH radicals generated by photoexcited nanoparticles. *Supramolecular Science, 5*, 469–473. https://doi.org/10.1016/S0968-5677(98)00053-4.

Eiampongpaiboon, T., Chung, W. O., Bryers, J. D., Chung, K. H., & Chan, D. C. N. (2015). Antibacterial activity of gold-titanates on Gram-positive cariogenic bacteria. *Acta Biomaterialia Odontologica Scandinavica, 1*, 51–58. https://doi.org/10.3109/23337931.2015.1084883.

Ferraris, S., & Spriano, S. (2016). Antibacterial titanium surfaces for medical implants. *Materials Science and Engineering C, 61*, 965–978. https://doi.org/10.1016/j.msec.2015.12.062.

Fotakis, G., & Timbrell, J. A. (2006). In vitro cytotoxicity assays: Comparison of LDH, neutral red, MTT and protein assay in hepatoma cell lines following exposure to cadmium chloride. *Toxicology Letters, 160*, 171–177. https://doi.org/10.1016/j.toxlet.2005.07.001.

Ge, L., Li, Q., Wang, M., Ouyang, J., Li, X., & Xing, M. M. Q. (2014). Nanosilver particles in medical applications: Synthesis, performance, and toxicity. *International Journal of Nanomedicine, 9*, 2399–2407. https://doi.org/10.2147/IJN.S55015.

Haase, H., Jordan, L., Keitel1, L., Keil1, C., & Mahltig, B. (2017). Comparison of methods for determining the effectiveness of antibacterial functionalized textiles. *Materials Science and Engineering C, 61*, 965–978. https://doi.org/10.1016/j.msec.2015.12.062.

Hazan, R., Que, Y. A., Maura, D., & Rahme, L. G. (2012). A method for high throughput determination of viable bacteria cell counts in 96-well plates. *BMC Microbiology, 12*, 259. http://www.biomedcentral.com/1471-2180/12/259.

Hirakawa, T., & Nosaka, Y. (2002). Properties of O2•− and OH• formed in TiO_2 aqueous suspensions by photocatalytic reaction and the influence of H_2O_2 and some ions. *Langmuir, 18*, 3247–3254. https://doi.org/10.1021/la015685a.

Hultin, H., Gustafsson, A., & Klinge, B. (2000). Long-term evaluation of osseointegrated dental implants in the treatment of partly edentulous patients. *Journal of Clinical Periodontology, 27*, 128–133. https://doi.org/10.1034/j.1600-051x.2000.027002128.x.

Itohiya, H., Matsushima, Y., Shirakawa, S., Kajiyama, S., Yashima, A., Nagano, T., et al. (2019). Organic resolution function and effects of platinum nanoparticles on bacteria and organic matter. *PLoS One, 14*(9), https://doi.org/10.1371/journal.pone.0222634 e0222634.

Jungner, M., Lundqvist, P., & Lundgren, S. (2005). Oxidized titanium implants (Nobel Biocare (R) TiUnite (TM)) compared with turned titanium implants (Nobel Biocare (R) mark III (TM)) with respect to implant failure in a group of consecutive patients treated with early functional loading and two-stage protocol. *Clinical Oral Implants Research, 16*, 308–312. https://doi.org/10.1111/j.1600-0501.2005.01101.x.

Khan, S., Qazi, I. A., Hashmi, I., Awan, M. A., & Zaidi, N. S. S. (2013). Synthesis of silver-doped titanium TiO_2 powder-coated surfaces and its ability to inactivate *Pseudomonas aeruginosa* and *Bacillus subtilis*. *Journal of Nanomaterials, 2013*, 8–18. https://doi.org/10.1155/2013/531010.

Li, J., Helmerhorst, E. J., Leone, C. W., Troxler, R. F., Yaskell, T., Haffajee, A. D., et al. (2004). Identification of early microbial colonizers in human dental biofilm. *Journal of Applied Microbiology, 97*, 1311–1318. https://doi.org/10.1111/j.1365-2672.2004.02420.x.

Li, X., Qi, M., Sun, X., Weir, M. D., Tay, F. R., Oates, T. W., et al. (2019). Surface treatments on titanium implants via nanostructured ceria for antibacterial and anti-inflammatory capabilities. *Acta Biomaterialia, 94*, 627–643. https://doi.org/10.1016/j.actbio.2019.06.023.

Ma, X., Dai, Y., Yu, L., & Huang, B. (2016). Energy transfer in plasmonic photocatalytic composites. *Light-Science & Applications, 5*. https://doi.org/10.1038/lsa.2016.17 e16017.

Masa, R., Deák, Á., Braunitzer, G., Tóth, Z., Kopniczky, J., Pelsőczi-Kovács, I., et al. (2018). TiO_2/Ag-TiO_2 nanohybrid films are cytocompatible with primary epithelial cells of human origin: An in vitro study. *Journal of Nanoscience and Nanotechnology, 18*, 3916–3924. https://doi.org/10.1166/jnn.2018.15261.

McShan, D., Ray, P. C., & Yu, H. (2014). Molecular toxicity mechanism of nanosilver. *Journal of Food and Drug Analysis, 22*, 116–127. https://doi.org/10.1016/j.jfda.2014.01.010.

Meerlo, J., Kaspers, G. J. L., & Cloos, J. (2011). Cell sensitivity assays: The MTT assay. *Methods in Molecular Biology (Clifton, NJ), 731*, 237–245. https://doi.org/10.1007/978-1-61779-080-5_20.

Meffert, R. M., Langer, B., & Fritz, M. E. (1992). Dental implants: A review. *Jornal of Periodontology, 63*, 859–870. https://doi.org/10.1902/jop.1992.63.11.859.

Mérai, L., Varga, N., Deák, Á., Sebők, D., Szenti, I., Kukovecz, Á., et al. (2019). Preparation of photocatalytic thin films with composition dependent wetting properties and self-healing ability. *Catalysis Today, 328*, 85–90. https://doi.org/10.1016/j.cattod.2018.10.015.

Monsees, T. K. (2016). Biocompatibility and anti-microbiological activity characterization of novel coatings for dental implants: A primer for non-biologists. *Frontiers in Materials, 3*(40), https://doi.org/10.3389/fmats.2016.00040.

Mosmann, T. (1983). Rapid colorimetric assay for cellular growth and survival: Application to proliferation and cytotoxicity assays. *Journal of Immunological Methods, 65*, 55–63. https://doi.org/10.1016/0022-1759(83)90303-4.

Perez-Benito, J. F. (2004). Iron (III)-hydrogen peroxide reaction: Kinetic evidence of a hydroxyl-mediated chain mechanism. *The Journal of Physical Chemistry A, 108*, 4853–4858. https://doi.org/10.1021/jp031339l.

Pokrowiecki, R., Mielczarek, A., Zareba, T., & Tyski, S. (2017). Oral microbiome and peri-implant diseases: where are we now? *Therapeutics and Clinical Risk Management, 13*, 1529–1542. https://doi.org/10.2147/TCRM.S139795.

Qi, M., Li, X., Sun, X., Li, C., Tay, F. R., Weir, M. D., et al. (2019). Novel nanotechnology and near-infrared photodynamic therapy to kill periodontitis-related biofilm pathogens and protect the periodontium. *Dental Materials, 35*, 1665–1681. https://doi.org/10.1016/j.dental.2019.08.115.

Rai, M. K., Deshmukh, S. D., Ingle, A. P., & Gade, A. K. (2012). Silver nanoparticles: The powerful nanoweapon against multidrug-resistant bacteria. *Journal of Applied Microbiology, 112*, 841–852. https://doi.org/10.1111/j.1365-2672.2012.05253.x.

Renvert, S., Roos-Jansaker, A. M., & Claffey, N. (2008). Non-surgical treatment of peri-implant mucositis and peri-implantitis: A literature review. *Journal of Clinical Periodontology, 35*, 305–315. https://doi.org/10.1111/j.1600-051X.2008.01276.x.

Sawada, T., Yoshino, F., Kimoto, K., Takahashi, Y., Shibata, T., Hamada, N., et al. (2010). ESR detection of ROS generated by TiO_2 coated with fluoridated apatite. *Journal of Dental Research, 8*, 848–853. https://doi.org/10.1016/j.surfcoat.2017.05.053.

Schmidlin, P. R., Müller, P., Attin, T., Wieland, M., Hofer, D., & Guggenheim, B. (2013). Polyspecies biofilm formation on implant surfaces with different surface characteristics. *Journal of Applied Oral Science, 21*, 48–55. https://doi.org/10.1590/1678-7757201302312.

Shany-Kdoshim, S., Polak, D., Houri-Haddad, Y., & Feuerstein, O. (2019). Killing mechanism of bacteria within multi-species biofilm by blue light. *Journal of Oral Microbiology, 11*, Article 1628577. https://doi.org/10.1080/20002297.2019.1628577.

Shi, C., Gao, J., Wang, M., Fu, J., Wang, D., & Zhu, Y. (2015). Ultra-trace silver-doped hydroxyapatite with non-cytotoxicity and effective antibacterial activity. *Materials Science and Engineering C, 55*, 497–505. https://doi.org/10.1016/j.msec.2015.05.078.

Stájer, A., Urban, E., Pelsőczi-Kovács, I., Mihalik, E., Rakonczay, Z., Nagy, K., et al. (2012). Effect of caries preventive products on the growth of bacterial biofilm on titanium surface. *Acta Microbiologica et Immunologica Hungarica, 59*, 51–61. https://doi.org/10.1556/AMicr.59.2012.1.6.

Sun, L., & Bolton, J. R. (1996). Determination of the quantum yield for the photochemical generation of hydroxyl radicals in TiO2 suspensions. *The Journal of Physical Chemistry, 100*, 4127–4134. https://doi.org/10.1021/jp9505800.

Tallósy, S. P., Janovák, L., Ménesi, J., Nagy, E., Juhász, Á., Balázs, L., et al. (2014). Investigation of the antibacterial effects of silver modified TiO_2 and ZnO plasmonic photocatalysts embedded in polymer thin films. *Environmental Science and Pollution Research - International, 19*, 11155–11167. https://doi.org/10.1007/s11356-014-2568-6.

Tallósy, S. P., Janovák, L., Nagy, E., Deák, Á., Juhász, Á., Csapó, E., et al. (2016). Adhesion and inactivation of Gram-negative and Gram-positive bacteria on photoreactive TiO_2/polymer and Ag–TiO_2/polymer nanohybrid films. *Applied Surface Science, 371*, 139–150. https://doi.org/10.1016/j.apsusc.2016.02.202.

Tanaka, A., Teramura, K., Hosokawa, S., Kominami, H., & Tanaka, T. (2017). Visible light-inudced water splitting in an aqueous suspension of a plasmonic Au/TiO_2 photocatalyst with metal co-catalysts. *Chemical Science, 8*, 2574–2580. https://doi.org/10.1039/C6SC05135A.

Veres, Á., Ménesi, J., Juhász, Á., Berkesi, O., Ábrahám, N., Bohus, G., et al. (2014). Photocatalytic performance of silver-modified TiO_2 embedded in poly(ethyl-acrylate-

co-methyl metacrylate) matrix. *Colloid and Polymer Science, 292*, 207–217. https://doi.org/10.1007/s00396-013-3063-1.

Veres, Á., Janovák, L., Bujdosó, T., Rica, T., Fodor, E., Tallósy, S. P., et al. (2012). Silver and phosphate functionalized reactive TiO_2/polymer composite films for destructions of resistent bacteria using visible light. *Journal of Advanced Oxidation Technologies, 15*, 205. https://doi.org/10.1515/jaots-2012-0124.

Veres, Á., Rica, T., Janovák, L., Dömök, M., Buzás, N., Zöllmer, V., et al. (2012). Silver and gold modified plasmonic TiO_2 hybrid films for photocatalytic decomposition of ethanol under visible light. *Catalysis Today, 181*, 156–162. https://doi.org/10.1016/j.cattod.2011.05.028.

Wen, H., Dan, M., Yang, Y., Lyu, J., Shao, A., Cheng, X., et al. (2017). Acute toxicity and genotoxicity of silver nanoparticle in rats. *PloS One, 12*(12), https://doi.org/10.1371/journal.pone.0185554 e0185554.

Xu, Y. X., Riedl, H., Holec, D., Chen, L., Du, Y., & Mayrhofer, P. H. (2017). Thermal stability and oxidation resistance of sputtered Ti\\Al\\Cr\\N hard coatings. *Surface & Coatings Technology, 324*, 48–56. https://doi.org/10.1177/0022034510370806.

Yoshino, F., & Yoshida, A. (2018). Effects of blue-light irradiation during dental treatment. *The Japanese Dental Science Review, 54*, 160–168. https://doi.org/10.1016/j.jdsr.2018.06.002.

Yuan, Z., Ouyang, P., Gu, K., Rehman, T., Zhang, T., Yin, Z., et al. (2019). The antibacterial mechanism of oridonin against methicillin-resistant *Staphylococcus aureus* (MRSA). *Pharmaceutical Biology, 57*, 710–716. https://doi.org/10.1080/13880209.2019.1674342.

Yuan, X., Ouyang, L., Luo, Y., Sun, Z., Yang, C., Wang, J., et al. (2019). Multifunctional sulfonated polyetheretherketone coating with beta-defensin-14 for yielding durable and broad-spectrum antibacterial activity and osseointegration. *Acta Biomaterialia, 86*, 323–337. https://doi.org/10.1016/j.actbio.2019.01.016.

Zhou, Y., Wang, S., Zhou, X., Zou, Y., Li, M., Peng, X., et al. (2019). Short-time antibacterial effects of dimethylaminododecyl methacrylate on oral multispecies biofilm *in vitro*. *BioMed Research International, 2019*. https://doi.org/10.1155/2019/6393470.

II.

AKADÉMIAI KIADÓ

Acta Microbiologica et Immunologica Hungarica

DOI:
10.1556/030.2020.01080

ORIGINAL ARTICLE

A simplified *in vitro* model for investigation of the antimicrobial efficacy of various antiseptic agents to prevent peri-implantitis

ANNAMÁRIA VENKEI[1*], GABRIELLA EÖRDEGH[2], KINGA TURZÓ[3], EDIT URBÁN[1], and KRISZTINA UNGVÁRI[2]

[1] Institute of Clinical Microbiology, Faculty of Medicine, University of Szeged, 6725, Semmelweis u. 6, Szeged, Hungary

[2] Department of Oral Biology and Experimental Dental Research, Faculty of Dentistry, University of Szeged, 6720, Tisza Lajos krt. 64, Szeged, Hungary

[3] Dentistry Program, Medical School, University of Pécs, 7621, Dischka Gy. u. 5, Pécs, Hungary

Received: November 8, 2019 • Accepted: January 1, 2020

ABSTRACT

The biofilm formation by oral bacteria on the implant surface is one of the most remarkable factors of peri-implant infections, which may eventually lead to bone resorption and loss of the dental implant. Therefore, the elimination of biofilm is an essential step for the successful therapy of implant-related infections. In this work we created a basic *in vitro* model to evaluate the antibacterial effect of three widely used antiseptics.

Commercially pure (CP4) titanium sample discs with sand blasted, acid etched, and polished surface were used. The discs were incubated with mono-cultures of *Streptococcus mitis* and *Streptococcus salivarius*. The adhered bacterial biofilms were treated with different antiseptics: chlorhexidine-digluconate (CHX), povidone-iodine (PI), and chlorine dioxide (CD) for 5 min and the control discs with ultrapure water. The antibacterial effect of the antiseptics was tested by colorimetric assay.

According to the results, the PI and the CD were statistically the most effective in the elimination of the two test bacteria on both titanium surfaces after 5 min treatment time. The CD showed significant effect only against *S. salivarius*.

Based on our results we conclude that PI and CD may be promising antibacterial agents to disinfecting the peri-implant site in the dental practice.

KEYWORDS

titanium, antimicrobial agents, peri-implantitis, *Streptococcus mitis*, *Streptococcus salivarius*

INTRODUCTION

Implantation is one of the most widely applied treatment options for tooth replacement. Titanium (Ti) and Ti alloys are the most common choices for dental implant materials because these materials are well tolerated by human tissues and they integrate easily with the bone to allow successful osseointegration [1]. Good clinical implantation intervention depends on various factors. Bacterial colonization, biofilm formation, and consequent peri-implantitis play major roles among the complications [2].

The oral microbiota is a diverse community, consisting of over 700 different bacterial and fungal species, which can form biofilm on soft and hard surfaces, including the implant surfaces [3]. Formation of a microbial biofilm is a complex and multi-step process. Most of the pioneer colonizers, belongs to *Streptococcus* genus and plays key role in the formation of multilayered dental plaque in oral cavity [4]. The formation and maturation of bacterial biofilm on the surfaces of dental implant have been associated with the etiology of peri-

*Corresponding author. Tel.: +36 (62) 54-5398; E-mail: venkei.annamaria@gmail.com

implant mucositis and peri-implantitis. Peri-implantitis is one of the major causes of unsuccessful implantation, since the periodontopathogenic bacteria can penetrate from the colonized neck part of an implant along the implant body in the gingiva and deeper hard tissue region, triggering inflammation around osseointegrated implants which may result in the loss of bone around an implant [5, 6].

Esposito et al. [7], published in their earlier study that 8–50% of implant removal processes are due to peri-implantitis. Because of the growing number of concerned patients every year, dentists need to address the proper treatment of peri-implant infections.

Currently, the treatment of peri-implantitis is done by mechanical debridement with or without adjunctive antiseptic agents. The most suitable chemical agent for disinfecting the peri-implant region has not yet been found because of the lack of comprehensive *in vitro* and *in vivo* experiments [8]. Several disinfectants have been tested with varying success.

In our earlier study we investigated the cytotoxic effect of three different disinfectant solutions (3% H_2O_2 solution, saturated citric acid (pH = 1) and CHX gel) on human epithelial cells attached to Ti surfaces [9]. Connecting to our previous study in this current work we done a basic research to observe the antimicrobial effects of decontaminant agents e.g., chlorhexidine-digluconate (CHX), chlorine dioxide (CD), and povidone-iodine (PI).

CHX has been the most frequently used agent in the adjuvant treatment of peri-implantitis for years as it has a broad-spectrum antimicrobial effect, both bactericidal and bacteriostatic, depending on the applied concentration [10]. CHX can also penetrate into the biofilm to damage the incorporated bacteria [11].

CD is used in various fields due to the excellent bactericidal and antiviral properties [12]. It can also diffuse easily into the biofilm and destroys the microbes forming the film [13].

PI has been used as a topical antiseptic in oral surgery and periodontal practice. PI has a wide spectrum of antibacterial and antiviral effects. The information regarding its effect on biofilms is limited [14]. Furthermore, the comparisons of antibacterial effect of CHX, CD, and PI have not yet been investigated.

The oral microbiota is a very complex ecological community that hard to model exactly, since it contains a huge number of culturable and unculturable bacteria which need special demands to their viability and proliferation [15, 16]. Our research group previously used *Streptococcus* strain as a model organism for dental research [17]. Therefore, in this study we also applied a simplified *in vitro* model and chose pioneer colonizers (*Streptococcus mitis*, *Streptococcus salivarius*) to our investigations.

MATERIALS AND METHODS

Preparation of disc surfaces for the experiment

In our experiments we used two different surface modified Ti discs. The discs (1.5 mm thick and 9 mm diameter) were cut from commercially pure (CP4) Ti rods (Denti System®, Hungary). One type of the discs surfaces were modified by sand blasting, acid etching technique and the surfaces of the other discs were polished by the manufacturer. Before the experiments the samples were cleaned with acetone, then with 70% ethanol for 15 min, and rinsed with ultrapure water three times. Finally, the samples were sterilized at 160 °C for 45 min.

Investigation of the antibacterial activity of the three different antiseptic agents on mono-species biofilms

S. mitis and *S. salivarius* isolates from patients who had clinical symptoms of peri-implantitis were used in our experiments. The isolates were previously identified by matrix assisted laser desorption ionization-time of flight mass spectrometer (MALDI-TOF MS) (Bruker Daltonics, Bremen, Germany).

After the isolation and identification, the bacteria were stored at −80 °C in Brain Heart Infusion (BHI) broth (Oxoid, UK) supplemented with 12% (v/v) glycerol. The strains were incubated at 37 °C for 24 h in 5% CO_2 atmosphere on blood agar plate containing 5% cattle blood (BioMérieux, S. A. Marcyl'Etoile, France) for experiments.

The mono-bacterial suspension was prepared in 1% glucose bouillon from the overnight blood agar plate of each strain. After incubation at 37 °C for 3 h under aerobic atmosphere, enriched with 5% CO_2, the optical density (OD) of the cultures reached the 0.5 McFarland density. The bacterial suspension was pipetted on the surfaces of discs in 24-well hydrophilic surface plate (Tissue Culture 24 well plate, Sarstedt, Nümbrecht, Germany).

We used different incubation time for the two test bacteria since our goal was to investigate the response of pioneer colonizer streptococci to antiseptic treatment in distinct laboratory conditions and create basic *in vitro* models for our further investigations. Therefore, we used a shorter incubation time for *S. mitis* (4.5 h) similarly to our previous experiment [17] and other researchers work [18]. However, we extended the incubation time to 48 h in case of *S. salivarius* where after 24 h we changed the culture medium for fresh 1% glucose bouillon. This was performed based on Rath et al. *in vitro* biofilm model who established in their work that already 24 h cultivation time of *S. salivarius* is enough for biofilm formation on titanium implant [19].

After incubation at 37 °C in CO_2 the developed biofilms were washed with 1× phosphate-buffered saline (PBS) (1×, pH: 7.2) to remove the less adherent cells. Than the attached bacterial cells were treated with 2 ml of three different oral antiseptics: CHX (Curasept ADS 220, 0.2%, Switzerland), PI (Betadine, 10%, Switzerland), and CD (Solumium dental, 0.12%, Hungary) for 5 min, since it can be optimal in the usual dental practice according our previous results [9] and other researchers [20]. The antiseptics were washed out from the implant surfaces by rinsed them with 1 ml 1× PBS.

In order to follow the metabolic activity of the bacterial biofilm 3-(4,5-dimethylthiazol-2-yl)-2,5-diphenyltetrazolium

bromide (MTT) (Sigma–Aldrich, Darmstadt, Germany) assay was used. This method was previously tested on epithelial cell culture by our research group [11]. After the antiseptic treatment and washing steps 50 µL MTT solution (1 mg/ml final concentration) was added to 0.5 ml 1× PBS on the samples and incubated at 37 °C for 4 h. Than the solution was removed from each well and the remaining formazan crystals, which indicates the level of cell metabolic activity, were solubilized with 200 µL of 0.04 mM HCl (Scharlab, Spain) in absolute isopropanol (Molar Chemicals, Hungary) and with 40 µL of 10% sodium dodecyl sulfate (Sigma–Aldrich GmbH, Germany). The OD of solubilized formazan crystals were measured at 550 nm with an ELISA reader (Anthos Labtech Elisa Reader, Hungary).

The antibacterial effect of the antiseptics was compared with untreated control Ti discs with the developed biofilm which were only rinsed with sterile 1× PBS.

Statistical analysis

Statistical analysis was carried out using Statistica 13 (Dell Inc. USA). After test of normality (Shapiro–Wilk test) the comparisons within group were evaluated using one-way analysis of variance (ANOVA) followed by Tukey's post hoc test and T-test was used for comparison of independent samples. The means ± SEM (standard error of the mean) were calculated for OD_{550nm} values measured by plate reader based on five parallel experiments (three measures in each group) carried out in different time points. Statistical significance was set at $P < 0.05$.

RESULTS

Disinfectant efficacy of oral antiseptics on *S. mitis* biofilm determined by MTT colorimetric assay

The results of antimicrobial activity of antiseptics against *S. mitis* are shown in Fig. 1. Evaluation of the three disinfectants antibacterial activity against the pioneer colonizer indicated that among antiseptics the PI and the CD showed significant difference both on the polished (ANOVA $P = 0.0005$) and the sand blasted, acid etched (ANOVA $P = 0.0004$) Ti surfaces compared with the untreated control Ti discs after the 5 min treatment time. We presented the measured OD values on Fig. 1 however, we converted these data to percent values and mentioned them in this way in the text (data are not shown here). The attachment to the control Ti surface was considered 100% (highest OD value) and the number of metabolically active cells on the surfaces was expressed in relative percentages in the results section.

Based on our MTT results all antiseptic decreased the cell metabolic activity in biofilm on sand blasted, acid etched and polished surfaces. However, the PI and CD showed significant cell reduction on both surfaces ($P < 0.05$).

The PI was the most effective antiseptic against the *S. mitis* cells incubated for 4.5 h, since it decreased the number of active cells with 37% ($OD_{550} = 0.043 \pm 0.001$) on polished surface compared with the control disc ($OD_{550} = 0.068 \pm 0.008$) after 5 min treatment time ($P = 0.0012$). We observed completely similar tendency with regard the sand blasted, acid etched surfaces. The decrease of the metabolically active cells was 33% ($OD_{550} = 0.044 \pm 0.001$) after rinsing with PI compared with the untreated control Ti discs ($OD_{550} = 0.065 \pm 0.007$) ($P = 0.0007$).

Disinfectant efficacy of oral antiseptics on *S. salivarius* biofilm determined by colorimetric MTT assay

The disinfectants dissolving effects on *S. salivarius* biofilm developed for a prolonged incubation time (48 h) are detailed in Fig. 2. According to our results all tested agents significantly decreased the amount of metabolically active cells in *S. salivarius* biofilm on polished surfaces compared with the untreated Ti surfaces *in vitro* (ANOVA $P < 0.0001$). The most pronounced antibacterial activity was attributed to PI, which is eliminated 65% ($OD = 0.048 \pm 0.003$) of biofilm forming cells on polished surface after 5 min treatment time ($P = 0.0002$). However, the CD also eliminated a remarkable percent of the biofilm (60%) ($OD = 0.056 \pm 0.001$) compared with the control polished discs ($OD = 0.139 \pm 0.01$, $P = 0.0002$). Considering the three agents significant differences could be observed between the PI and CHX ($P = 0.0002$) and in this respect between the CD and CHX ($P = 0.0006$) as well.

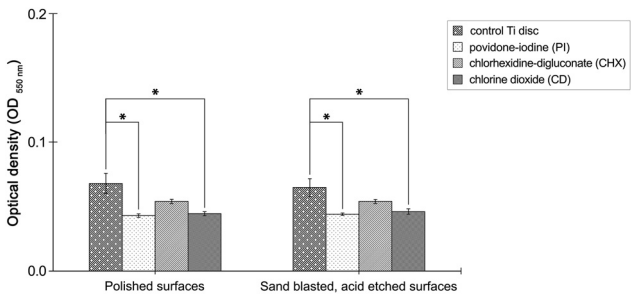

Figure 1. Determination of the antibacterial efficiency of different antiseptic agents by MTT colorimetric assay for *S. mitis*. The values were calculated from five independent experiments and are shown as mean ± SEM. Asterisks denote significant differences (*$P < 0.05$)

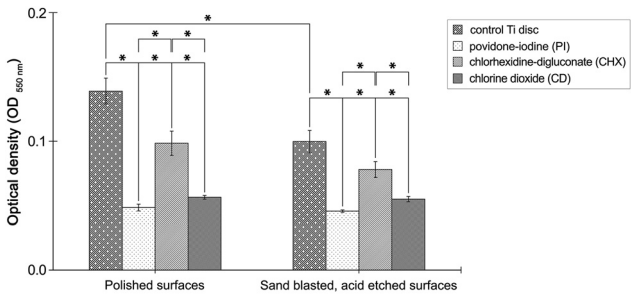

Figure 2. Effect of antiseptics on the *S. salivarius* cells using MTT colorimetric assay. The values were calculated from five independent experiments and are shown as mean ± SEM. Asterisks denote significant differences (*$P < 0.05$)

On the sand blasted, acid etched surface the metabolic activity of *S. salivarius* cells decreased in the biofilm when treated with all three antiseptics compared with the control discs (ANOVA $P < 0.0001$). Furthermore, the PI and CD showed significantly higher antibacterial activity against *S. salivarius* compared with the CHX treatment (PI vs. CHX $P = 0.0007$, CD vs. CHX $P = 0.0212$).

Besides these results the quantitative evaluation of bacterial adhesion to different control Ti surfaces revealed that the density of metabolically active cell was significantly lower on the polished surface than on the sand blasted, acid etched groups, respectively ($P = 0.0063$). We did not found such difference at *S. mitis* between non treated control polished and sand blasted acid etched surfaces (Fig. 1).

DISCUSSION

In dentistry the dental implants are widely used for tooth replacement however, the implant surfaces similarly to the tooth surfaces provides possibility for attachment of bacteria and for formation of a complex biofilm which can cause inflammation around peri-implant tissues and influence the long-term success of osseointegration of implants [21].

Generally in dentistry a smooth Ti surface is developed to provide epithelial attachment and prevent plaque formation. The rough part of Ti implant responsible for proper connective tissue attachment, and grant the anchorage of implant in the bone. The peri-implant inflammation caused by pathogens can spread apically from the colonized neck part of Ti implant toward the deeper bone tissue region therefore, we used two different surface roughness of dental implant (polished and sand blasted, acid etched) to model this complex process on two test bacteria (*S. mitis*, *S. salivarius*) in our *in vitro* model [22].

According to McDonnell and Russell [10] CHX is one of the most well-known and widely used antiseptic agent in dentistry, but based on our results it is showed significant cell reduction only in case of *S. salivarius* after 5 min exposure time. The CHX reduced 29% of metabolically active cells while the other two agents destroyed double amount of proliferating *S. salivarius*.

Based on MTT data the PI and CD were the two most effective antiseptic agents against *S. mitis* and *S. salivarius*. Moreover, both agents are proved to be significantly better compared with CHX in the elimination of the *S. salivarius* biofilm developed for 48 h. Our results are in concordance with Herczegh et al. [23] who established in their work that the CD was more effective compared with CHX after 5 min treatment time.

Our model demonstrated that the PI was the most effective in the *in vitro* elimination of both bacterial biofilms. However, in case of *S. mitis* we could not observe significant difference between PI and CD. Hosaka et al. [24] reported that even 0.5 min application of PI was effective in the *in vitro* killing both of *Porphyromonas gingivalis* and *Fusobacterium nucleatum* and according to other studies the CD was also effective in reducing the plaque of *F. nucleatum*. [25] Currently there are no data in the literature about the comparison of the effectiveness of PI and CD in the same *in vitro* experimental setting.

Besides these three antiseptics there are several other agents to control biofilm associated peri-implantitis. [10] However, choosing an ideal antiseptic to the therapy of peri-implantitis is influenced not only by effectiveness but also by the lack of side effects of agent. CHX is the most widely used gold standard antiseptic for plaque control [26] but CHX have some adverse properties. It stains teeth or it can cause oral mucosa desquamation or the burning sensation of the oral mucosa [27, 28]. However, the anti discoloration system (ADS) presented in Curasept used by our experiment can reduce the risk of discoloration and eliminates the unpleasant taste-disturbance [29]. PI has also adverse effects including allergy or hypersensitivity to the solution, and it can cause a reversible yellowish discoloration as well, however the short durations of using PI in low concentration could decrease these effects [30, 31]. In our experiment we used a short 5 min exposure time, furthermore, Kanagalingam et al. reported in their review that there have been no clinical reports on development of microbial resistance after the PI treatment while, in contrast bacterial resistance to CHX has been observed [32]. Based on our MTT assay data, we determined that PI could be a promising oral antiseptic in the prevention of peri-implantitis.

According to other researchers [33] CD can react with four amino acids (cysteine, methionine, tyrosine, tryptophan) which have vital role in living organism and microbes can not develop resistance against CD, it can not cause real harm to humans as it is not able to penetrate into the deep tissues [33]. CD is effective in relatively low concentrations and the new membrane technology developed by Noszticziusz et al. [33] allows the production of high purity CD solution without any by-products. These properties could make it an ideal antiseptic beside PI in dental practice to treat inflammation caused by microoganisms.

CONCLUSION

In our study we compared the antimicrobial effect of three antiseptics (CHX, PI, CD) on *S. mitis* and *S. salivarius* in mono-species biofilm models adhering to Ti surfaces using MTT colorimetric assay. The antimicrobial property of all tested disinfectants have been known, however there are limited information in the literature about their comparison.

Our data indicated, that PI and CD had remarkable eliminating property against *S. mitis* and *S. salivarius* cells in biofilm after 5 min of treatment time. Considering the conflicts in available literature regarding the cytotoxic properties of agents we established that the PI and CD means advantageous disinfectants, since they are effective *in vitro* against the biofilms of the pioneer colonizers under aerobic conditions.

In the light of our results we plan the further optimization of our *in vitro* model by using other pathogenic anaerobic bacteria or pathogenic fungal species and changing the treatment time or concentration of antiseptics for their most effective clinical application.

ACKNOWLEDGMENTS

The present study was supported by the following grants: GINOP-2.3.2-15-2016-00011- Molecular research of oral diseases. The autors are grateful to Denti System Ltd for supplying our research group with commercially pure Ti for the experiments.

Conflict of interest: The authors declared no potential conflicts of interest with respect to the research, authorship, and publication of this article.

REFERENCES

[1] Abrahamsson I, Berglundh T, Lindhe J. Soft tissue response to plaque formation at different implant systems. A comparative study in the dog. Clin Oral Implants Res 1998; 9: 73–73.

[2] Berglundh T, Persson L, Klinge B. A systematic review of the incidence of biological and technical complications in implant dentistry reported in prospective longitudinal studies of at least 5 years. J Clin Periodontol 2002; 29: 197–212.

[3] Dewhirst FE, Chen T, Izard J, Paster BJ, Tanner AC, Yu WH, et al. The human oral microbiome. J Bacteriol 2010; 192: 5002–17.

[4] Huang R, Li M, Gregory R. Bacterial interactions in dental biofilm. Virulence 2011; 2: 435–44.

[5] Zitzmann ZU, Berglundh T. Definition and prevalence of peri-implant diseases. J Clin Periodontol 2008; 35: 286–91.

[6] Gristina A. Biomaterial-centered infection: microbial adhesion versus tissue integration. Science 1987; 237: 1588–95.

[7] Esposito M, Hirsch JM, LekholmU, ThomsenP. Failure patterns of four osseointegrated oral implant systems. J Mater Sci Mater Med 1997; 8: 812–47.

[8] Machtei EE. Treatment alternatives to negotiate peri-implantitis. Advances Med 2014; 2014: 13.

[9] Ungvari K, Pelsoczi IK, Kormos B, Oszko A, Rakonczay Z, Kemeny L, et al. Effects on titanium implant surfaces of chemical agents used for the treatment of peri-implantitis. J Biomed Mater Res B Appl Biomater 2010; 94: 222–9.

[10] McDonnell G, Russell AD. Antiseptics and disinfectants: activity, action, and resistance. Clin Microbiol Rev 1999; 12: 147–79.

[11] Southard SR, Drisko CL, Killoy WJ, Cobb CM, Tira DE. The effect of 2% chlorhexidine digluconate irrigation on clinical parameters and the level of bacteroides gingivalis in periodontal pockets. J Periodontol 1989; 60: 302–9.

[12] Grootveld M, Silwood C, Gill D, Lynch E. Evidence for the microbicidal activity of a chlorine dioxide-containing oral rinse formulation *in vivo*. J Clin Dent 2001; 12: 67–70.

[13] Benarde MA, Snow WB, Olivieri VP, Davidson B. Kinetics and mechanism of bacterial disinfection by chlorine dioxide. Appl Microbiol 1967; 15: 257–65.

[14] Durani P, Leaper D. Povidone-iodine: use in hand disinfection, skin preparation and antiseptic irrigation. Int Wound J 2008; 5: 376–87.

[15] Stewart EJ. Growing unculturable bacteria. J Bacteriology 2012; 194: 4151–60.

[16] Aas JA, Paster BJ, Stokes LN, Olsen I, Dewhirst FE. Defining the normal bacterial flora of the oral cavity. J Clin Microbiol 2005; 43: 5721–32.

[17] Györgyey Á, Janovák L, Ádám A, Kopniczky J, Tóth LK, Deák Á, et al. Investigation of the *in vitro* photocatalytic antibacterial activity of nanocrystalline TiO_2 and coupled TiO_2/Ag containing copolymer on the surface of medical grade titanium. J Biomater Appl 2016; 31: 55–67.

[18] Montanaro L, Campoccia D, Rizzi S, Donati EM, Breschi L, Prati C, et al. Evaluation of bacterial adhesion of *Streptococcus mutans* on dental restorative materials. Biomaterials 2004; 24: 4457–63.

[19] Rath H, Stumpp NS, Stiesch M. Development of a flow chamber system for the reproducible *in vitro* analysis of biofilm formation on implant materials. PLoS One 2017; 12: e0172095.

[20] Schou S, Berglundh T, Lang PN. Surgical treatmnet of peri-implantitis. Int J Oral Maxillofac Implants 2004; 19: 140–9.

[21] Wilson M. Bacterial biofilms and human disease. Sci prog 2001; 84: 235–54.

[22] Dhir S. Biofilm and dental implant: the microbial link. J Indian Soc Periodontology 2013; 17: 5–11.

[23] Herczegh A, Gyurkovics M, Agababyan H, Ghidán Á, Lohinai Z. Comparing the efficacy of hyper-pure chlorine-dioxide with other oral antiseptics on oral pathogen microorganisms and biofilm *in vitro*. Acta Microbiol Immunol Hung 2013; 60: 359–73.

[24] Hosaka Y, Saito A, Maeda R, Fukaya C, Morikawa S, Makino A, et al. Antibacterial activity of povidone-iodine against an artificial biofilm of *Porphyromonas gingivalis* and *Fusobacterium nucleatum*. Arch Oral Biol 2012; 57: 364–8.

[25] Shinada K, Ueno M, Konishi C, Takehara S, Yokoyama S, Zaitsu T, et al. Effects of a mouthwash with chlorine dioxide on oral malodor and salivary bacteria: a randomized placebo-controlled 7-day trial. Trials 2010; 11: 14–14.

[26] Mathur S, Mathur T, Srivastava R, Khatri R. Chlorhexidine: the gold standard in chemical plaque control. Natl J Physiol Pharm Pharmacol 2011; 1: 45–50.

[27] Addy M, Moran J, Griffiths AA, Wills-Wood NJ. Extrinsic tooth discoloration by metals and chlorhexidine. I. Surface protein denaturation or dietary precipitation?. Br Dent J 1985; 159: 281–5.

[28] Kenrad B. Toxin effects from chlorhexidine gluconate: case report. Tandlaegebladet 1990; 94: 489–91.

[29] Marrelli M, Amantea M, Tatullo M. A comparative, randomized, controlled study on clinical efficacy and dental staining reduction of a mouthwash containing chlorhexidine 0.20% and Anti Discoloration System (ADS). Ann Stomatol (Roma) 2015; 6: 35–42.

[30] Rath T, Meissl G. Induction of hyperthyroidism in burn patients treated topically with povidone-iodine. Burns Incl Therm Inj 1988; 14: 320–2.

[31] Chua J, Dominguez E, Mae C, Sison CMC, Berba R. The efficacy of povidone-iodine oral rinse in preventing ventilator-

associated pneumonia: a randomized, double blind, placebo-controlled (VAPOR) trial: preliminary report. Philipp J Microbiol Infect Dis 2004; 33: 153–61.

[32] Kanagalingam J, Feliciano R, Hah JH, Labib H, Le TA, Lin JC. Practical use of povidone-iodine antiseptic in the maintenance of oral health and in the prevention and treatment of common oropharyngeal infections. Int J Clin Pract 2015; 69: 1247–56.

[33] Noszticzius Z, Wittmann M, Kaly-Kullai K, Beregvari Z, Kiss I, Rosivall L, et al. Chlorine dioxide is a size-selective antimicrobial agent. PLoS One 2013; 8: e79157.